US 20100036252A1

(19) **United States**

(12) **Patent Application Publication**

Chalana et al.

(10) **Pub. No.: US 2010/0036252 A1**

(43) **Pub. Date: Feb. 11, 2010**

(54) **ULTRASOUND SYSTEM AND METHOD FOR MEASURING BLADDER WALL THICKNESS AND MASS**

(76) Inventors: **Vikram Chalana**, Mill Creek, WA (US); **Stephen Dudycha**, Bothell, WA (US); **Gerald McMorrow**, Kirkland, WA (US); **Jongtae Yuk**, Redmond, WA (US); **Tim Shelton**, North Bend, WA (US); **Bill Barnard**, Woodville, WA (US)

Correspondence Address:
BLACK LOWE & GRAHAM, PLLC
701 FIFTH AVENUE, SUITE 4800
SEATTLE, WA 98104 (US)

(21) Appl. No.: **12/497,509**

(22) Filed: **Jul. 2, 2009**

Related U.S. Application Data

(63) Continuation-in-part of application No. 10/704,996, filed on Nov. 10, 2003, which is a continuation-in-part of application No. 10/701,955, filed on Nov. 5, 2003, now Pat. No. 7,087,022, which is a continuation-in-part of application No. 10/633,186, filed on Jul. 31, 2003, now Pat. No. 7,004,904, Continuation-in-part of application No. 10/165,556, filed on Jun. 7, 2002, now Pat. No. 6,676,605, Continuation-in-part of application No. PCT/US03/24368, filed on Aug. 1, 2003, Continuation-in-part of application No. PCT/US03/14785, filed on May 9, 2003, which is a continuation of application No. 10/165,556, filed on Jun. 7, 2002, now Pat. No. 6,676,605, Continuation-in-part of application No. 10/633,186, filed on Jul. 31, 2003, now Pat. No. 7,004,904.

(60) Provisional application No. 60/400,624, filed on Aug. 2, 2002, provisional application No. 60/423,881, filed on Nov. 5, 2002, provisional application No. 60/423,881, filed on Nov. 5, 2002, provisional application No. 60/400,624, filed on Aug. 2, 2002.

Publication Classification

(51) **Int. Cl.**
A61B 8/00 (2006.01)

(52) **U.S. Cl.** **600/449**

(57) **ABSTRACT**

An ultrasound transceiver scans an organ and processes the echogenic signals to produce three-dimensional, two-dimensional, and one-dimensional information of the organ. The 3-D, 2-D, and 1-D information is utilized to determine the thickness, surface area, volume, and mass of the organ wall.

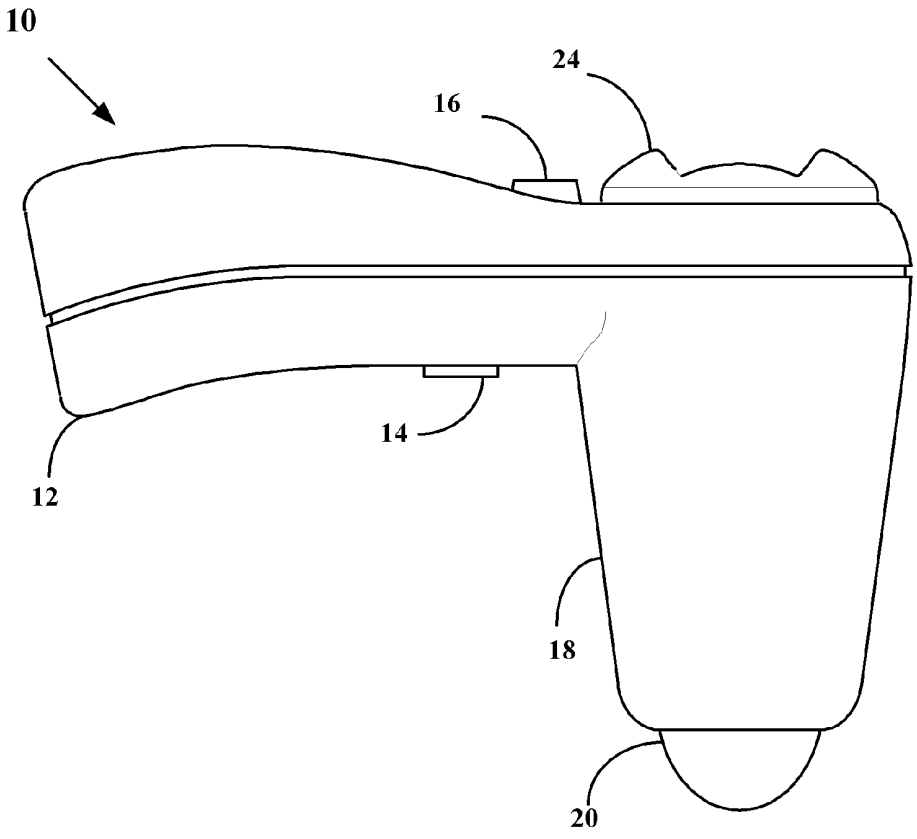

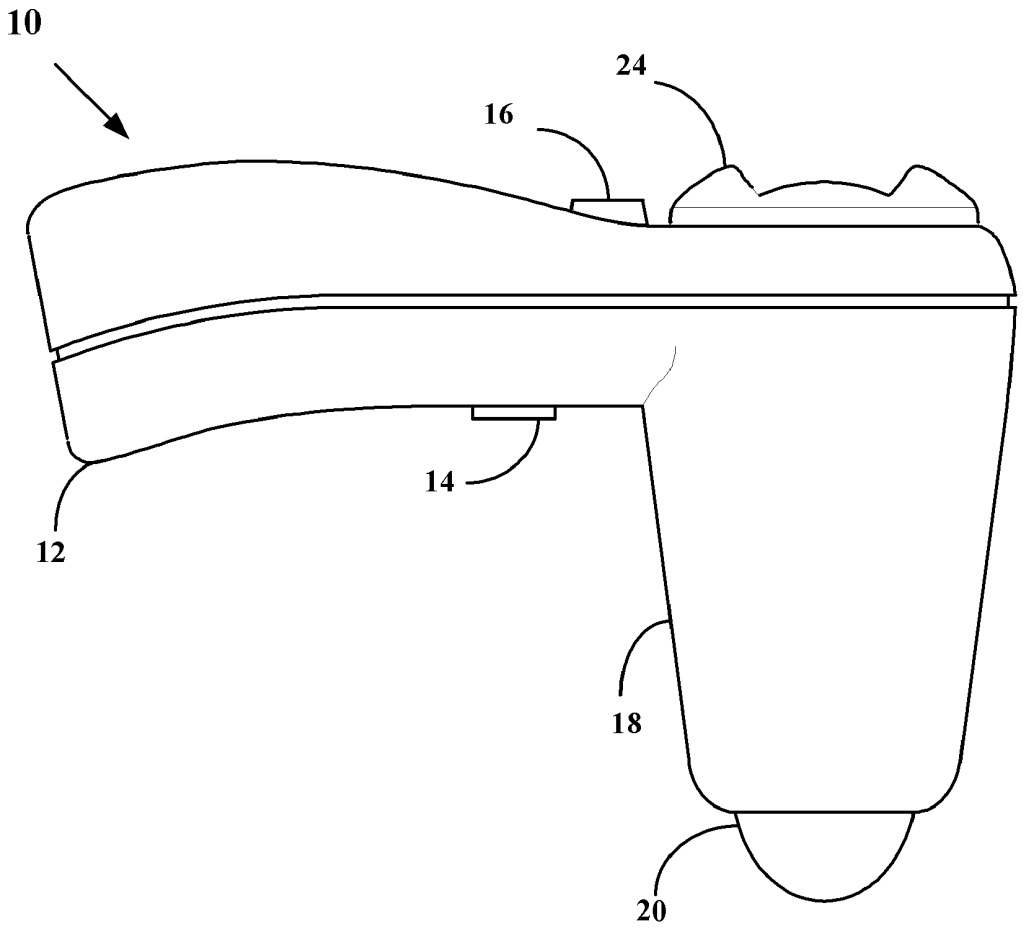

FIG. 1

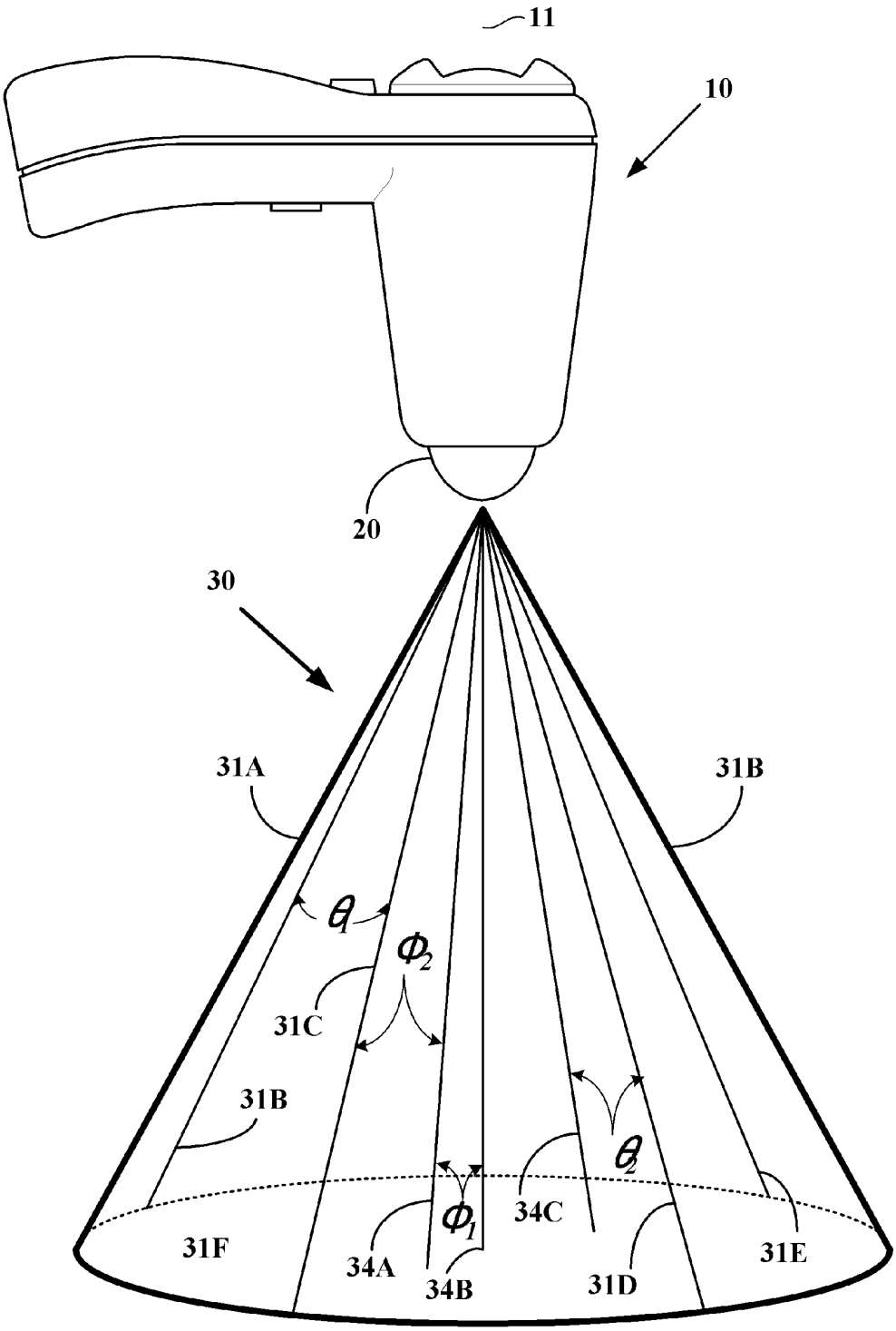

Fig. 2

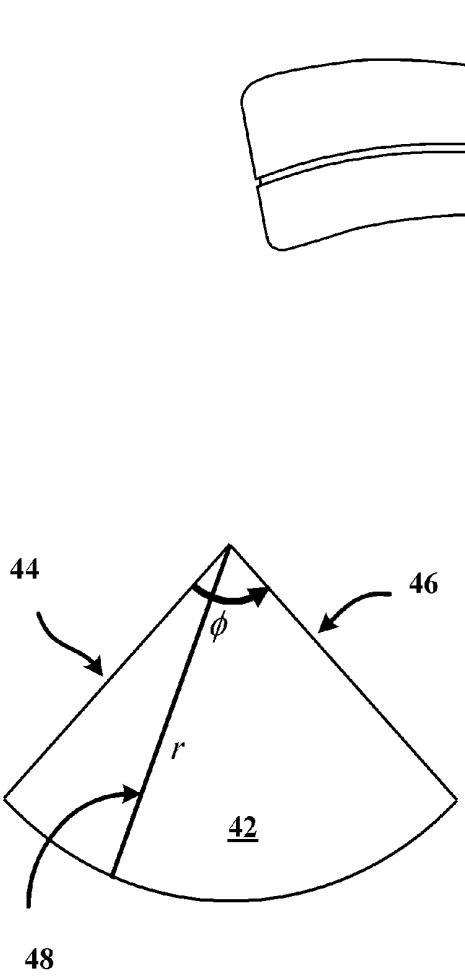

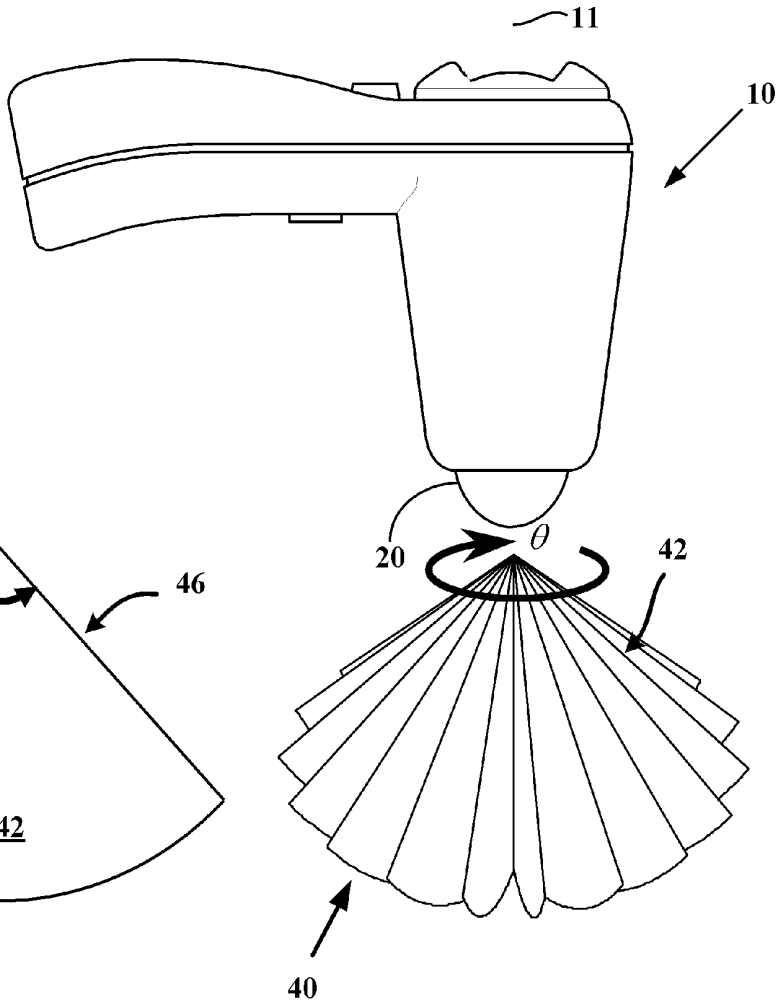

Fig. 3B

Fig. 3A

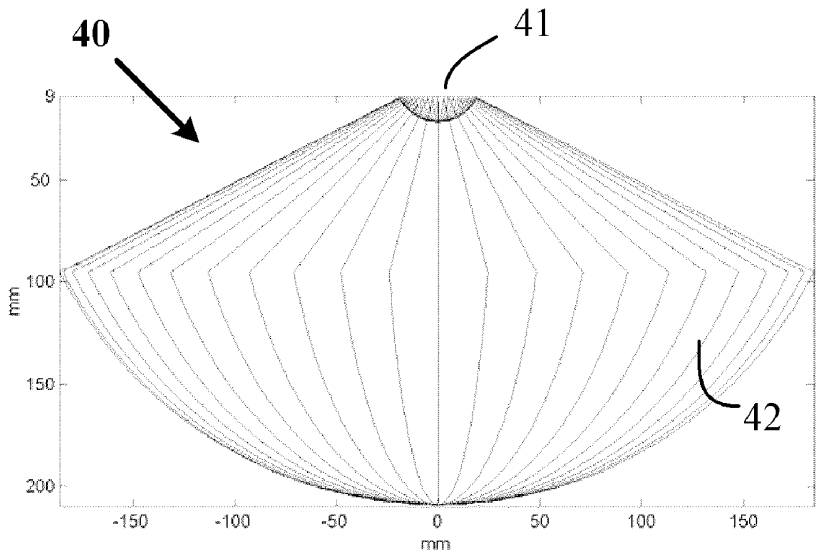
40
41
42
mm
9
50
100
150
200
-150
-100
-50
0
50
100
150
mm

FIG. 3C

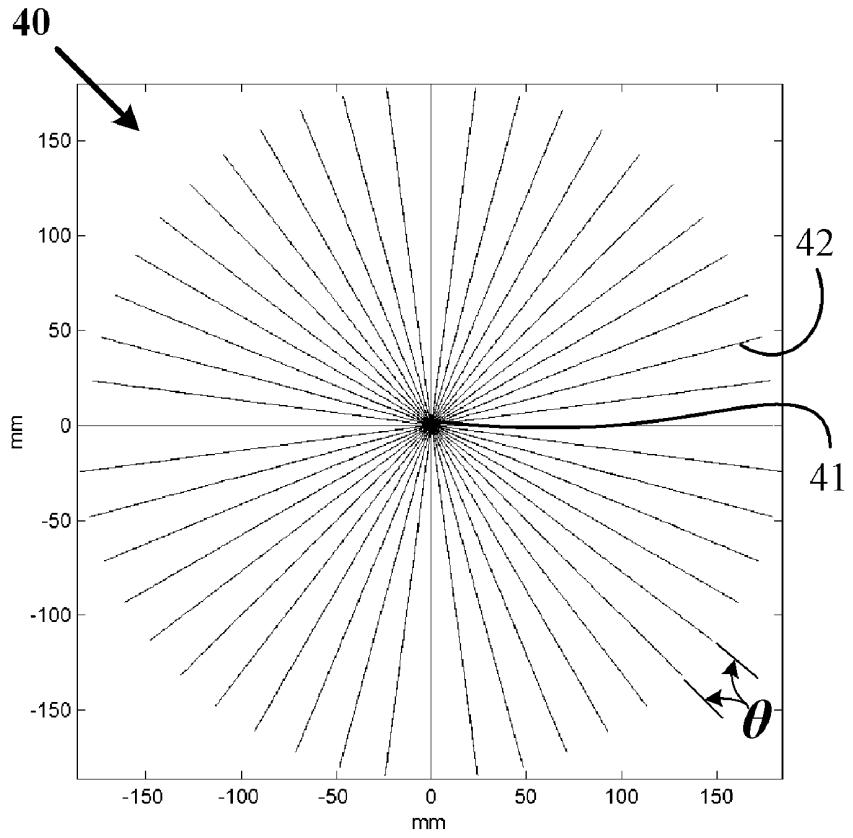
40
42
41
θ
mm
150
100
50
0
-50
-100
-150
-150
-100
-50
0
50
100
150
mm

FIG. 3D

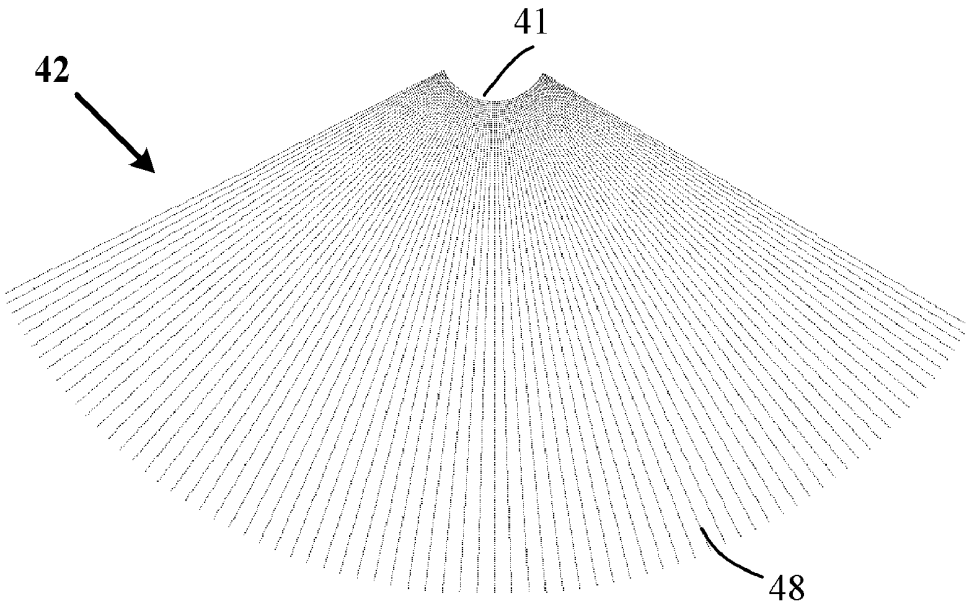

FIG. 3E

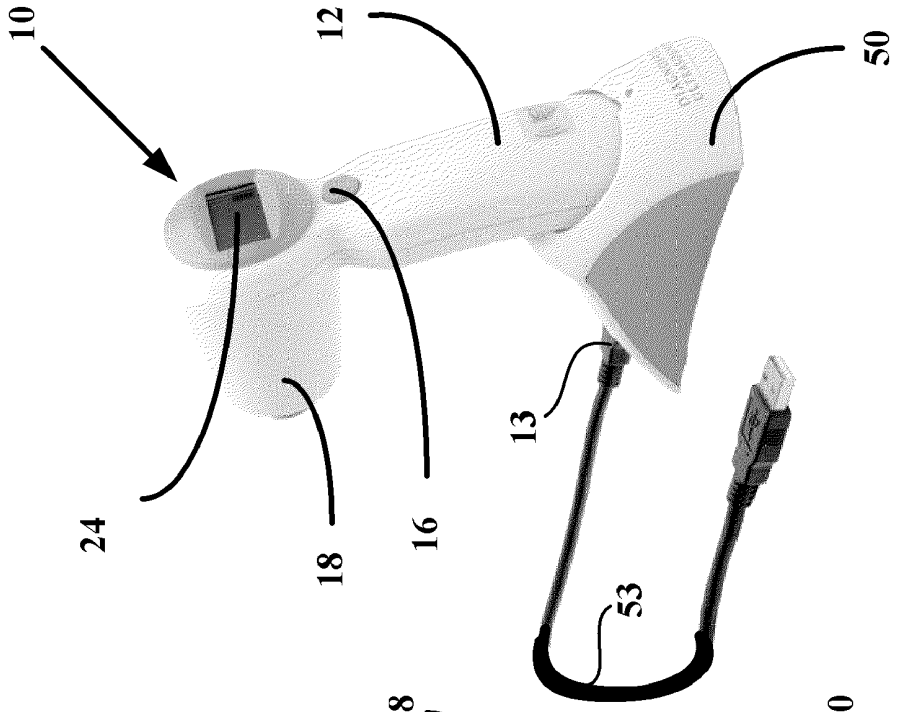

Fig. 4B

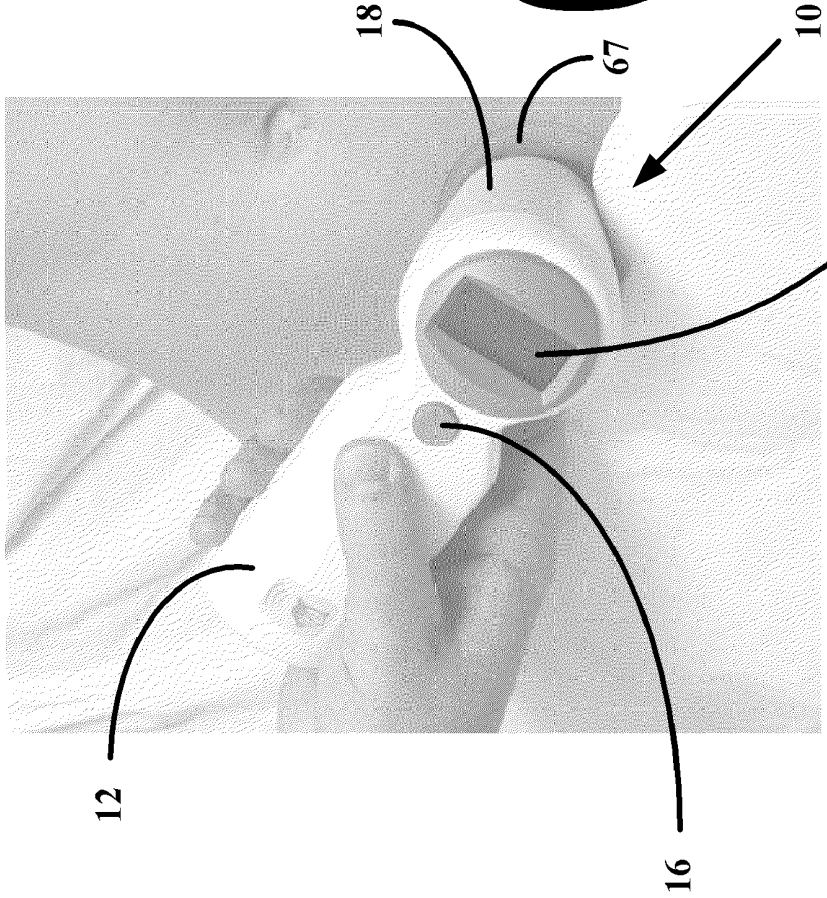

Fig. 4A

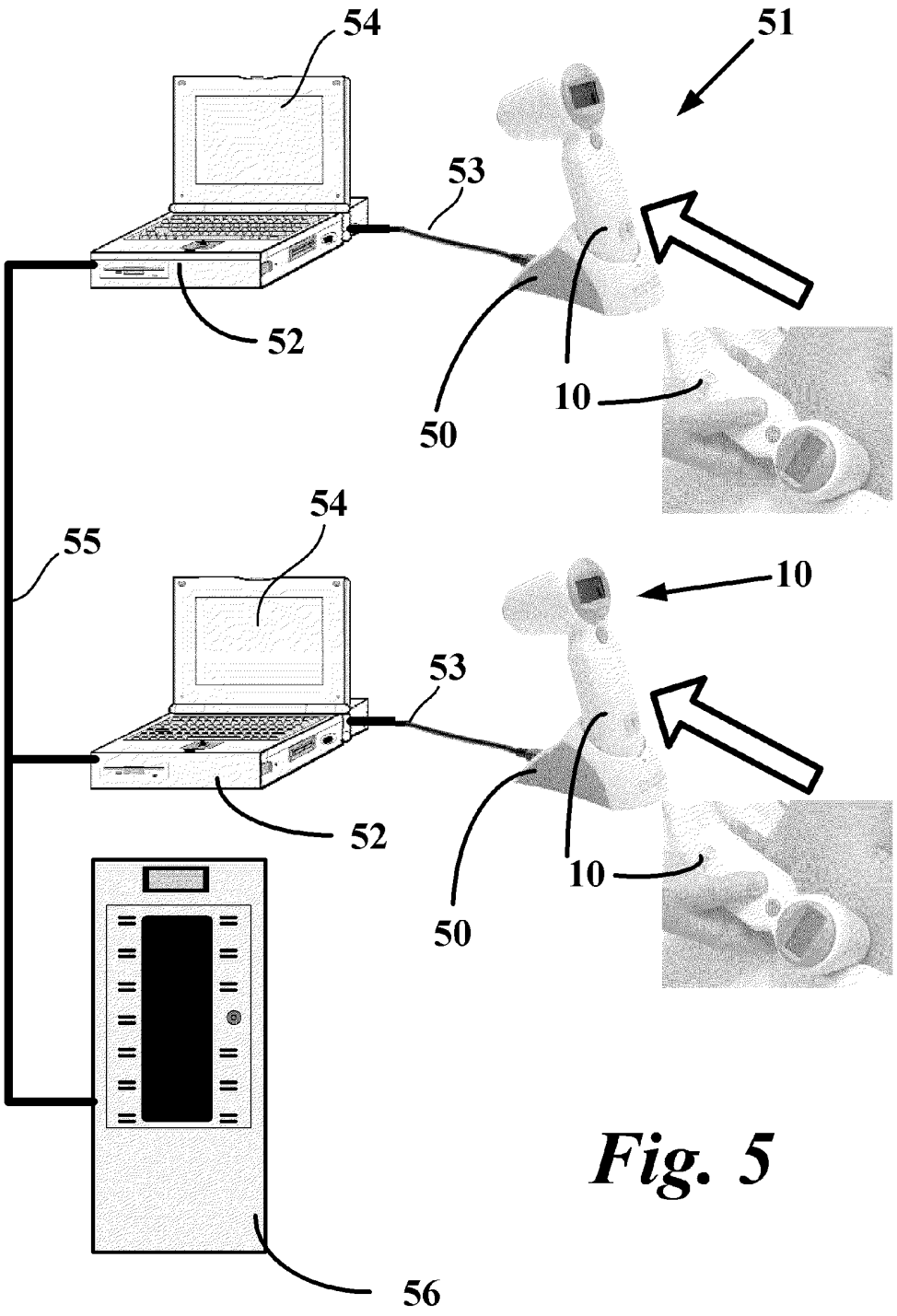

Fig. 5

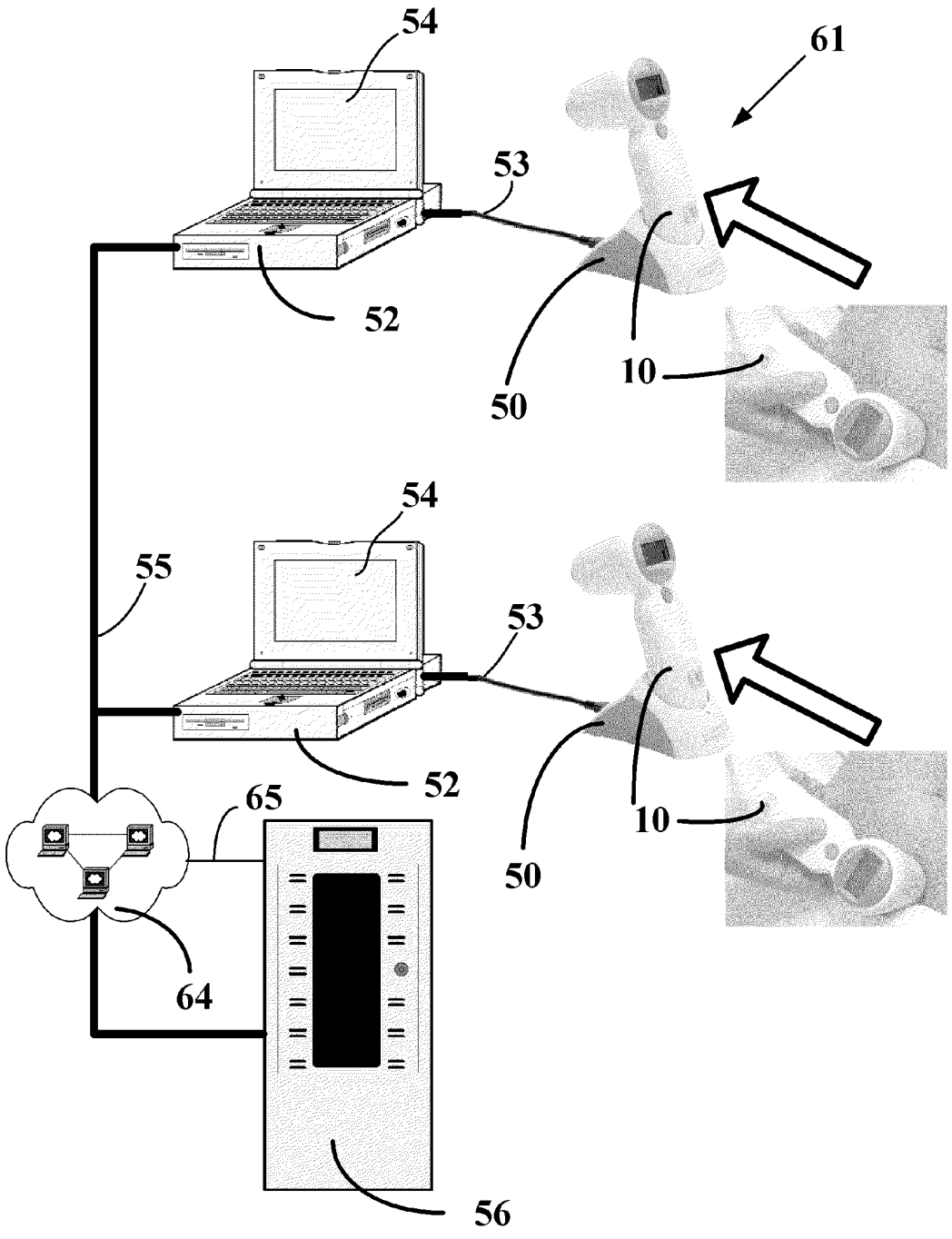

Fig. 6

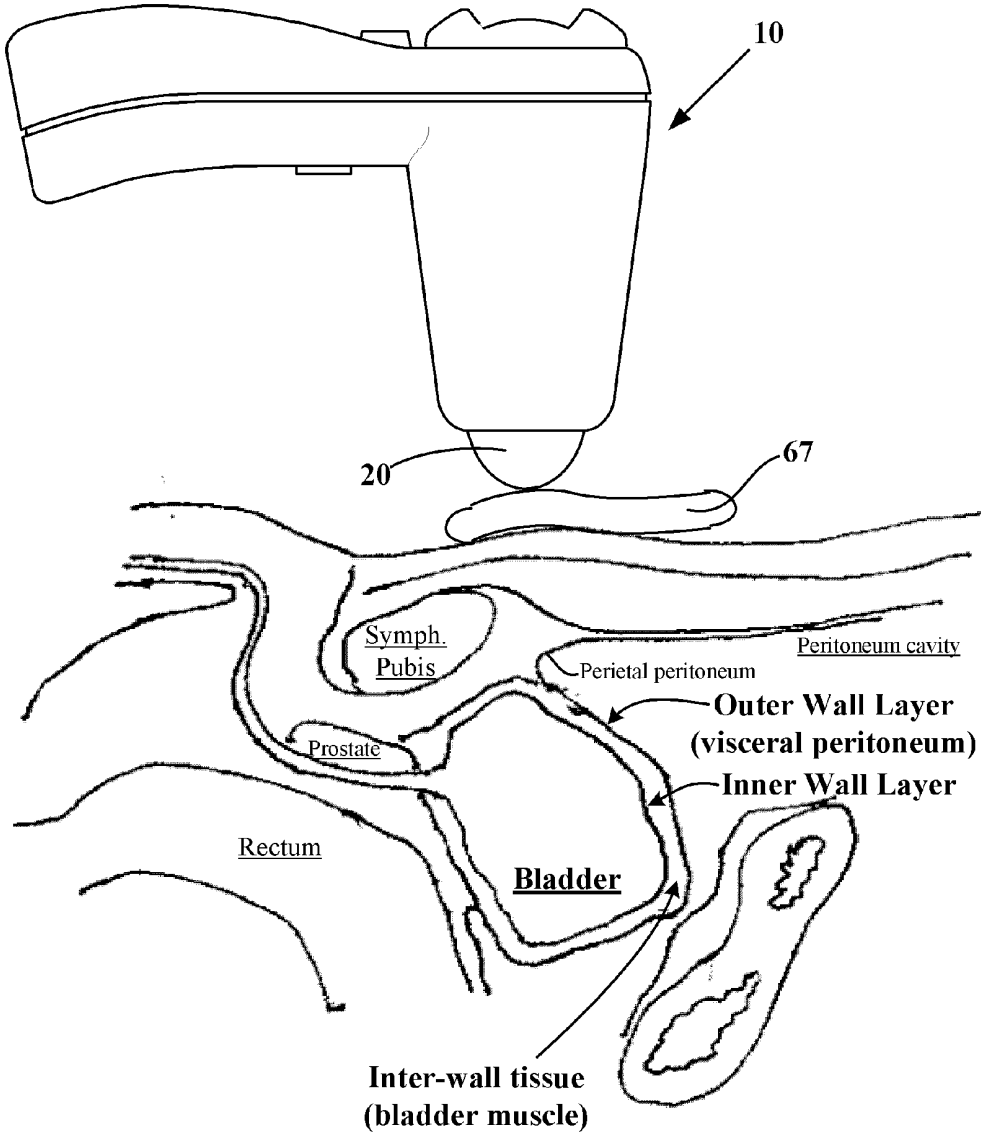
10
20
67
Symph.
Pubis
Peritoneum cavity
Perietal peritoneum
Outer Wall Layer
(visceral peritoneum)
Inner Wall Layer
Prostate
Rectum
Bladder
Inter-wall tissue
(bladder muscle)

Fig. 7

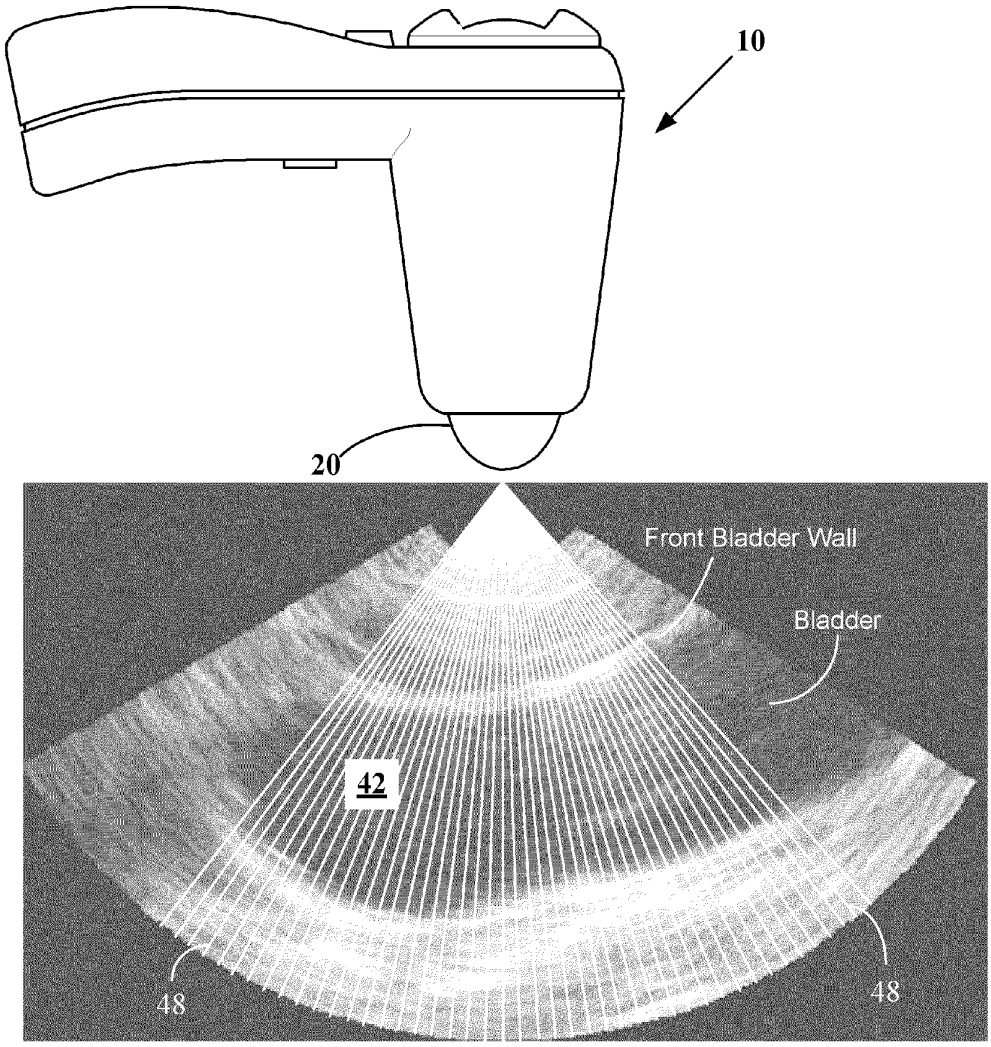

Fig. 8

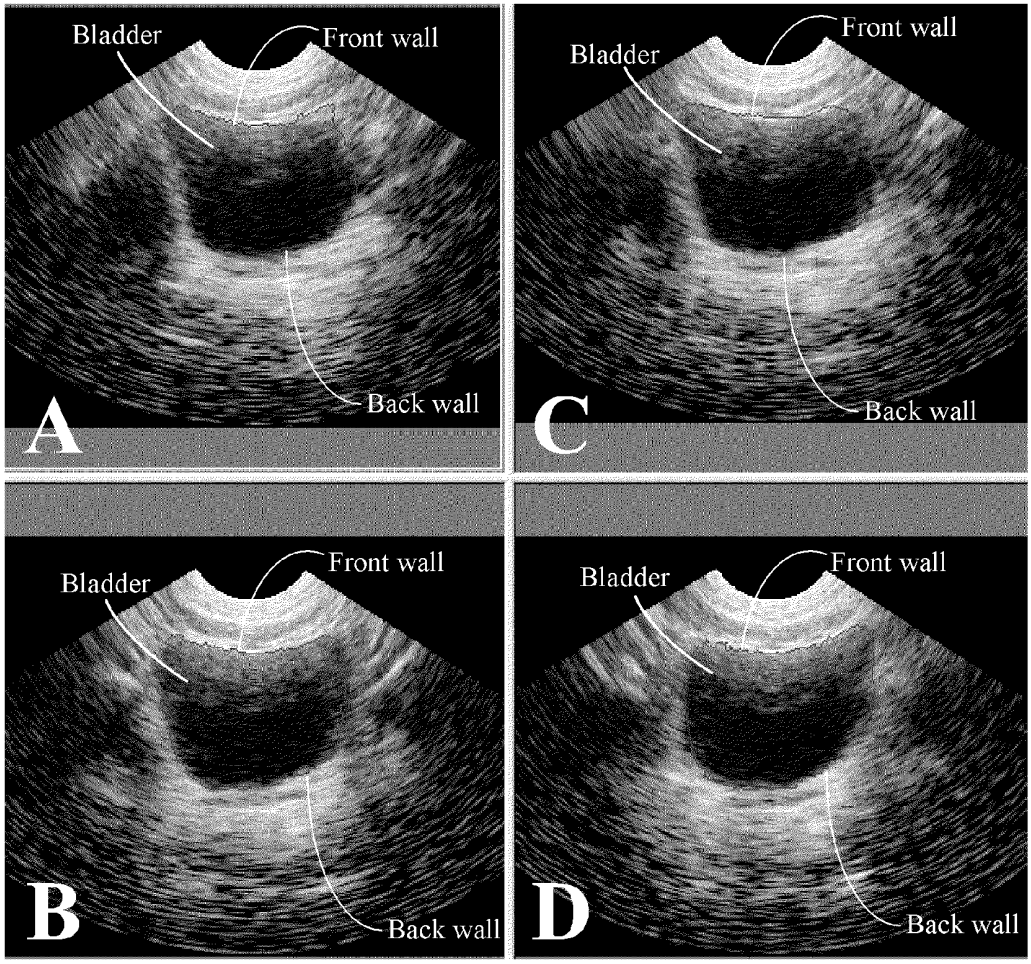
Bladder
Front wall
Back wall
A
Bladder
Front wall
Back wall
C
Bladder
Front wall
Back wall
B
Bladder
Front wall
Back wall
D

Fig. 9A-D

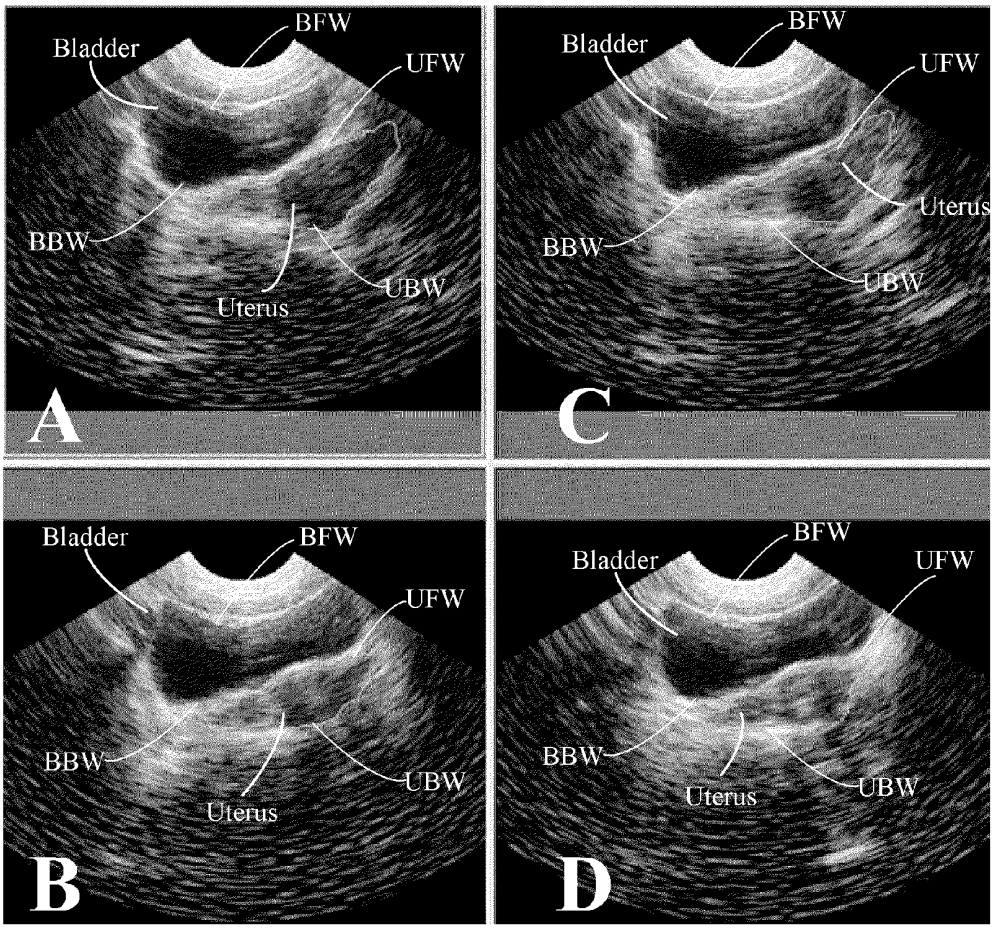
Bladder
BFW
UFW
BBW
Uterus
UBW
A
Bladder
BFW
UFW
Uterus
BBW
UBW
C
Bladder
BFW
UFW
BBW
Uterus
UBW
B
Bladder
BFW
UFW
BBW
Uterus
UBW
D

Fig. 10 A-D

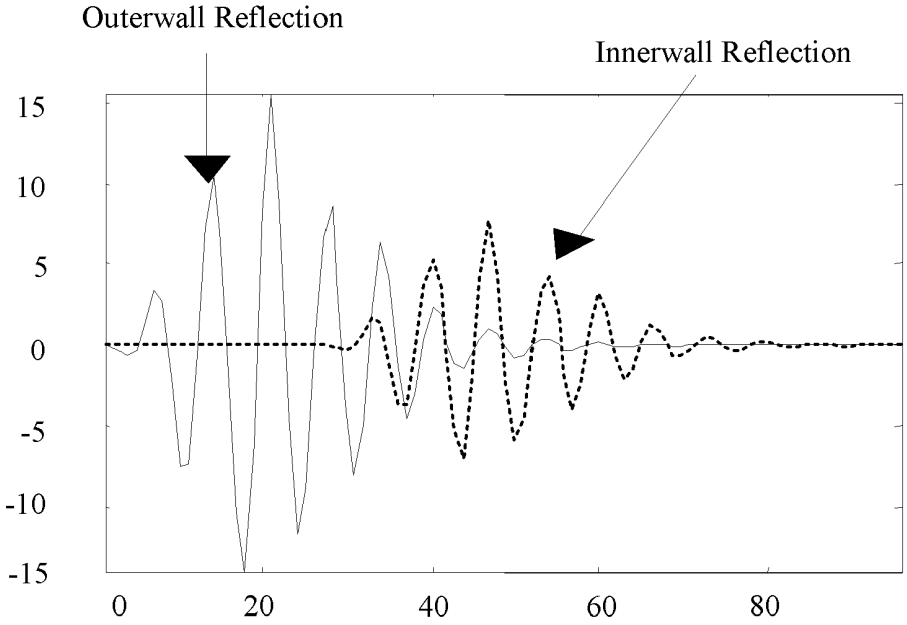
Outerwall Reflection
Innerwall Reflection
15
10
5
0
-5
-10
-15
0
20
40
60
80

Fig. 11

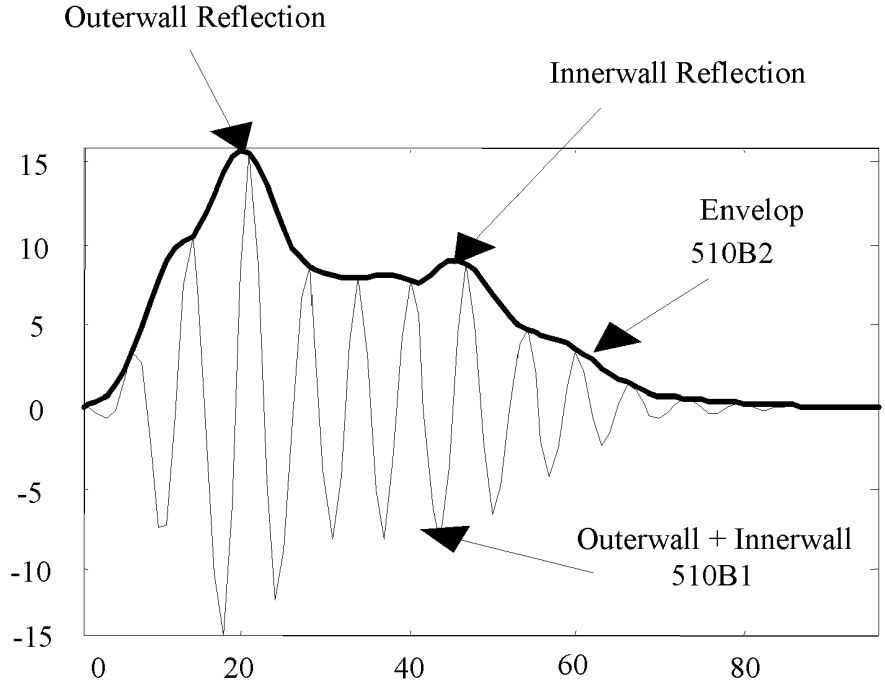
Outerwall Reflection
Innerwall Reflection
Envelop
510B2
Outerwall + Innerwall
510B1
15
10
5
0
-5
-10
-15
0
20
40
60
80

Fig. 12

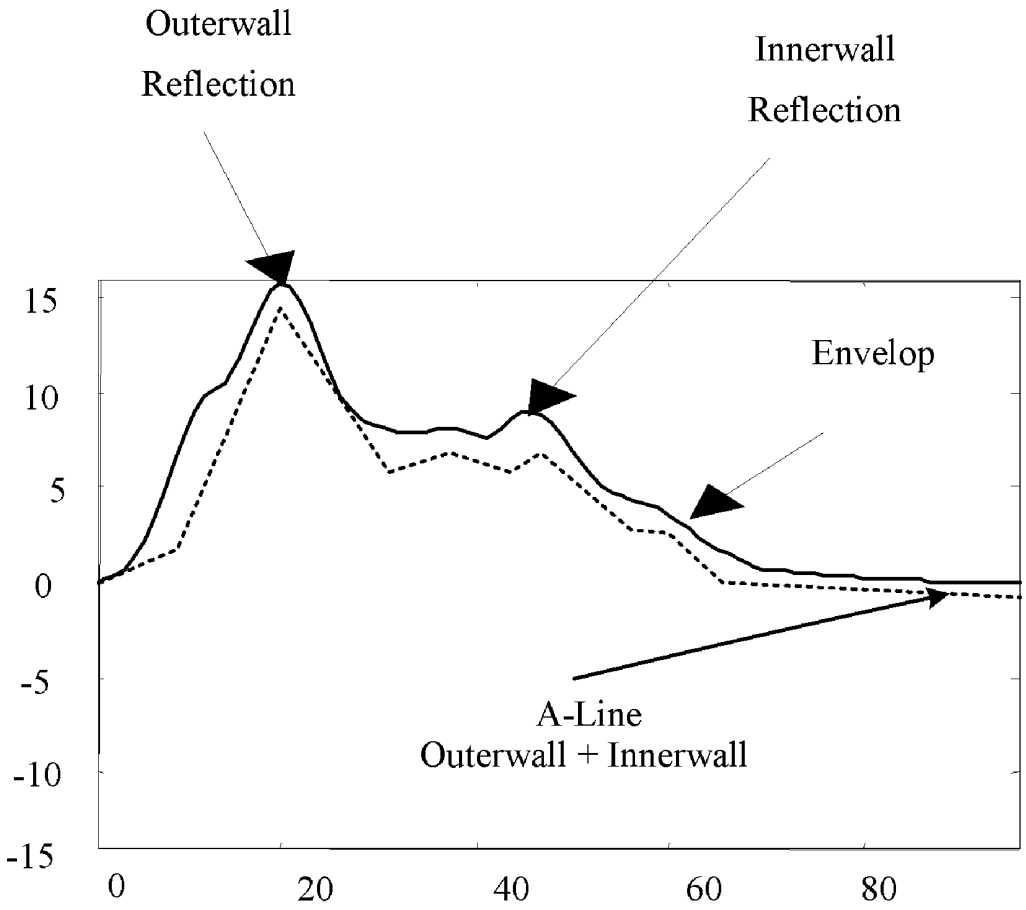
Outerwall
Reflection
Innerwall
Reflection
Envelop
A-Line
Outerwall + Innerwall
15
10
5
0
-5
-10
-15
0
20
40
60
80

Fig. 13

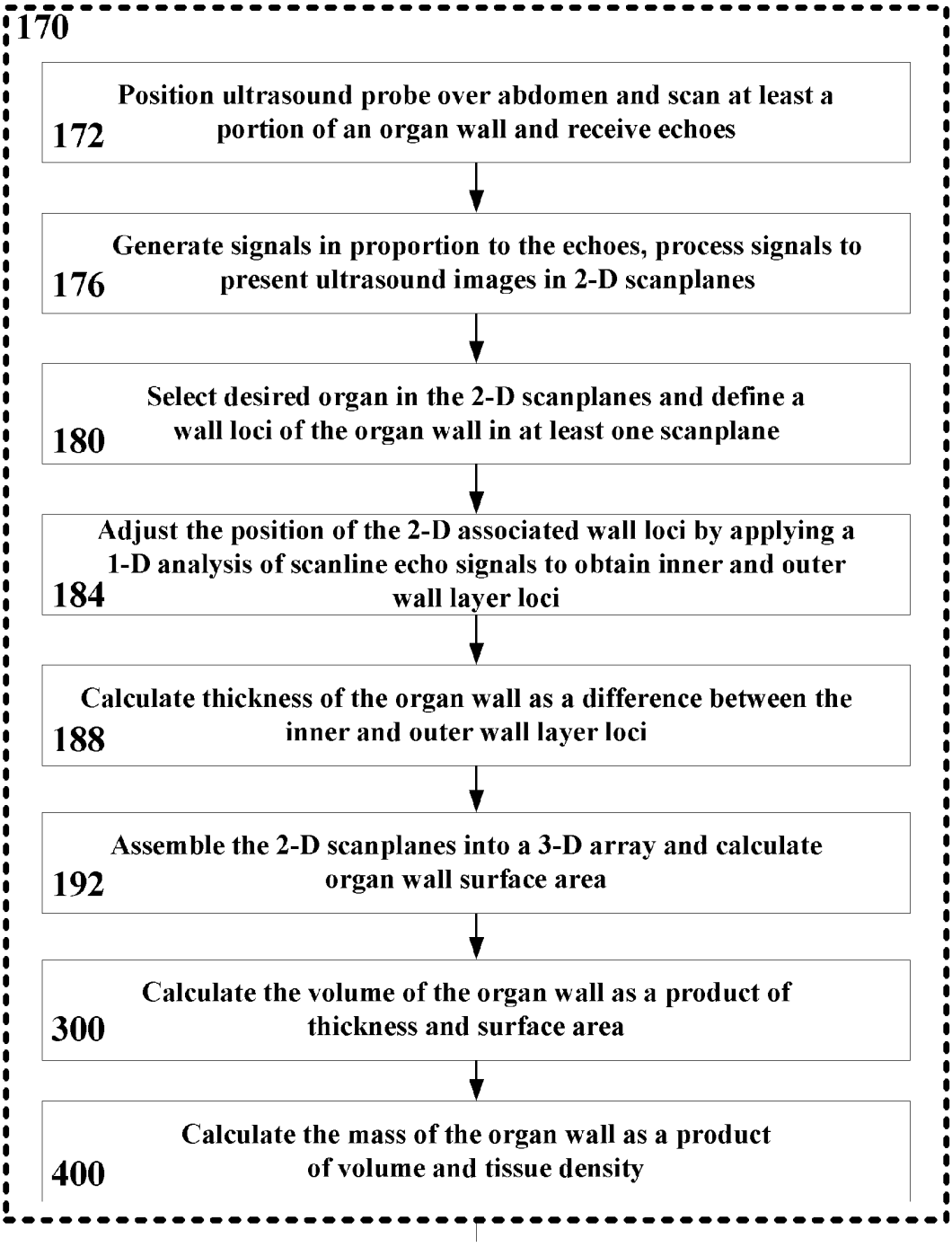
170
Position ultrasound probe over abdomen and scan at least a portion of an organ wall and receive echoes
172
Generate signals in proportion to the echoes, process signals to present ultrasound images in 2-D scanplanes
176
Select desired organ in the 2-D scanplanes and define a wall loci of the organ wall in at least one scanplane
180
Adjust the position of the 2-D associated wall loci by applying a 1-D analysis of scanline echo signals to obtain inner and outer wall layer loci
184
Calculate thickness of the organ wall as a difference between the inner and outer wall layer loci
188
Assemble the 2-D scanplanes into a 3-D array and calculate organ wall surface area
192
Calculate the volume of the organ wall as a product of thickness and surface area
300
Calculate the mass of the organ wall as a product of volume and tissue density
400

Fig. 14

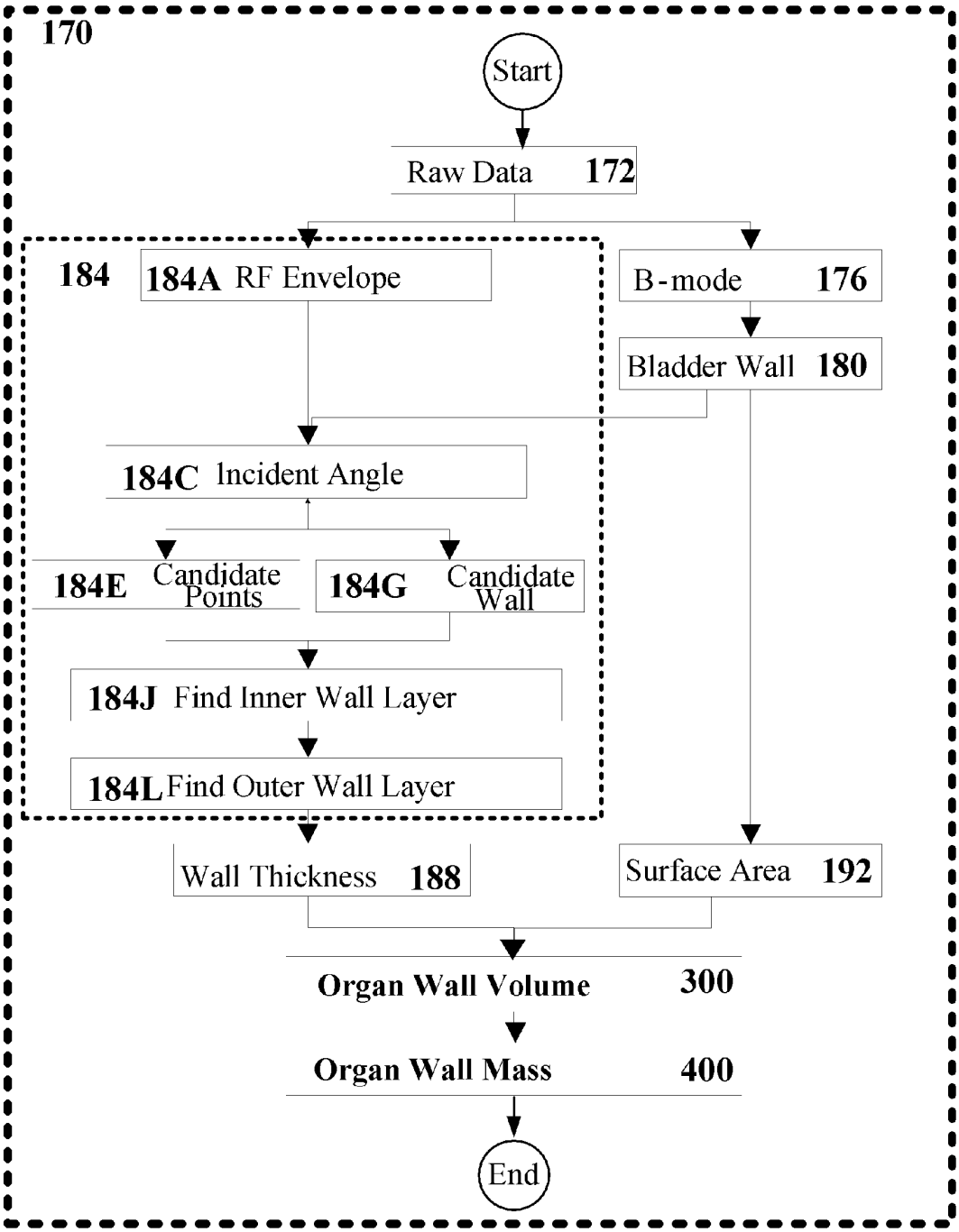
170
Start
Raw Data 172
184
184A RF Envelope
B-mode 176
Bladder Wall 180
184C Incident Angle
184E Candidate Points
184G Candidate Wall
184J Find Inner Wall Layer
184L Find Outer Wall Layer
Wall Thickness 188
Surface Area 192
Organ Wall Volume 300
Organ Wall Mass 400
End

Fig. 15

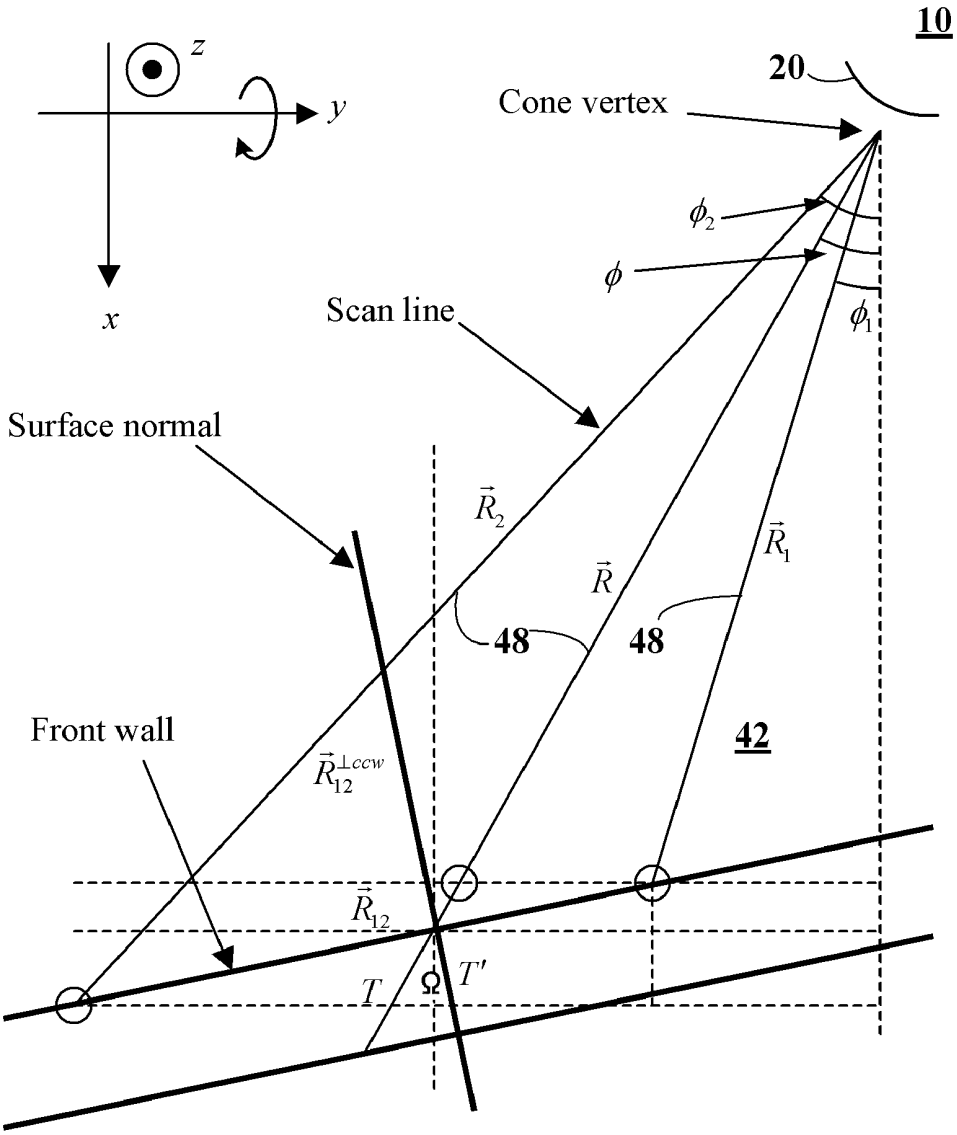
10
20
Cone vertex
z
y
x
ϕ_2
ϕ
ϕ_1
Scan line
Surface normal
$\vec{R}_2$
$\vec{R}$
$\vec{R}_1$
48
48
42
Front wall
$\vec{R}_{12}^{\perp ccw}$
$\vec{R}_{12}$
T
Ω
T'

Fig. 16

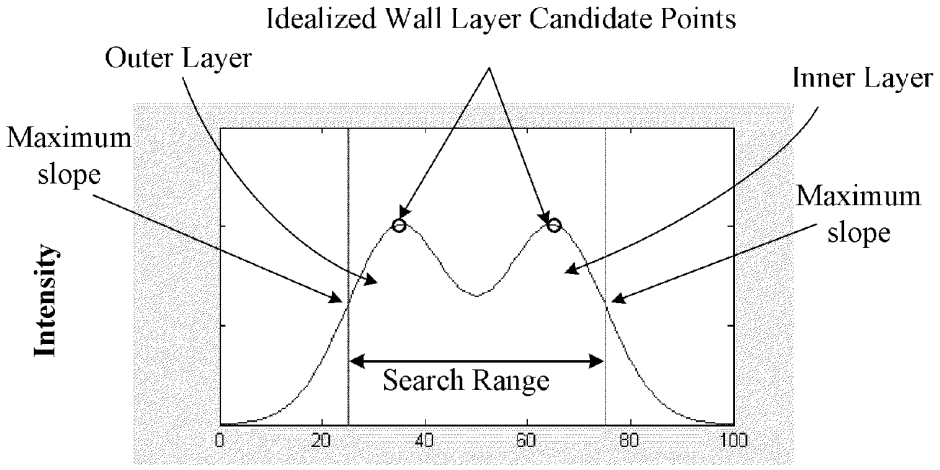
Idealized Wall Layer Candidate Points
Outer Layer
Inner Layer
Maximum slope
Maximum slope
Intensity
Search Range
0
20
40
60
80
100

Fig. 17

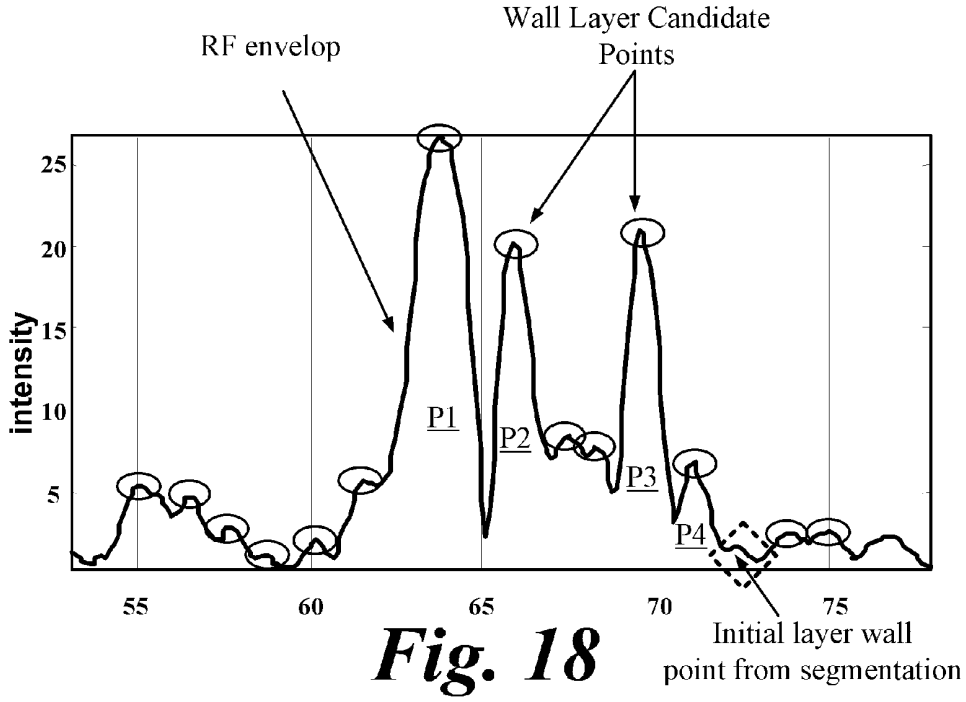
RF envelop
Wall Layer Candidate Points
intensity
25
20
15
10
5
P1
P2
P3
P4
55
60
65
70
75
Initial layer wall point from segmentation

Fig. 18

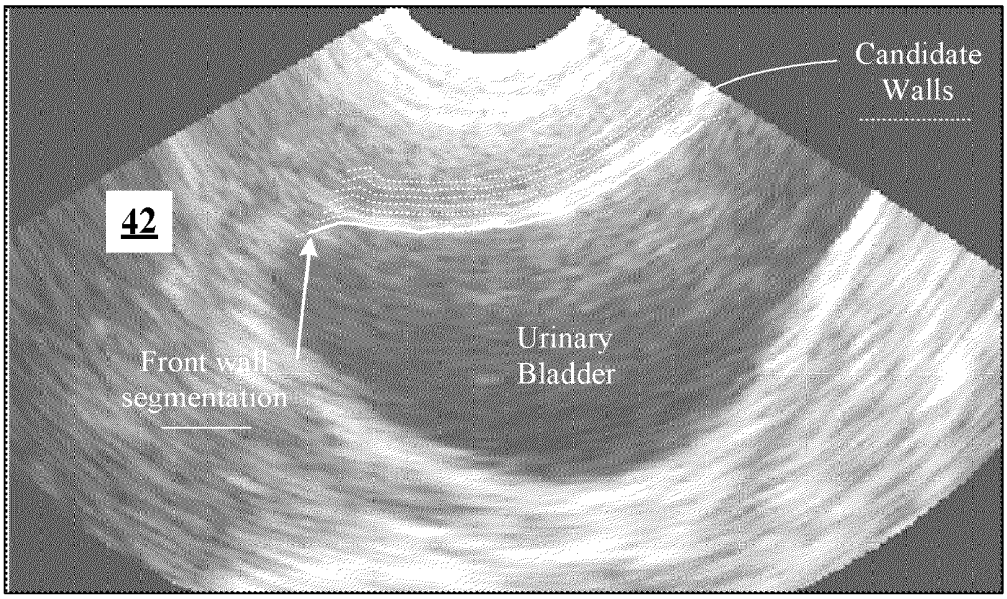
Candidate
Walls
42
Front wall
segmentation
Urinary
Bladder

Fig. 19

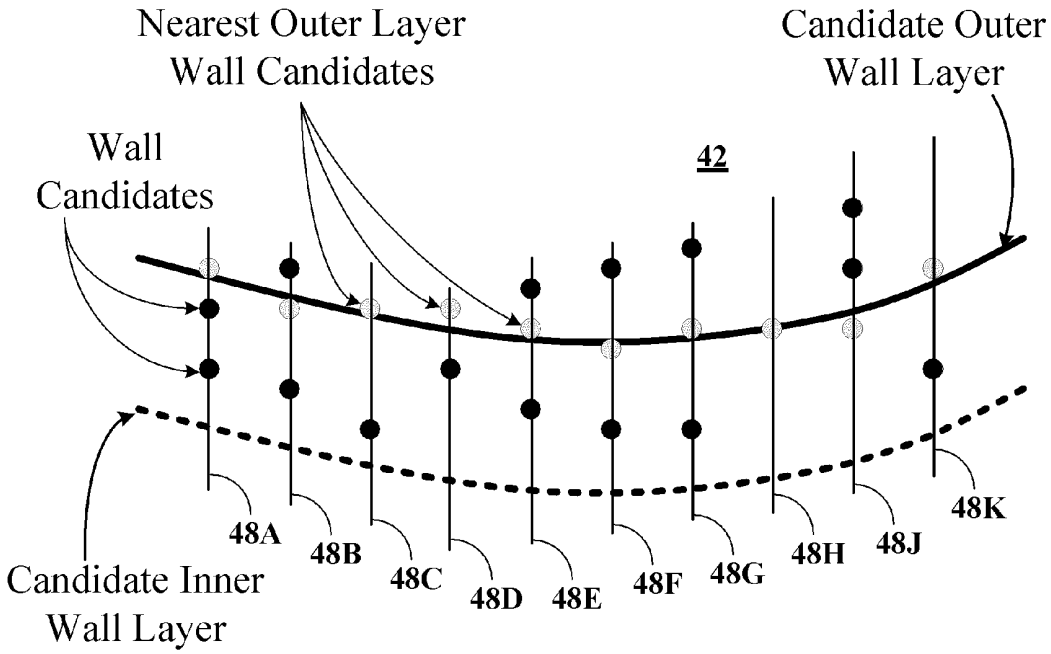
Nearest Outer Layer
Wall Candidates
Candidate Outer
Wall Layer
Wall
Candidates
42
48A
48B
48C
48D
48E
48F
48G
48H
48J
48K
Candidate Inner
Wall Layer

Fig. 20

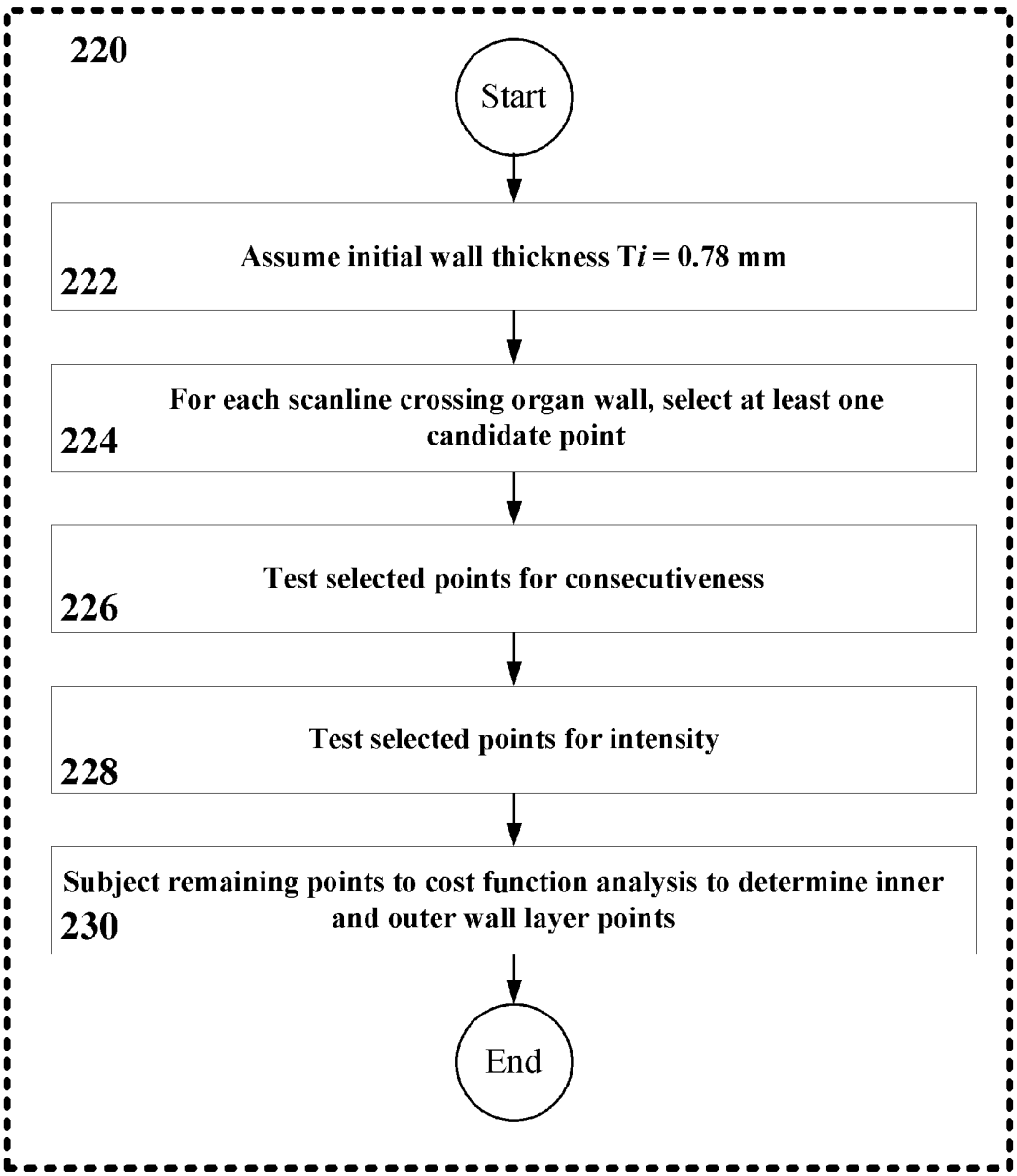
220
Start
Assume initial wall thickness Ti = 0.78 mm
222
For each scanline crossing organ wall, select at least one candidate point
224
Test selected points for consecutiveness
226
Test selected points for intensity
228
Subject remaining points to cost function analysis to determine inner and outer wall layer points
230
End

Fig. 21A

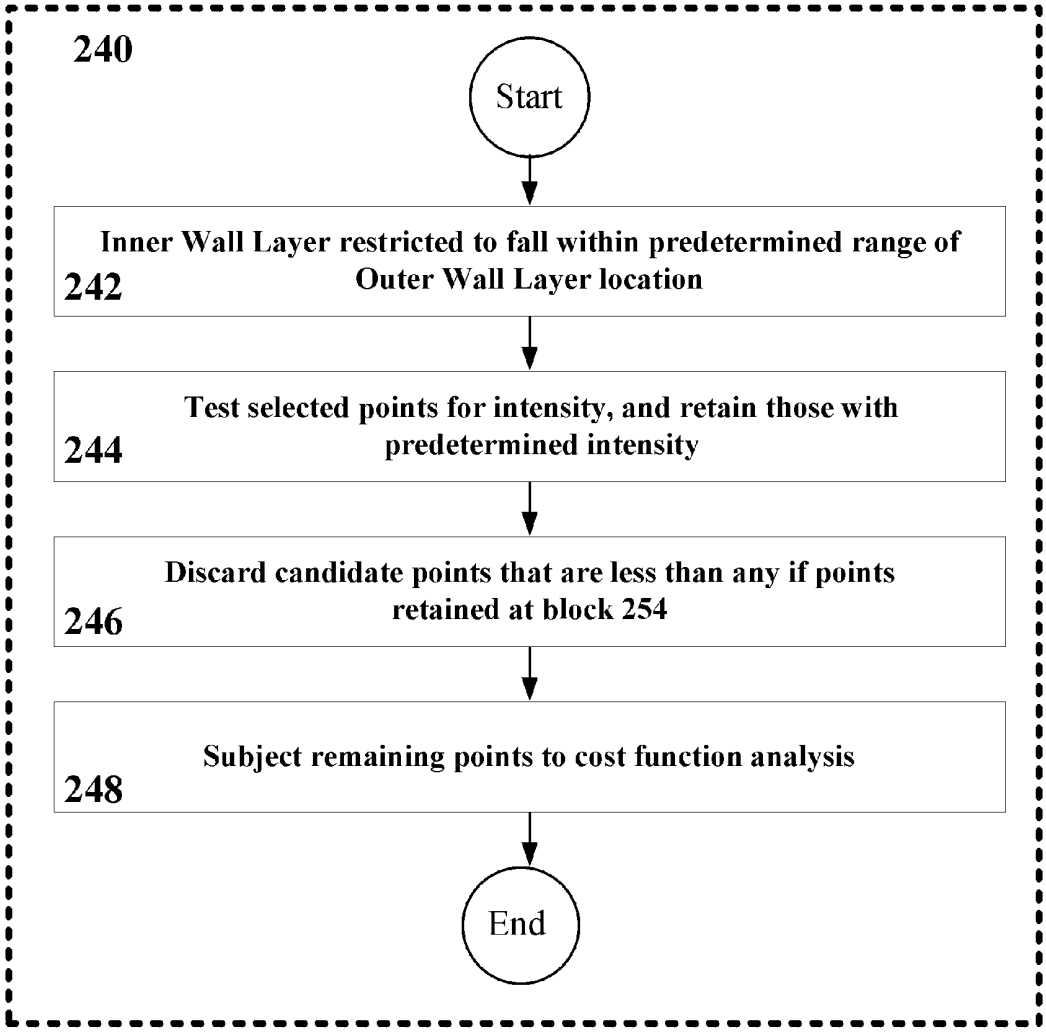
240
Start
Inner Wall Layer restricted to fall within predetermined range of Outer Wall Layer location
242
Test selected points for intensity, and retain those with predetermined intensity
244
Discard candidate points that are less than any if points retained at block 254
246
Subject remaining points to cost function analysis
248
End

Fig. 21B

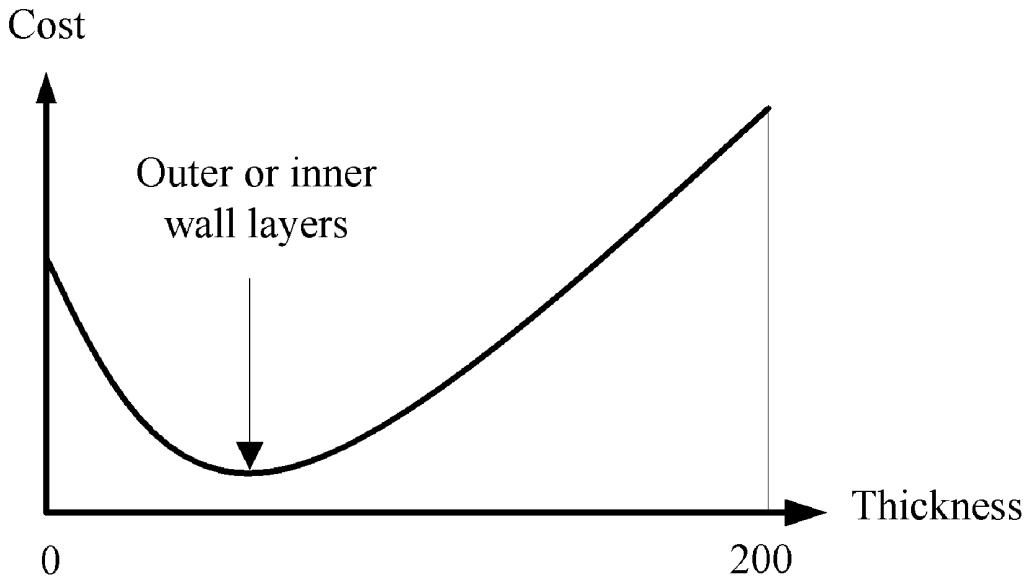

Fig. 22

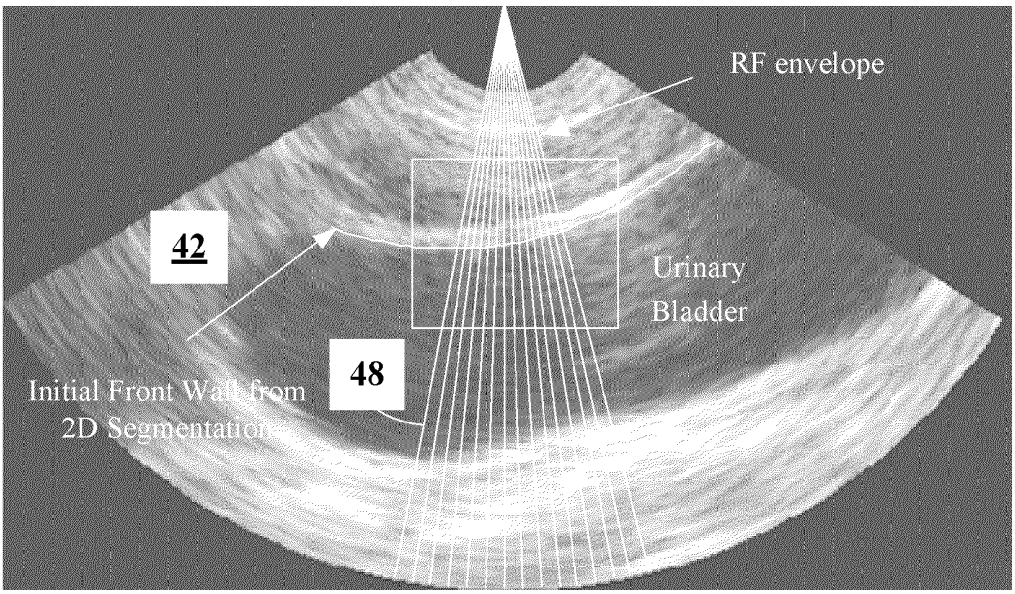
RF envelope
42
Urinary
Bladder
48
Initial Front Wall from
2D Segmentation

Fig. 23

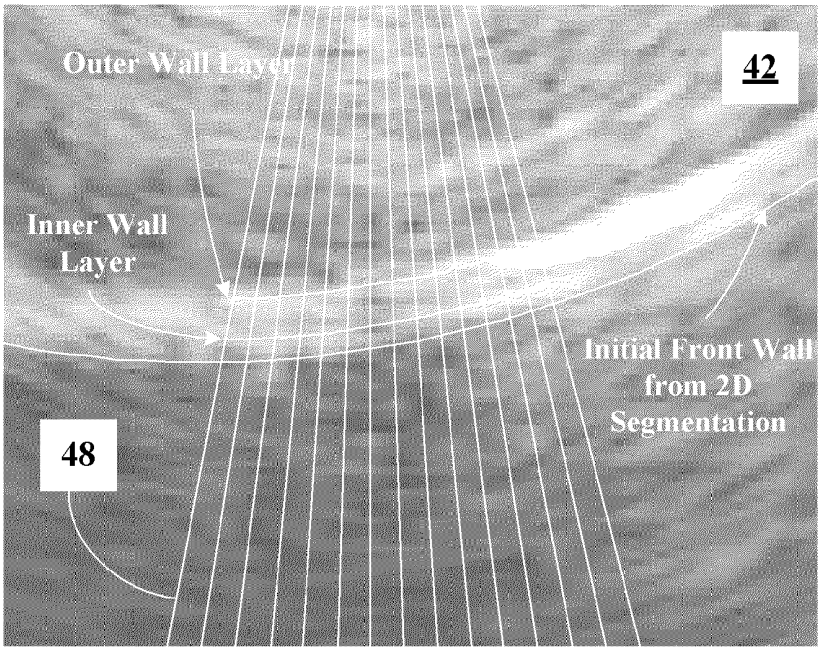
Outer Wall Layer
42
Inner Wall
Layer
Initial Front Wall
from 2D
Segmentation
48

Fig. 24

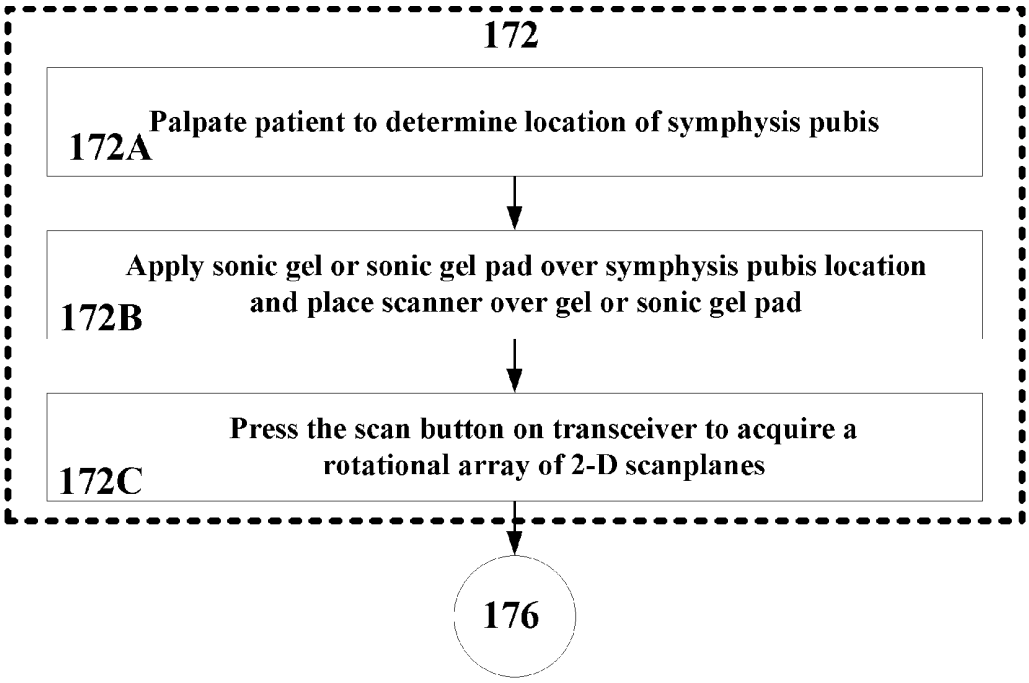
172
172A
Palpate patient to determine location of symphysis pubis
172B
Apply sonic gel or sonic gel pad over symphysis pubis location and place scanner over gel or sonic gel pad
172C
Press the scan button on transceiver to acquire a rotational array of 2-D scanplanes
176

Fig. 25

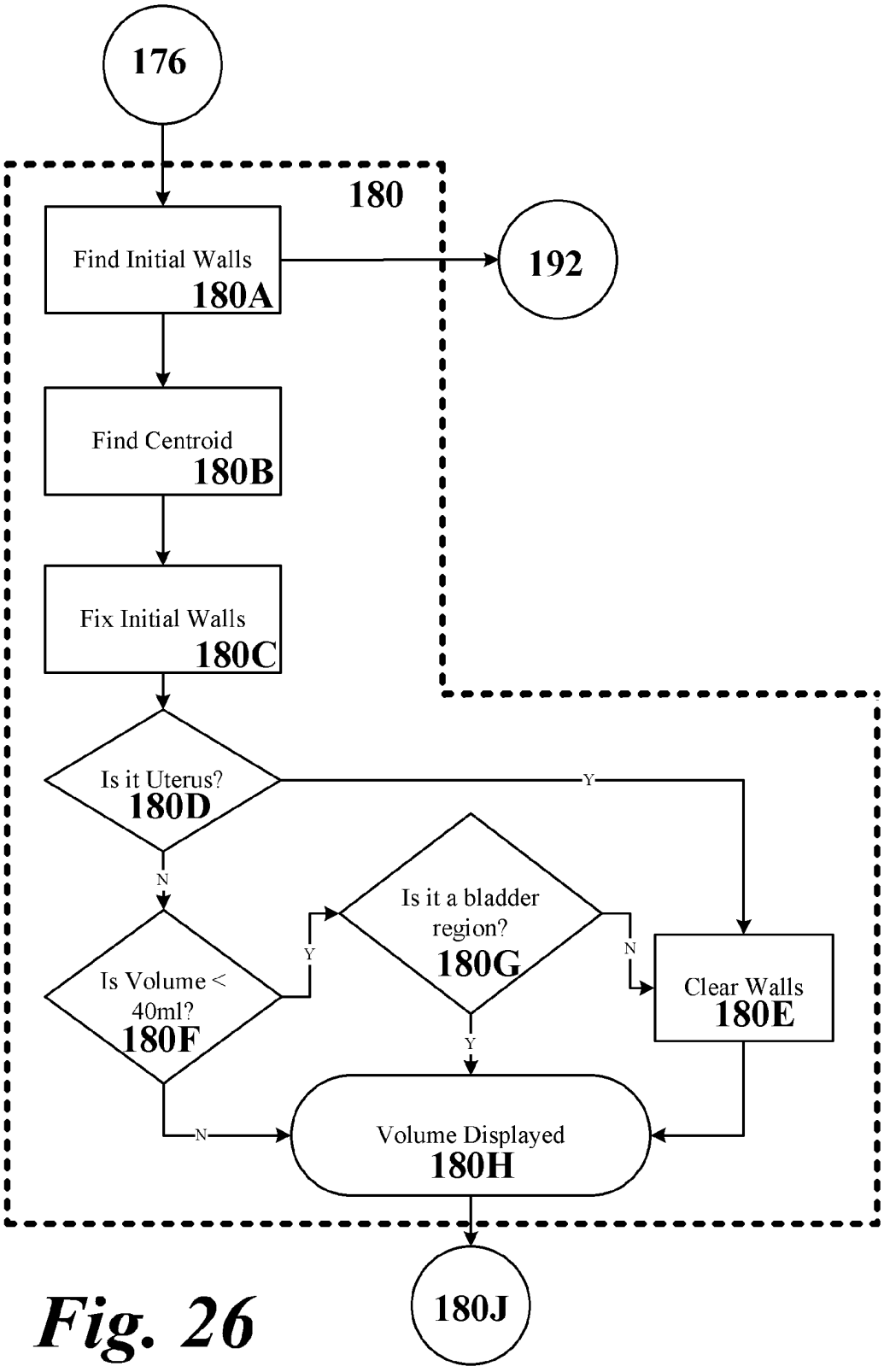
176
180
Find Initial Walls
180A
192
Find Centroid
180B
Fix Initial Walls
180C
Is it Uterus?
180D
Y
N
Is it a bladder region?
180G
Y
N
Is Volume < 40ml?
180F
Y
N
Clear Walls
180E
Volume Displayed
180H
180J

Fig. 26

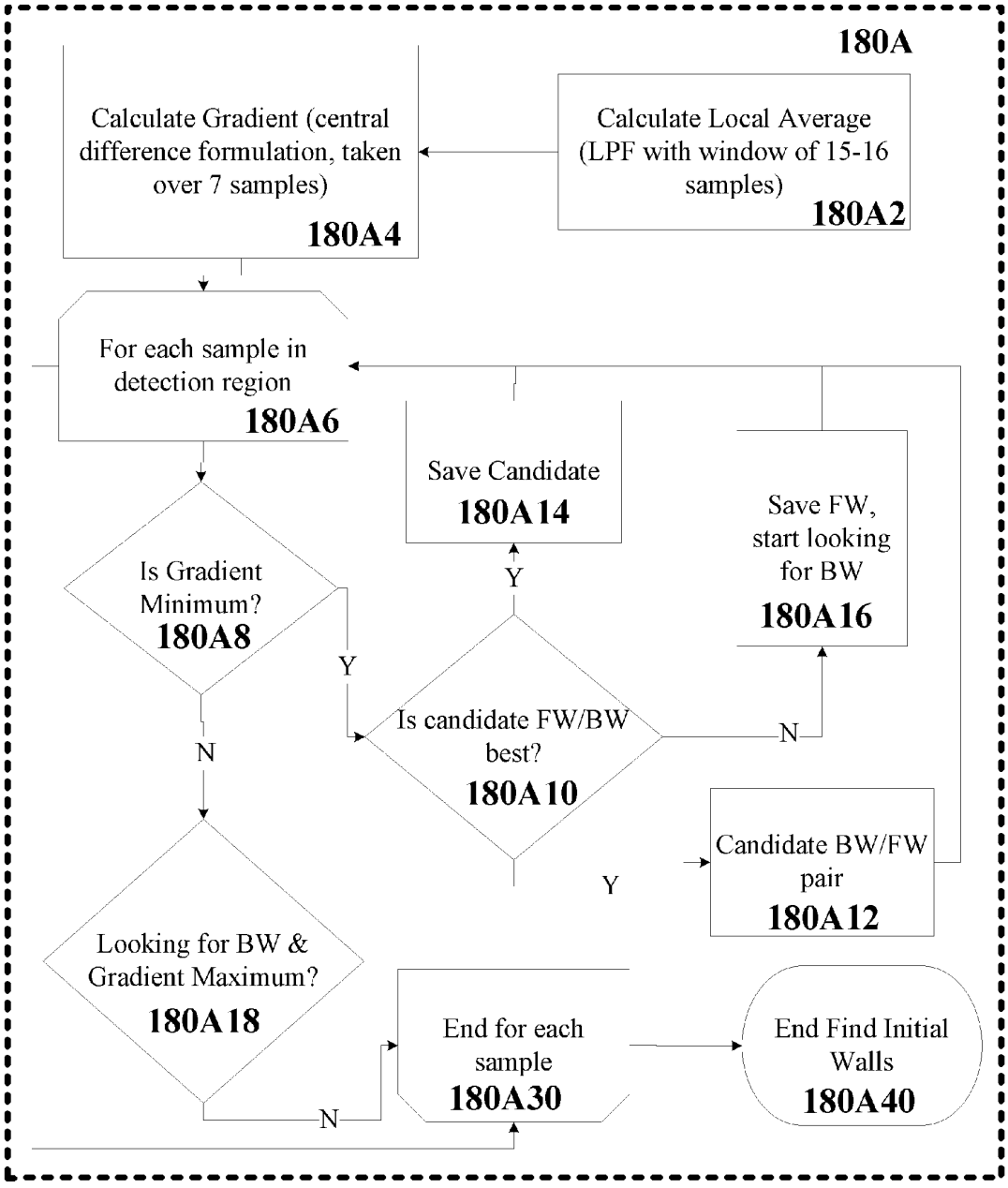
180A
Calculate Gradient (central difference formulation, taken over 7 samples)
180A4
Calculate Local Average (LPF with window of 15-16 samples)
180A2
For each sample in detection region
180A6
Save Candidate
180A14
Save FW, start looking for BW
180A16
Is Gradient Minimum?
180A8
Y
N
Is candidate FW/BW best?
180A10
Y
N
Candidate BW/FW pair
180A12
Looking for BW & Gradient Maximum?
180A18
N
End for each sample
180A30
End Find Initial Walls
180A40

Fig. 27

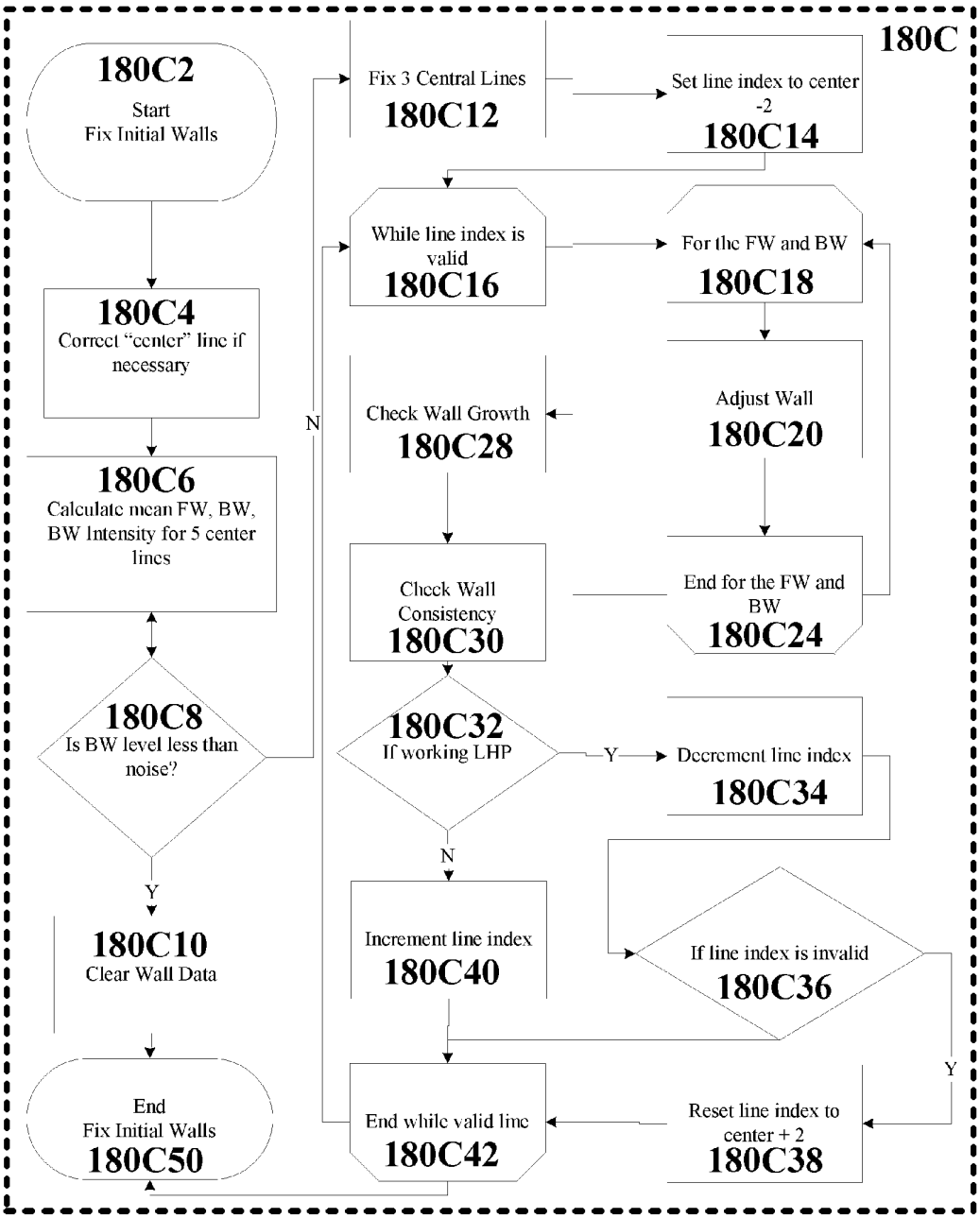
180C
180C2
Start
Fix Initial Walls
Fix 3 Central Lines
180C12
Set line index to center -2
180C14
While line index is valid
180C16
For the FW and BW
180C18
180C4
Correct "center" line if necessary
Adjust Wall
180C20
Check Wall Growth
180C28
N
180C6
Calculate mean FW, BW, BW Intensity for 5 center lines
End for the FW and BW
180C24
Check Wall Consistency
180C30
180C8
Is BW level less than noise?
180C32
If working LHP
Y
Decrement line index
180C34
N
Y
180C10
Clear Wall Data
Increment line index
180C40
If line index is invalid
180C36
Y
End
Fix Initial Walls
180C50
End while valid line
180C42
Reset line index to center + 2
180C38

Fig. 28

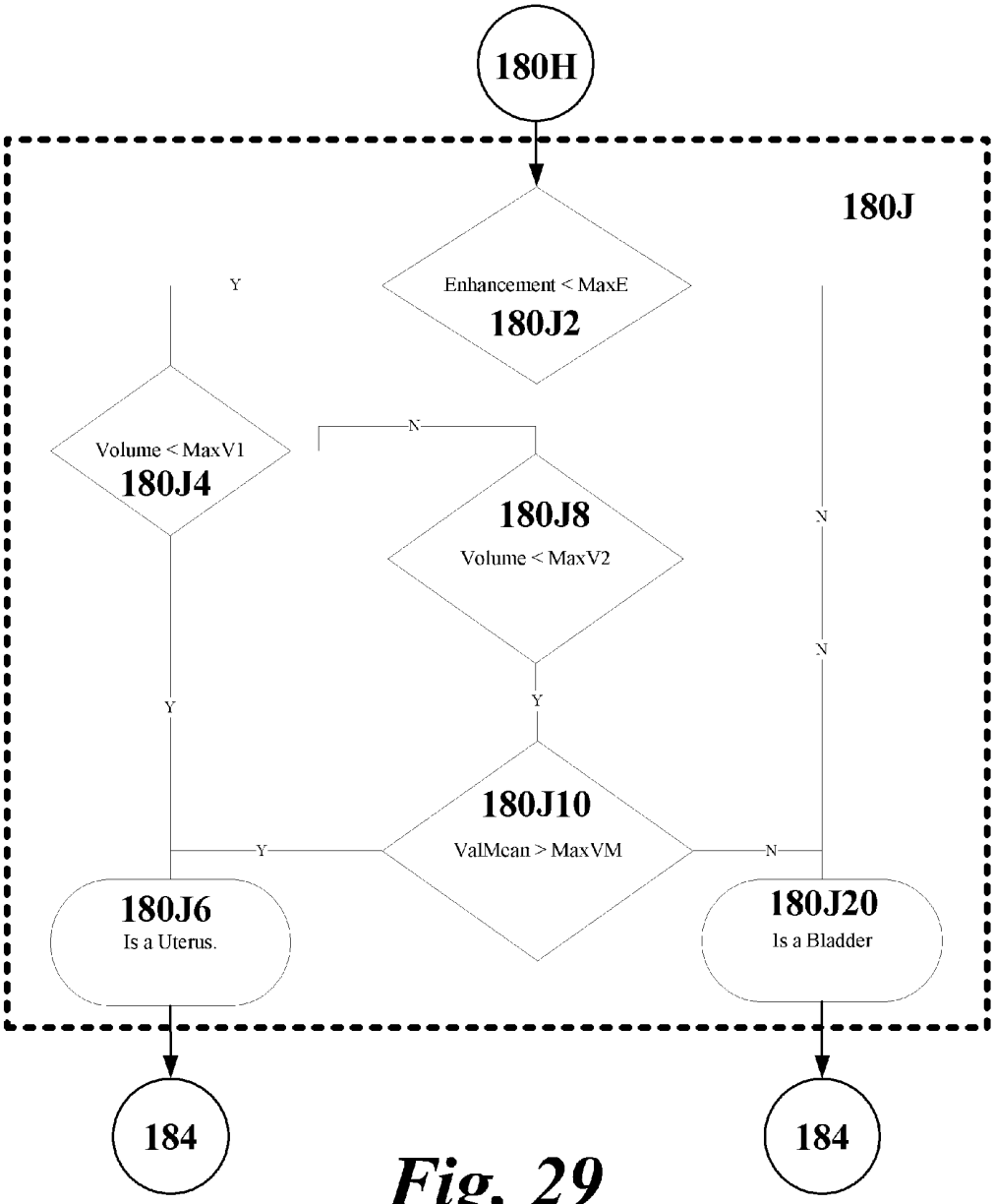
180H
180J
Enhancement < MaxE
180J2
Y
N
Volume < MaxV1
180J4
180J8
Volume < MaxV2
N
N
Y
Y
180J10
ValMean > MaxVM
Y
N
180J6
Is a Uterus.
180J20
Is a Bladder
184
184

Fig. 29

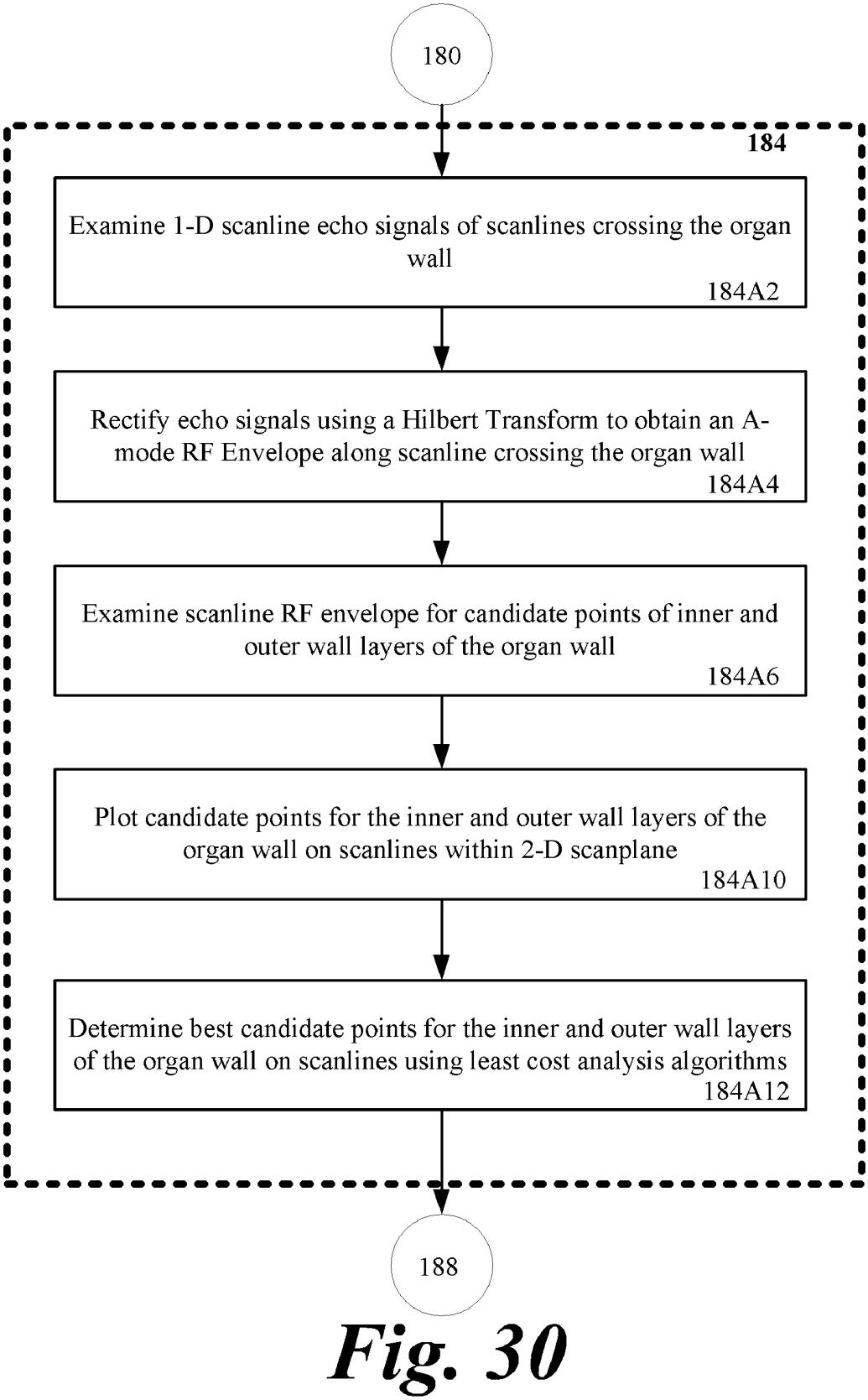
180
184
Examine 1-D scanline echo signals of scanlines crossing the organ wall
184A2
Rectify echo signals using a Hilbert Transform to obtain an A-mode RF Envelope along scanline crossing the organ wall
184A4
Examine scanline RF envelope for candidate points of inner and outer wall layers of the organ wall
184A6
Plot candidate points for the inner and outer wall layers of the organ wall on scanlines within 2-D scanplane
184A10
Determine best candidate points for the inner and outer wall layers of the organ wall on scanlines using least cost analysis algorithms
184A12
188

Fig. 30

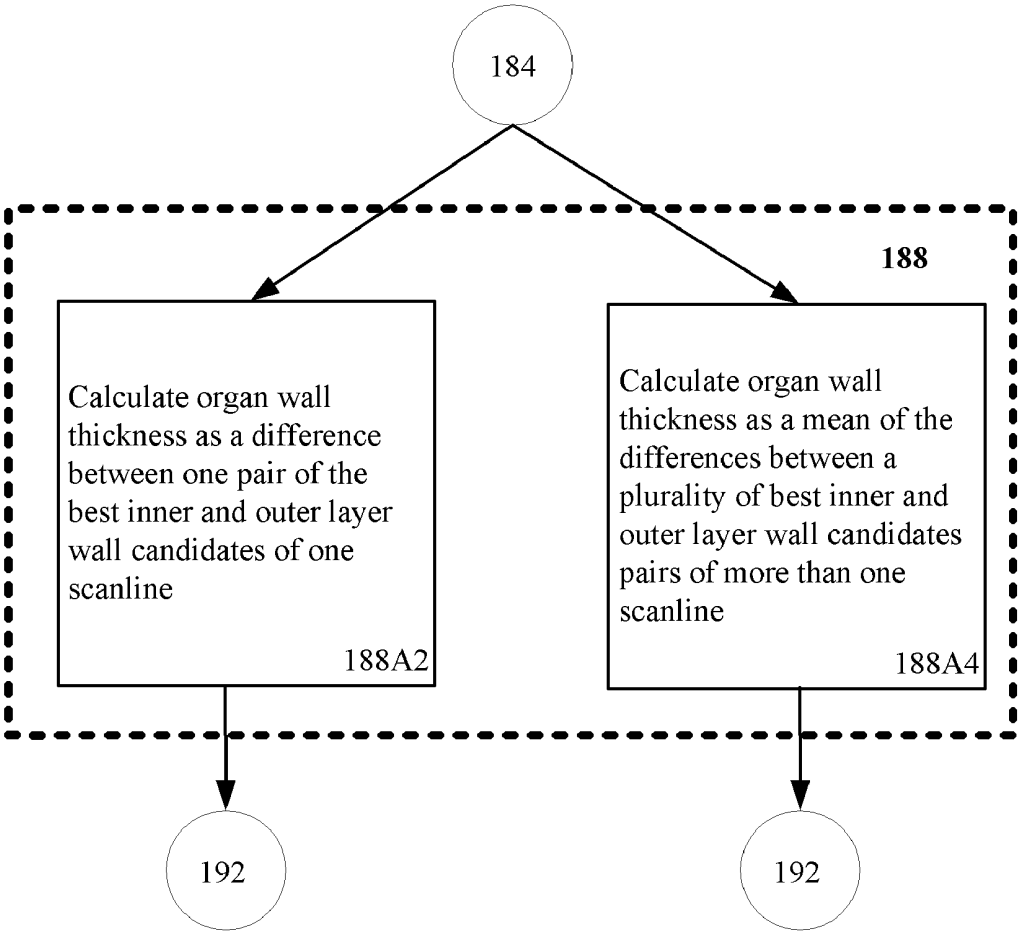
184
188
Calculate organ wall thickness as a difference between one pair of the best inner and outer layer wall candidates of one scanline
188A2
Calculate organ wall thickness as a mean of the differences between a plurality of best inner and outer layer wall candidates pairs of more than one scanline
188A4
192
192

Fig. 31

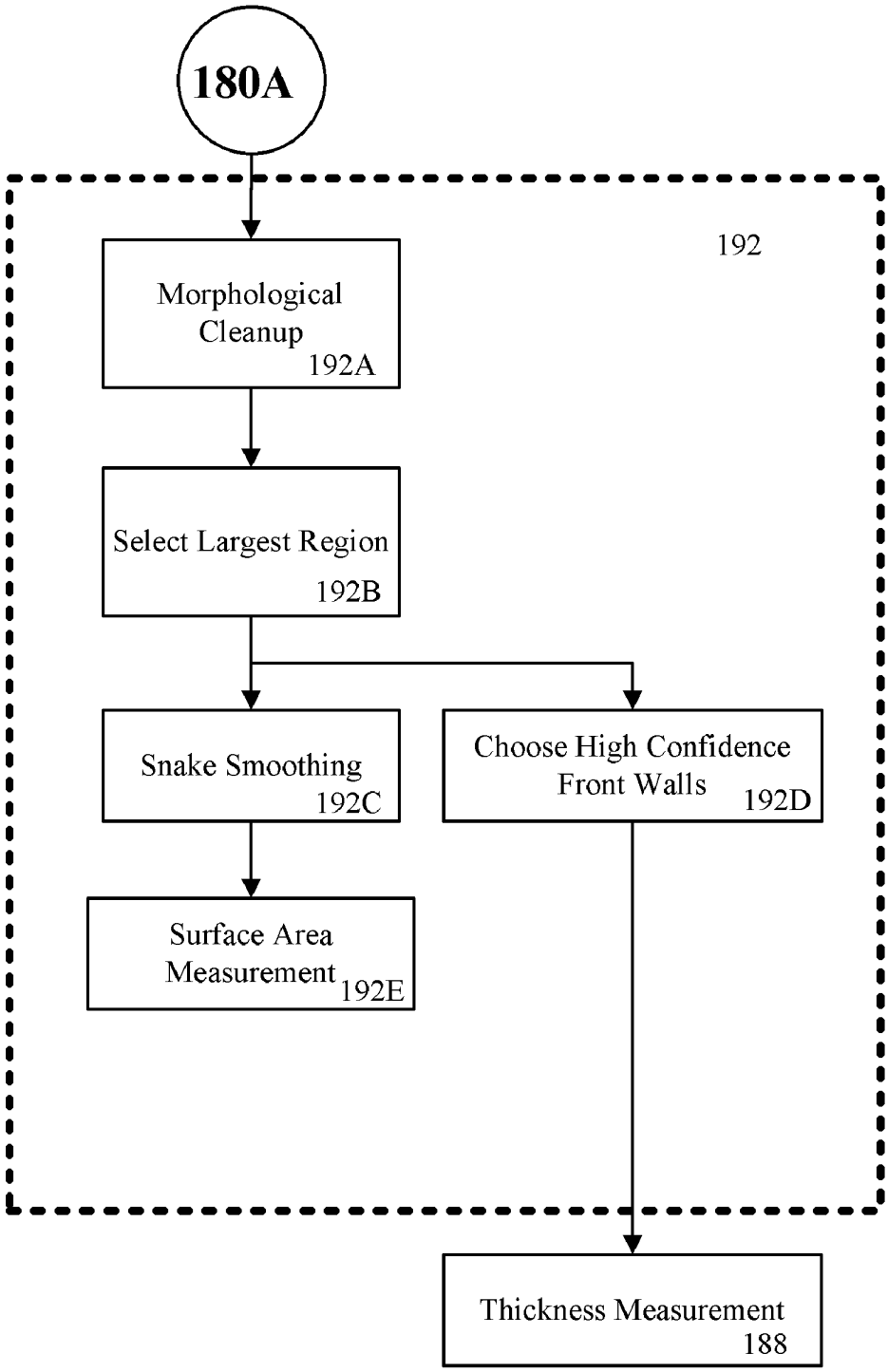
180A
192
Morphological Cleanup 192A
Select Largest Region 192B
Snake Smoothing 192C
Choose High Confidence Front Walls 192D
Surface Area Measurement 192E
Thickness Measurement 188

Fig. 32

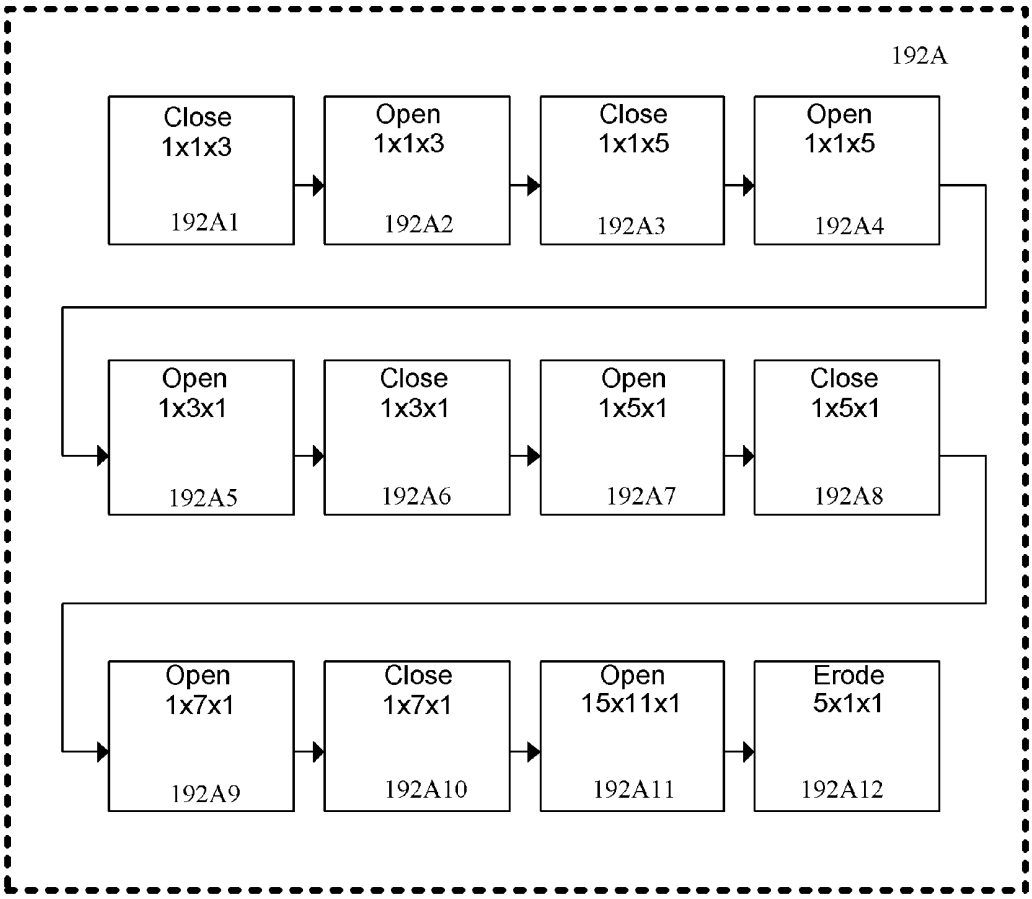
192A
Close 1x1x3
192A1
Open 1x1x3
192A2
Close 1x1x5
192A3
Open 1x1x5
192A4
Open 1x3x1
192A5
Close 1x3x1
192A6
Open 1x5x1
192A7
Close 1x5x1
192A8
Open 1x7x1
192A9
Close 1x7x1
192A10
Open 15x11x1
192A11
Erode 5x1x1
192A12

Fig. 33

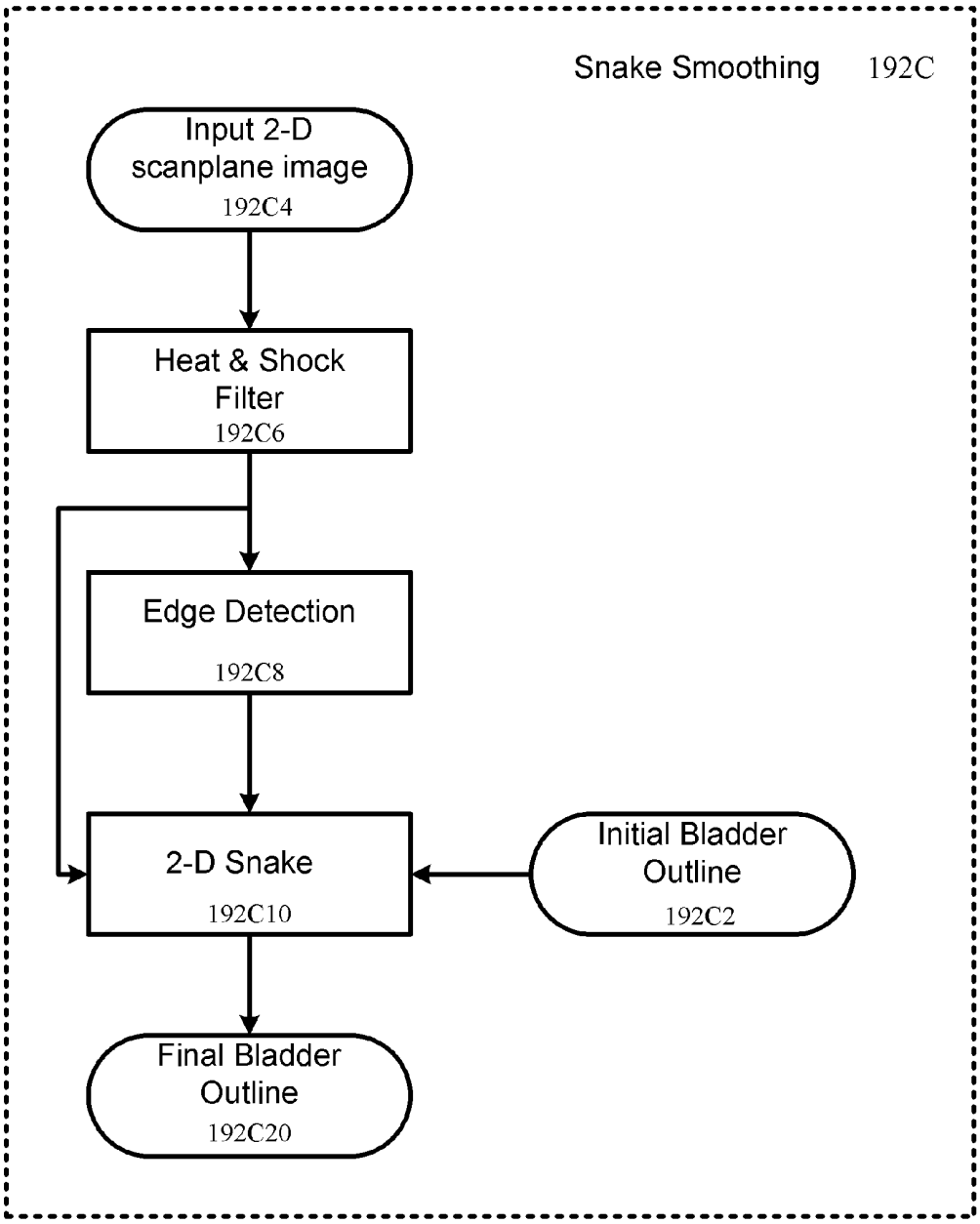
Snake Smoothing 192C
Input 2-D scanplane image 192C4
Heat & Shock Filter 192C6
Edge Detection 192C8
2-D Snake 192C10
Initial Bladder Outline 192C2
Final Bladder Outline 192C20

Fig. 34

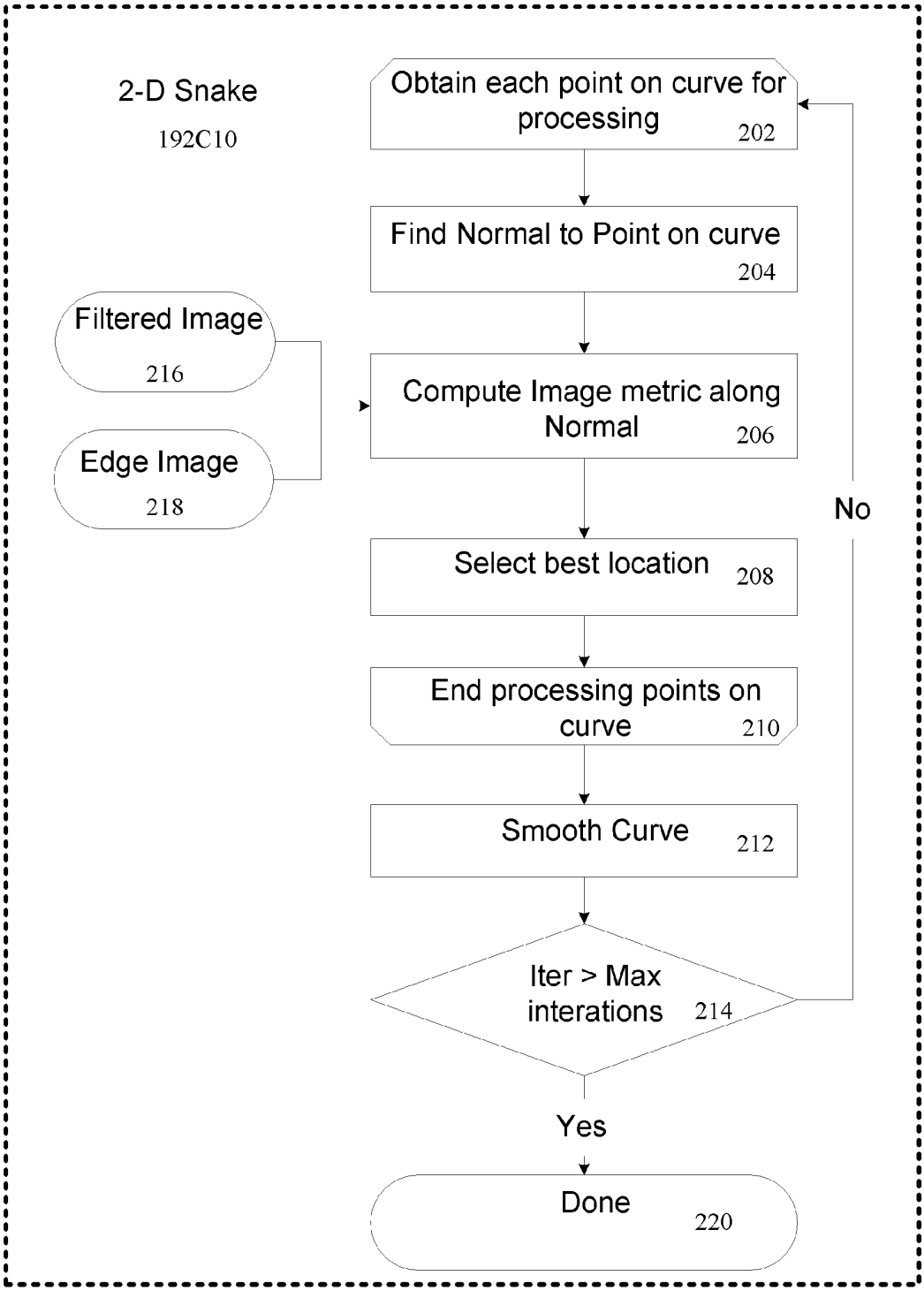
2-D Snake
192C10
Obtain each point on curve for processing
202
Find Normal to Point on curve
204
Filtered Image
216
Edge Image
218
Compute Image metric along Normal
206
No
Select best location
208
End processing points on curve
210
Smooth Curve
212
Iter > Max interations
214
Yes
Done
220

Fig. 35

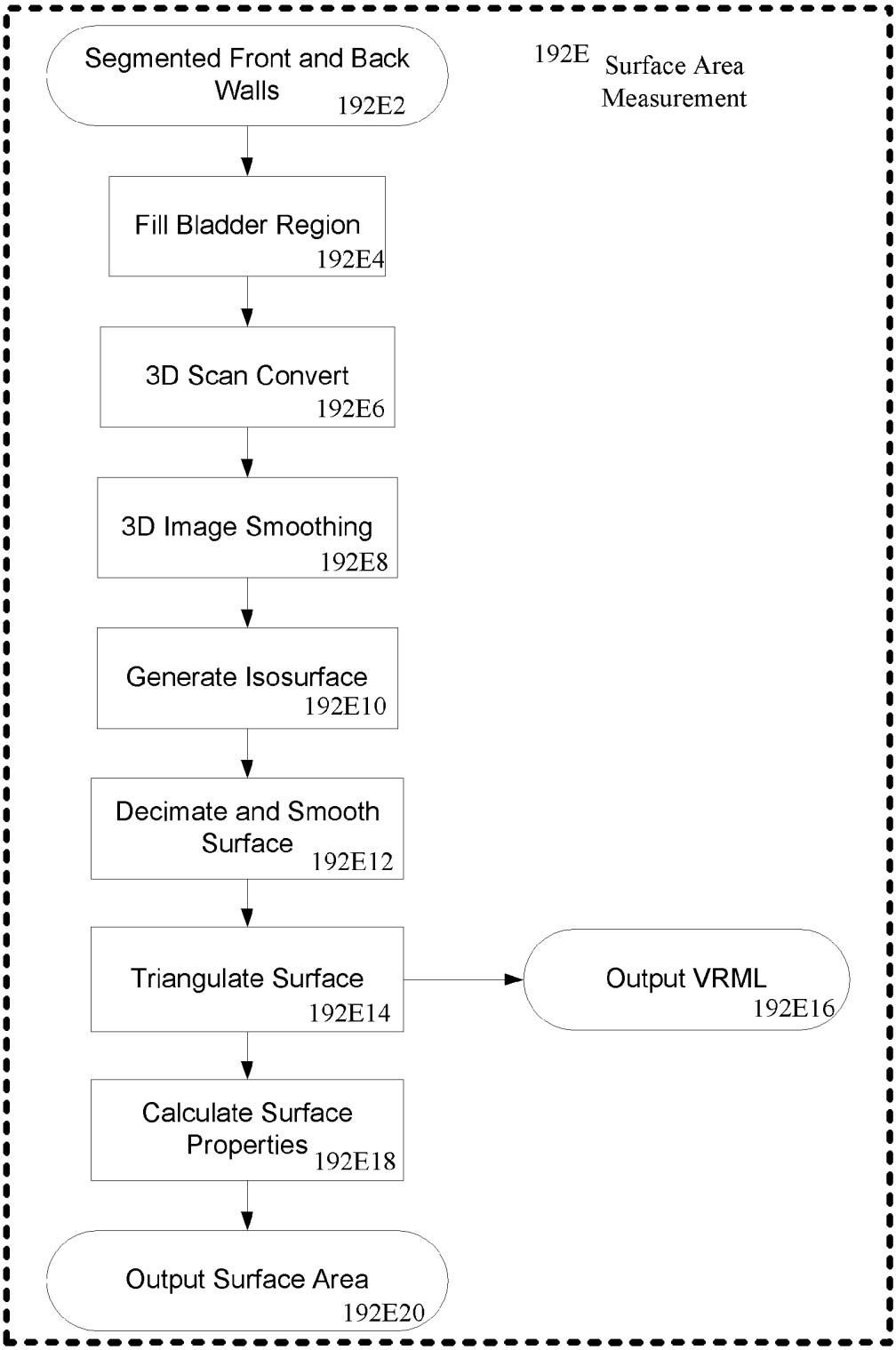
192E Surface Area Measurement
Segmented Front and Back Walls 192E2
Fill Bladder Region 192E4
3D Scan Convert 192E6
3D Image Smoothing 192E8
Generate Isosurface 192E10
Decimate and Smooth Surface 192E12
Triangulate Surface 192E14
Output VRML 192E16
Calculate Surface Properties 192E18
Output Surface Area 192E20

Fig. 36

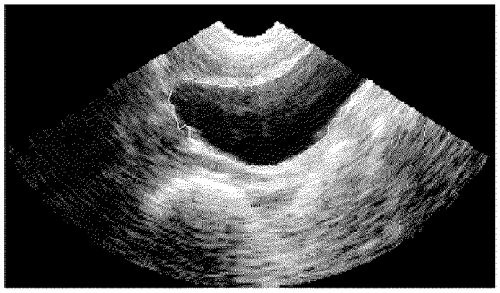

Fig. 37A

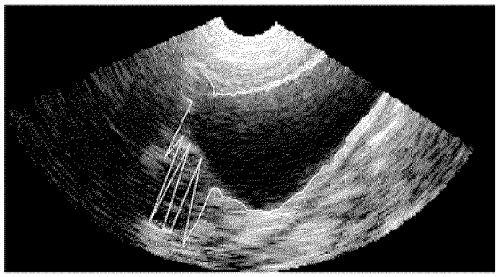

Fig. 37B

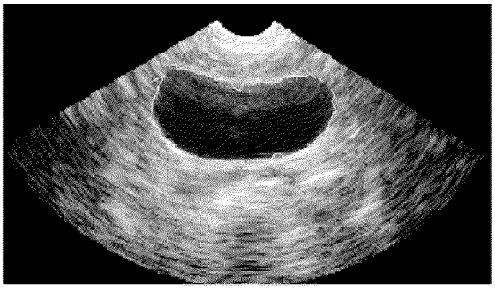

Fig. 37C

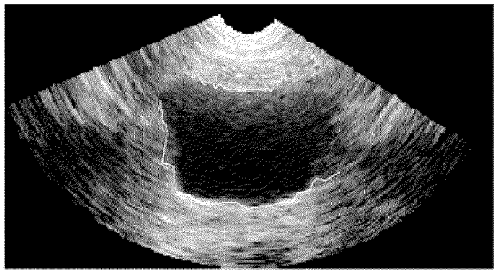

Fig. 37D

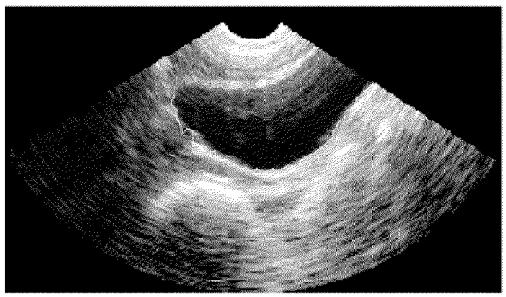

Fig. 38A

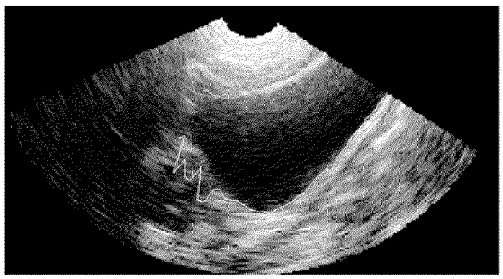

Fig. 38B

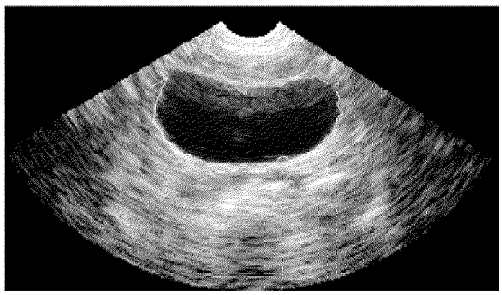

Fig. 38C

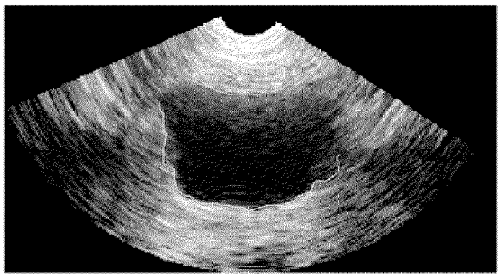

Fig. 38D

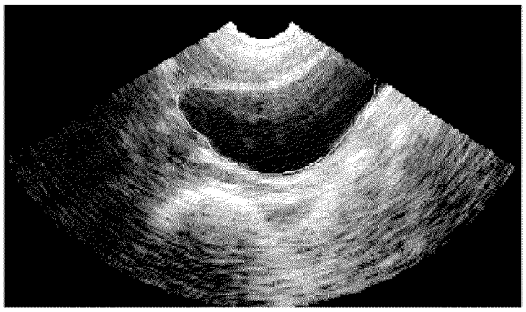

Fig. 39A

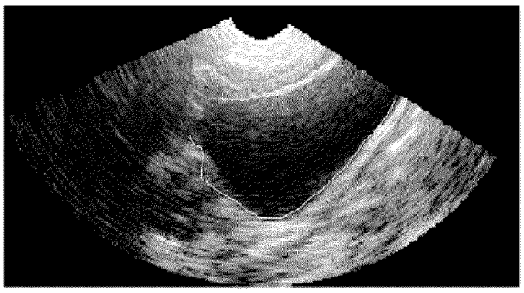

Fig. 39B

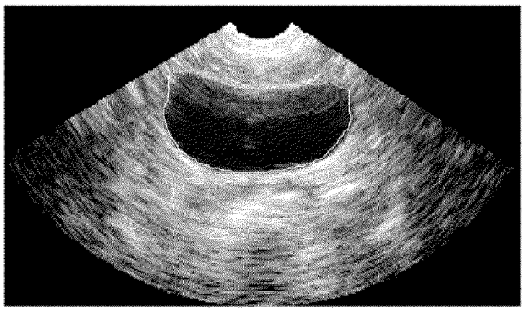

Fig. 39C

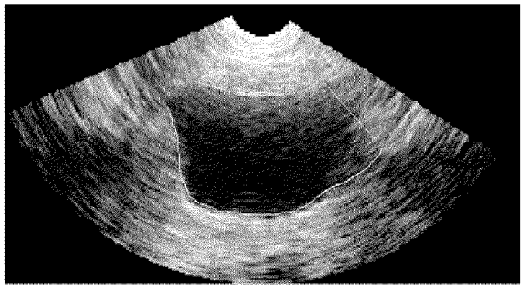

Fig. 39D

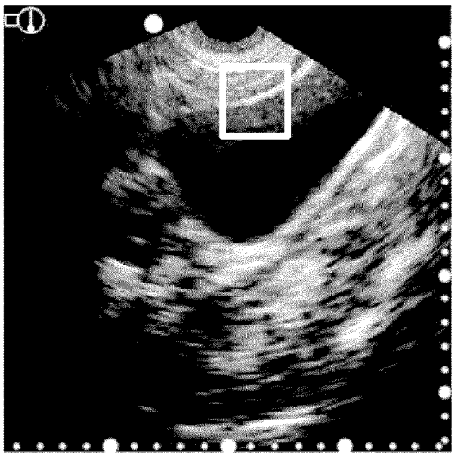

Fig. 40A

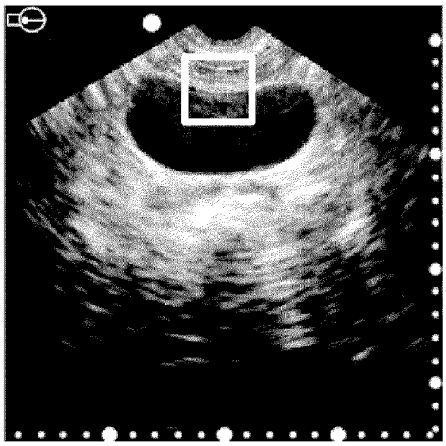

Fig. 41A

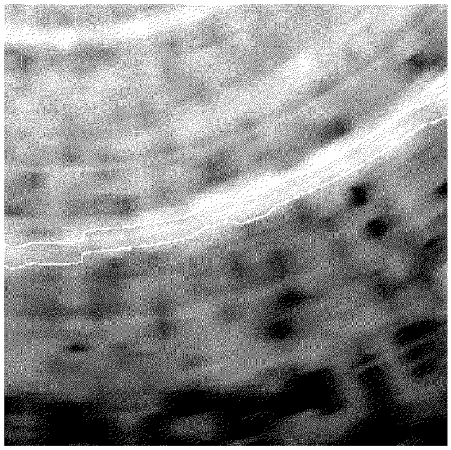

Fig. 40B

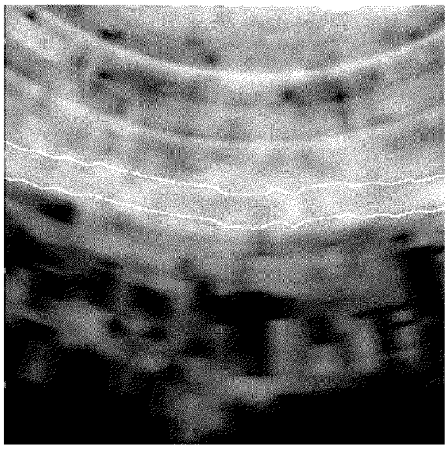

Fig. 41B

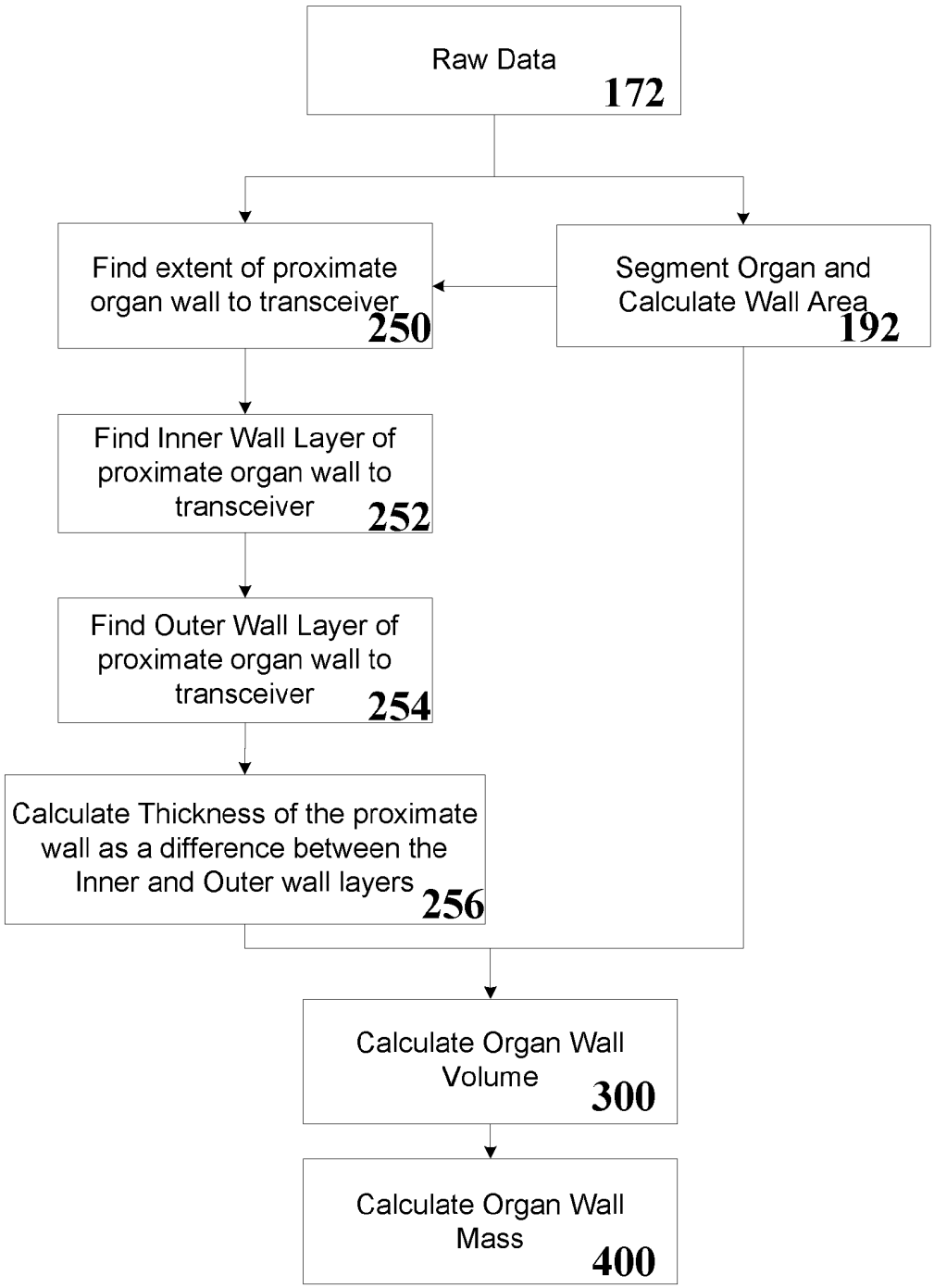
Raw Data
172
Find extent of proximate organ wall to transceiver
250
Segment Organ and Calculate Wall Area
192
Find Inner Wall Layer of proximate organ wall to transceiver
252
Find Outer Wall Layer of proximate organ wall to transceiver
254
Calculate Thickness of the proximate wall as a difference between the Inner and Outer wall layers
256
Calculate Organ Wall Volume
300
Calculate Organ Wall Mass
400

Fig. 42

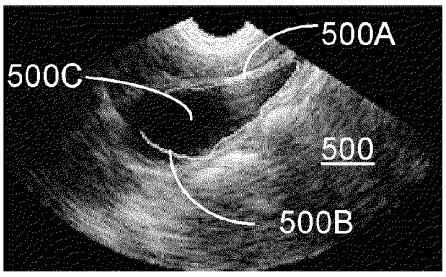

Fig. 43A

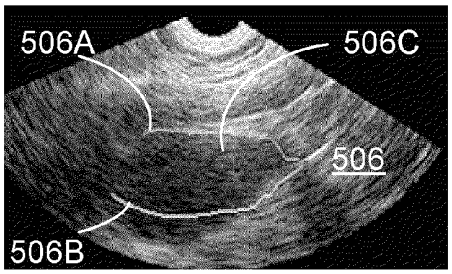

Fig. 44A

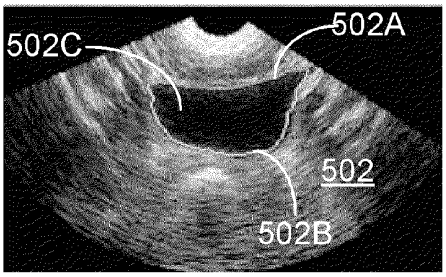

Fig. 43B

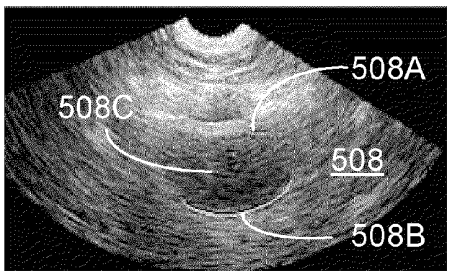

Fig. 44B

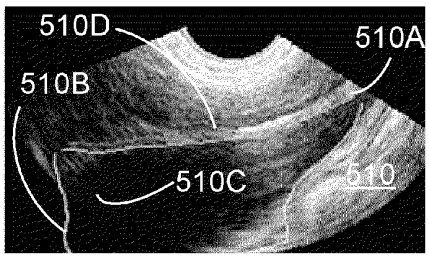

Fig. 45A

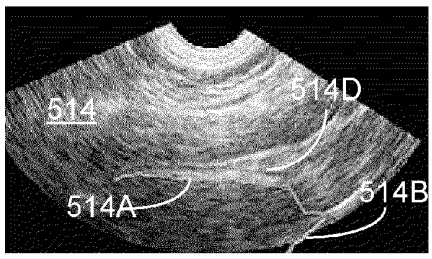

Fig. 46A

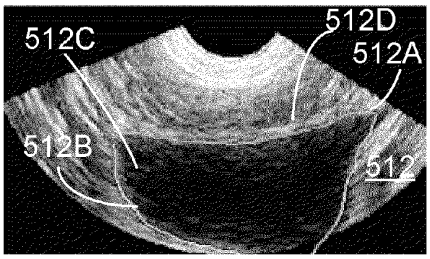

Fig. 45B

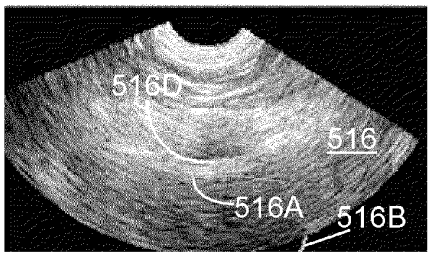

Fig. 46B

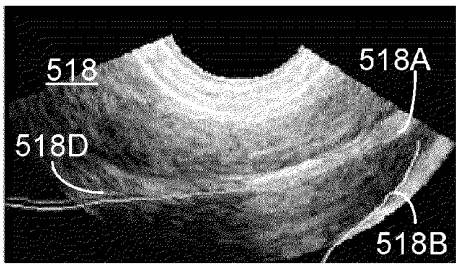

Fig. 47A

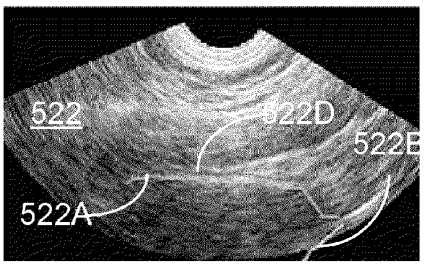

Fig. 48A

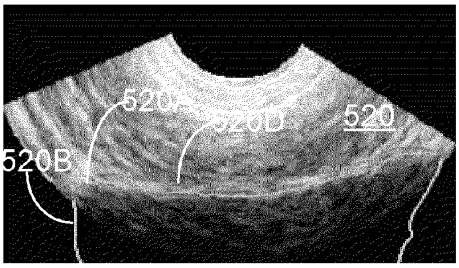

Fig. 47B

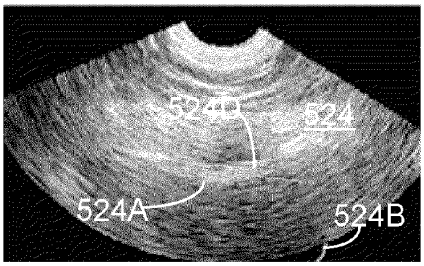

Fig. 48B

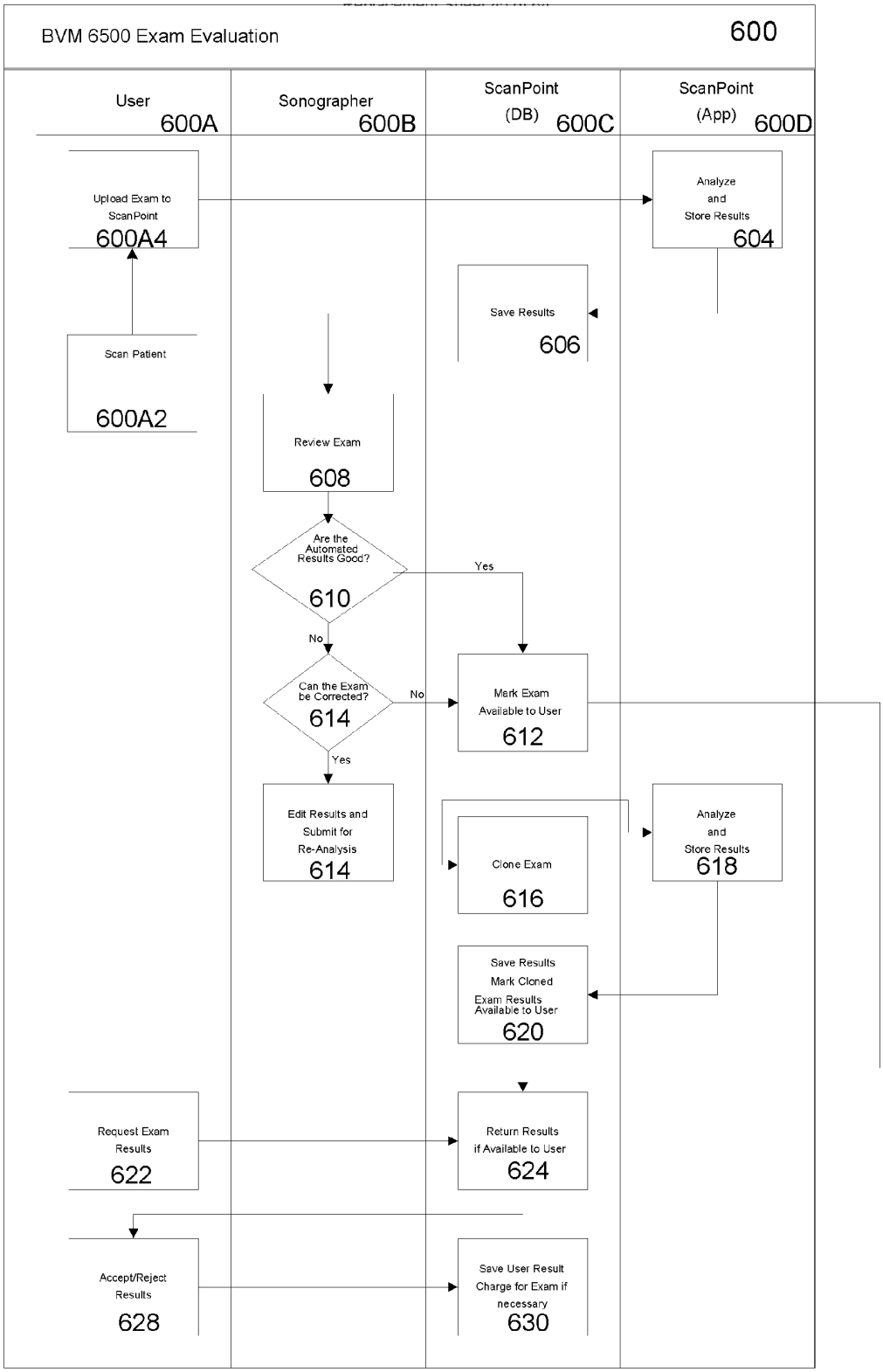
BVM 6500 Exam Evaluation
600
User
600A
Sonographer
600B
ScanPoint
(DB)
600C
ScanPoint
(App)
600D
Upload Exam to ScanPoint
600A4
Analyze and Store Results
604
Save Results
606
Scan Patient
600A2
Review Exam
608
Are the Automated Results Good?
610
Yes
No
Can the Exam be Corrected?
614
No
Mark Exam Available to User
612
Yes
Edit Results and Submit for Re-Analysis
614
Clone Exam
616
Analyze and Store Results
618
Save Results Mark Cloned Exam Results Available to User
620
Request Exam Results
622
Return Results if Available to User
624
Accept/Reject Results
628
Save User Result Charge for Exam if necessary
630

Fig. 49

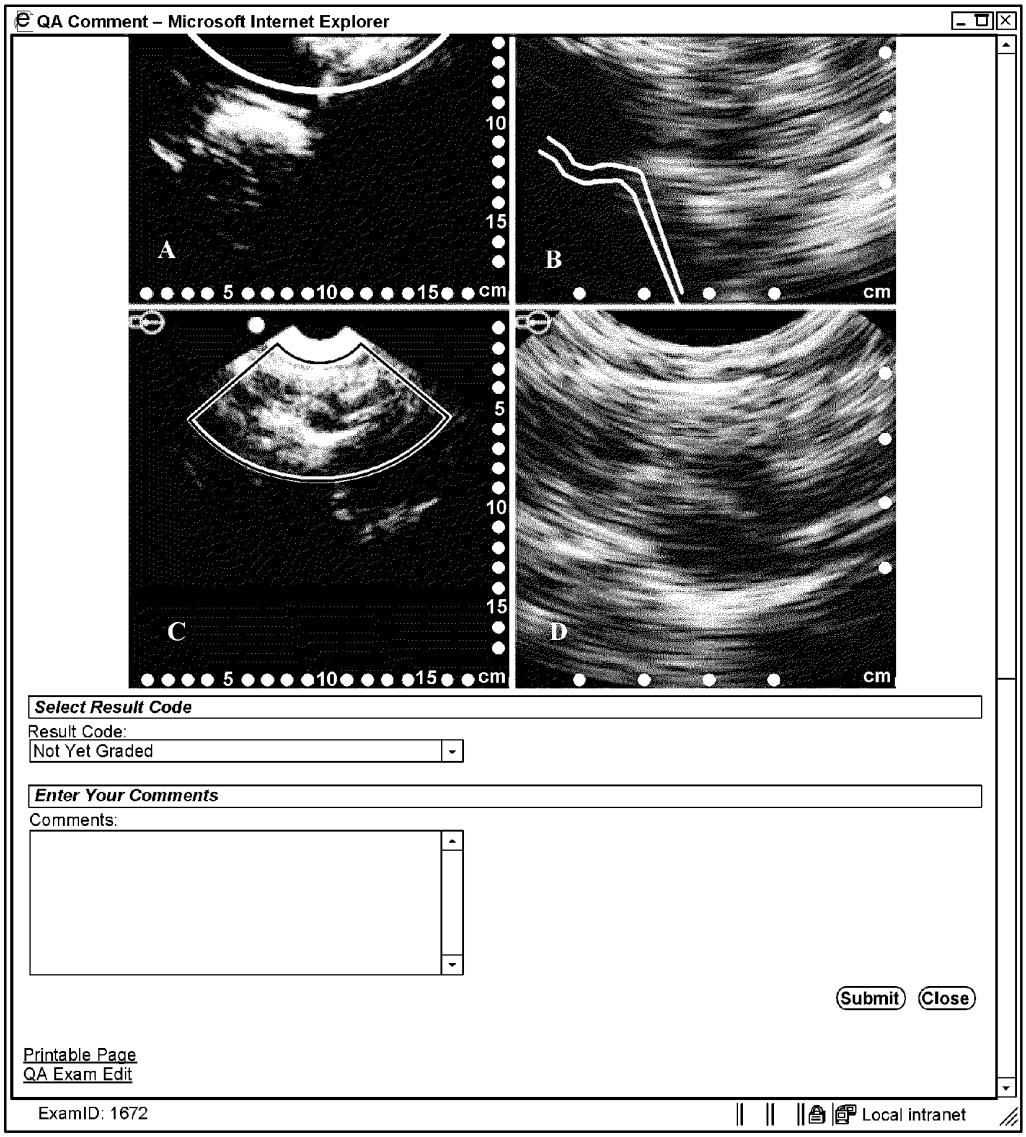
QA Comment – Microsoft Internet Explorer
A
B
C
D
cm
Select Result Code
Result Code:
Not Yet Graded
Enter Your Comments
Comments:
Submit
Close
Printable Page
QA Exam Edit
ExamID: 1672
Local intranet

Fig. 50

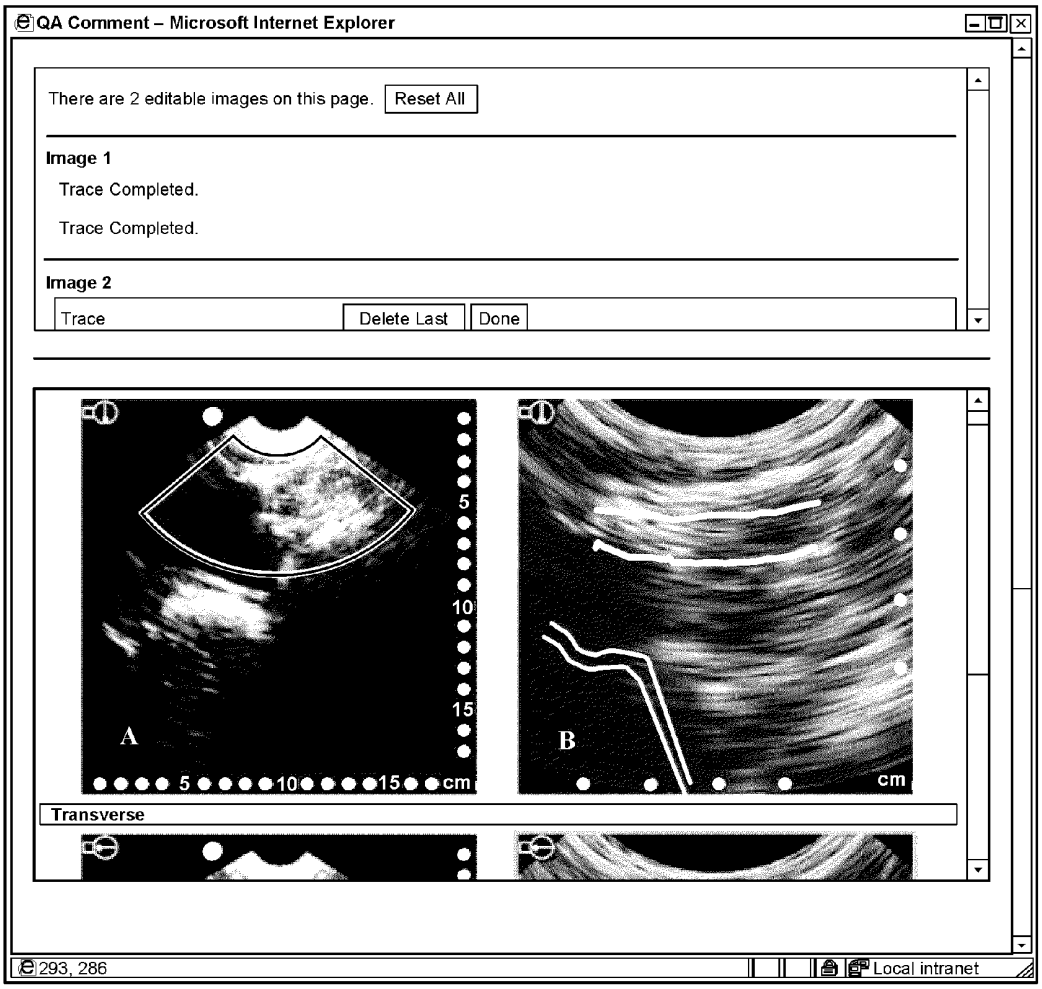
QA Comment – Microsoft Internet Explorer
There are 2 editable images on this page.
Reset All
Image 1
Trace Completed.
Trace Completed.
Image 2
Trace
Delete Last
Done
A
B
5
10
15
cm
Transverse
293, 286
Local intranet

Fig. 51

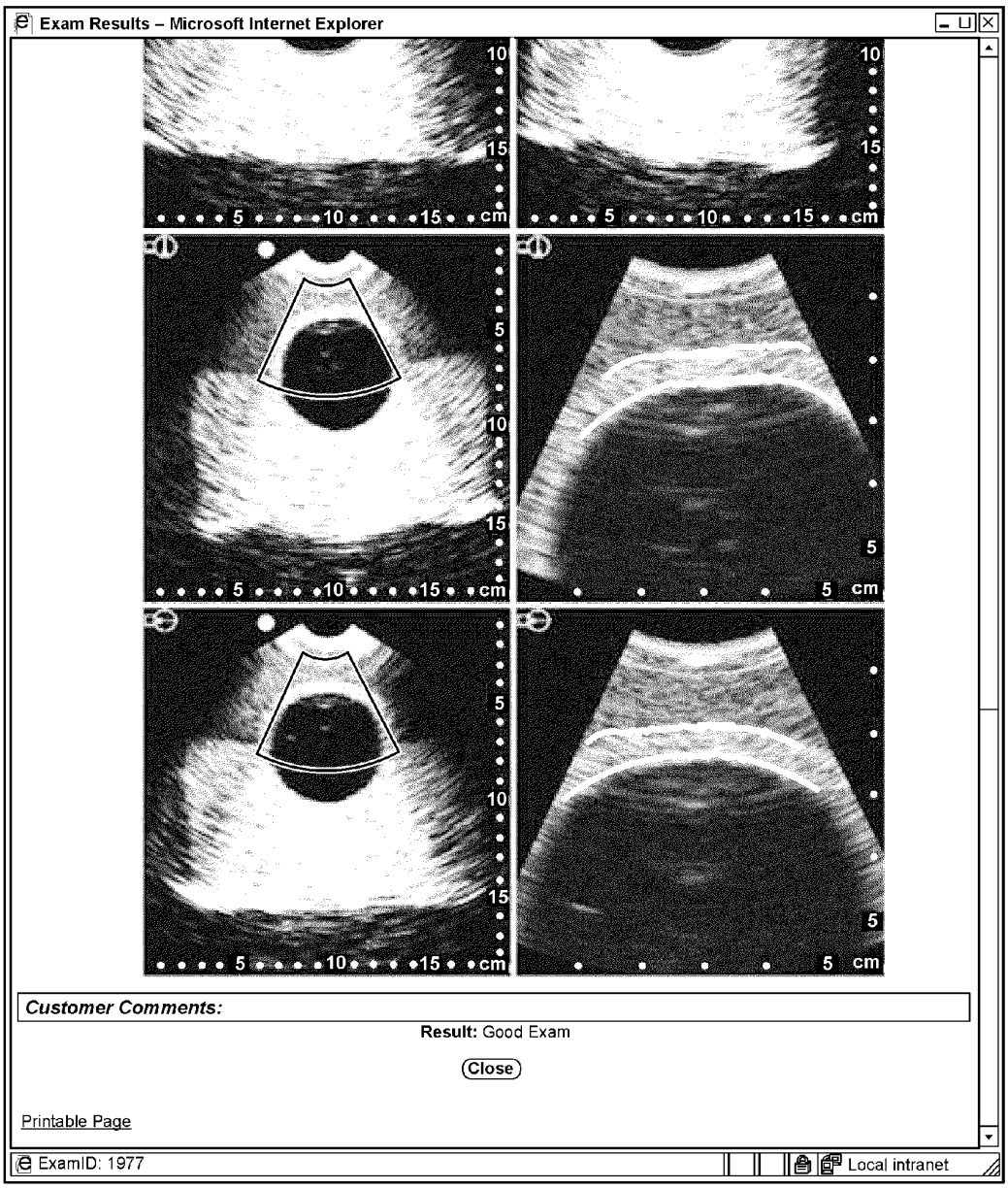
Exam Results – Microsoft Internet Explorer
10
15
5 10 15 cm
10
15
5 10 15 cm
5
10
15
5 10 15 cm
5
5 cm
5
10
15
5 10 15 cm
5
5 cm
Customer Comments:
Result: Good Exam
Close
Printable Page
ExamID: 1977
Local intranet

Fig. 52

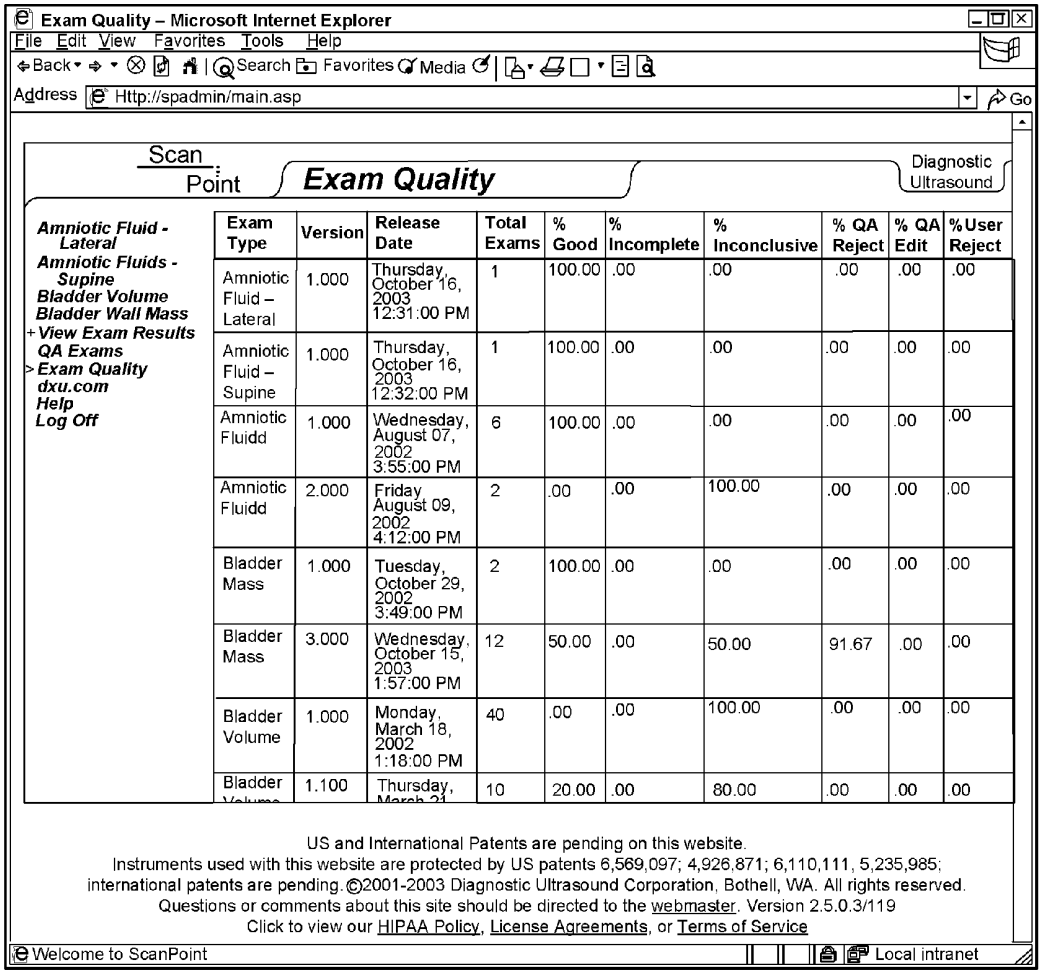
Exam Quality – Microsoft Internet Explorer
File Edit View Favorites Tools Help
Back Search Favorites Media
Address Http://spadmin/main.asp
Go
Scan Point
Exam Quality
Diagnostic Ultrasound
Amniotic Fluid - Lateral
Amniotic Fluids - Supine
Bladder Volume
Bladder Wall Mass
+ View Exam Results
QA Exams
> Exam Quality
dxu.com
Help
Log Off
Exam Type | Version | Release Date | Total Exams | % Good | % Incomplete | % Inconclusive | % QA Reject | % QA Edit | % User Reject
Amniotic Fluid – Lateral | 1.000 | Thursday, October 16, 2003 12:31:00 PM | 1 | 100.00 | .00 | .00 | .00 | .00 | .00
Amniotic Fluid – Supine | 1.000 | Thursday, October 16, 2003 12:32:00 PM | 1 | 100.00 | .00 | .00 | .00 | .00 | .00
Amniotic Fluidd | 1.000 | Wednesday, August 07, 2002 3:55:00 PM | 6 | 100.00 | .00 | .00 | .00 | .00 | .00
Amniotic Fluidd | 2.000 | Friday August 09, 2002 4:12:00 PM | 2 | .00 | .00 | 100.00 | .00 | .00 | .00
Bladder Mass | 1.000 | Tuesday, October 29, 2002 3:49:00 PM | 2 | 100.00 | .00 | .00 | .00 | .00 | .00
Bladder Mass | 3.000 | Wednesday, October 15, 2003 1:57:00 PM | 12 | 50.00 | .00 | 50.00 | 91.67 | .00 | .00
Bladder Volume | 1.000 | Monday, March 18, 2002 1:18:00 PM | 40 | .00 | .00 | 100.00 | .00 | .00 | .00
Bladder | 1.100 | Thursday, | 10 | 20.00 | .00 | 80.00 | .00 | .00 | .00
US and International Patents are pending on this website.
Instruments used with this website are protected by US patents 6,569,097; 4,926,871; 6,110,111, 5,235,985; international patents are pending. ©2001-2003 Diagnostic Ultrasound Corporation, Bothell, WA. All rights reserved.
Questions or comments about this site should be directed to the webmaster. Version 2.5.0.3/119
Click to view our HIPAA Policy, License Agreements, or Terms of Service
Welcome to ScanPoint
Local intranet

Fig. 53

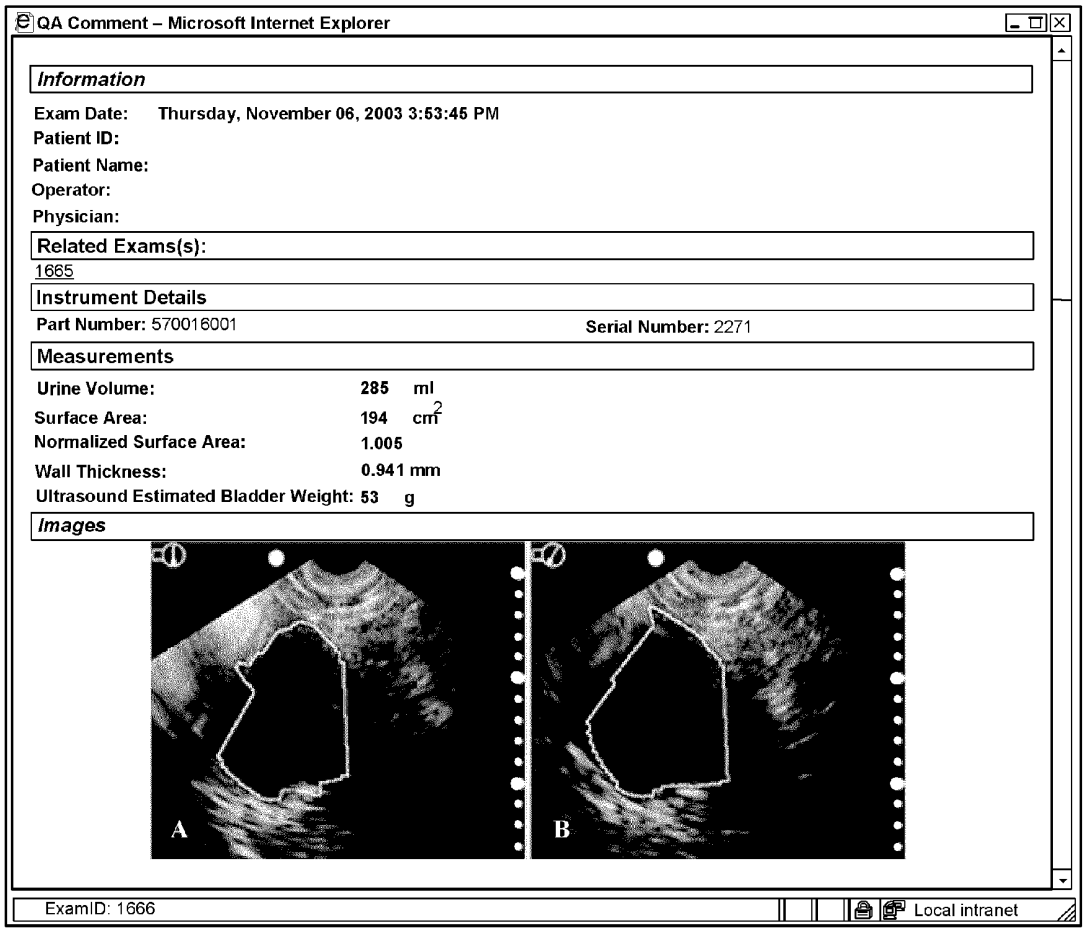
QA Comment – Microsoft Internet Explorer
Information
Exam Date: Thursday, November 06, 2003 3:53:45 PM
Patient ID:
Patient Name:
Operator:
Physician:
Related Exams(s):
1665
Instrument Details
Part Number: 570016001
Serial Number: 2271
Measurements
Urine Volume: 285 ml
Surface Area: 194 cm2
Normalized Surface Area: 1.005
Wall Thickness: 0.941 mm
Ultrasound Estimated Bladder Weight: 53 g
Images
A
B
ExamID: 1666
Local intranet

Fig. 54

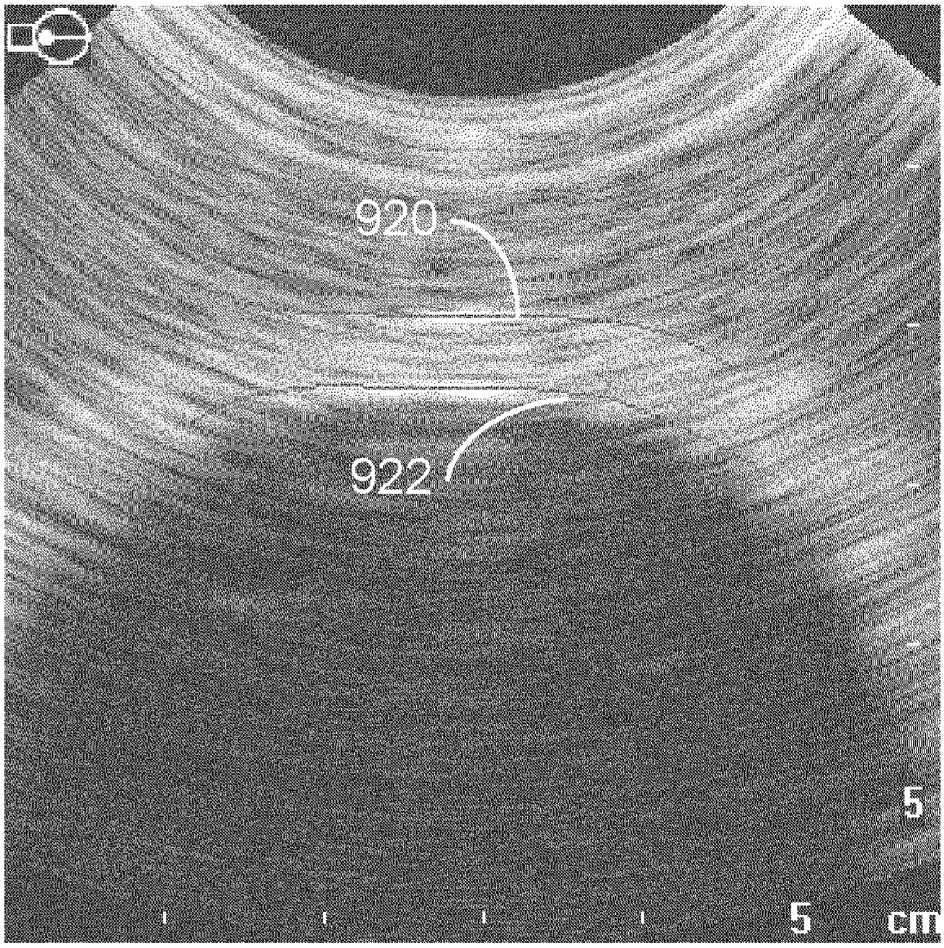

Fig. 55

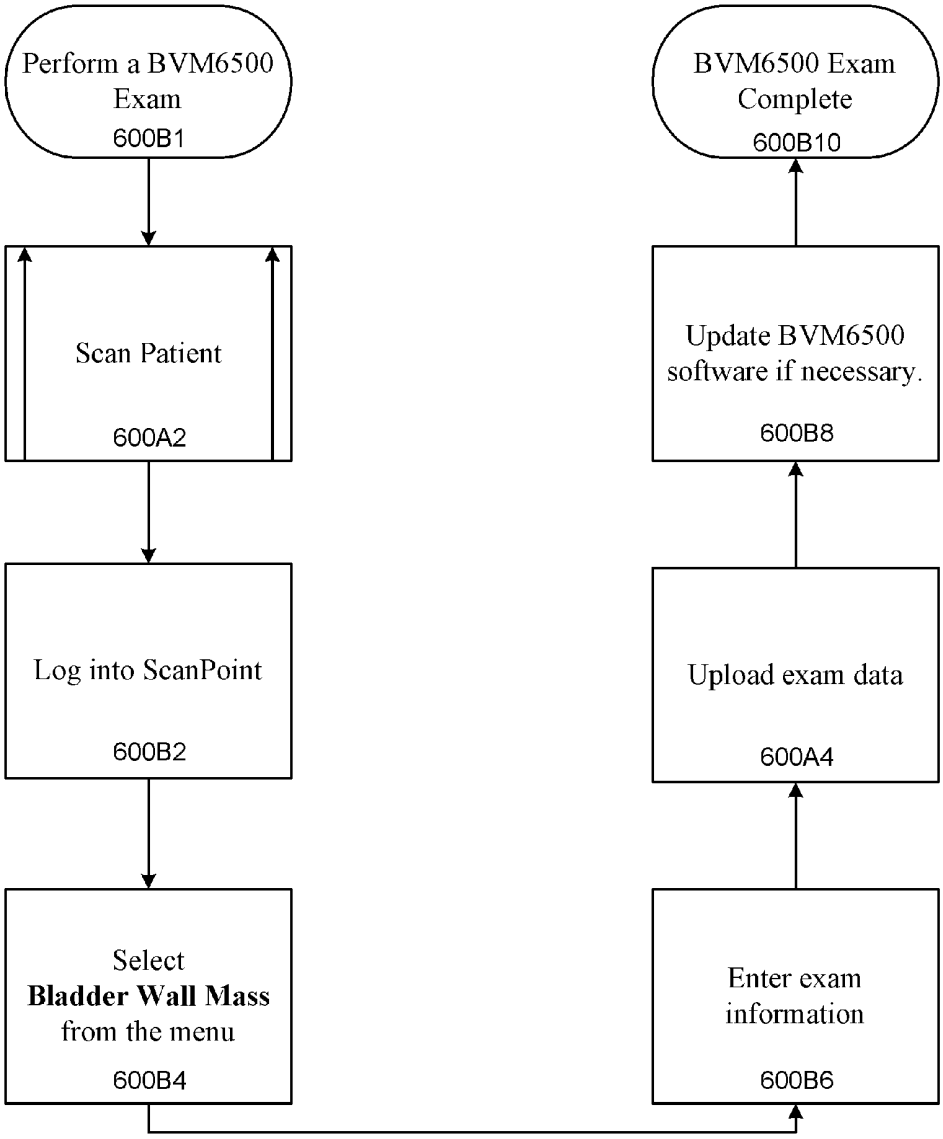
Perform a BVM6500 Exam
600B1
Scan Patient
600A2
Log into ScanPoint
600B2
Select
Bladder Wall Mass
from the menu
600B4
Enter exam information
600B6
Upload exam data
600A4
Update BVM6500 software if necessary.
600B8
BVM6500 Exam Complete
600B10

Fig. 56

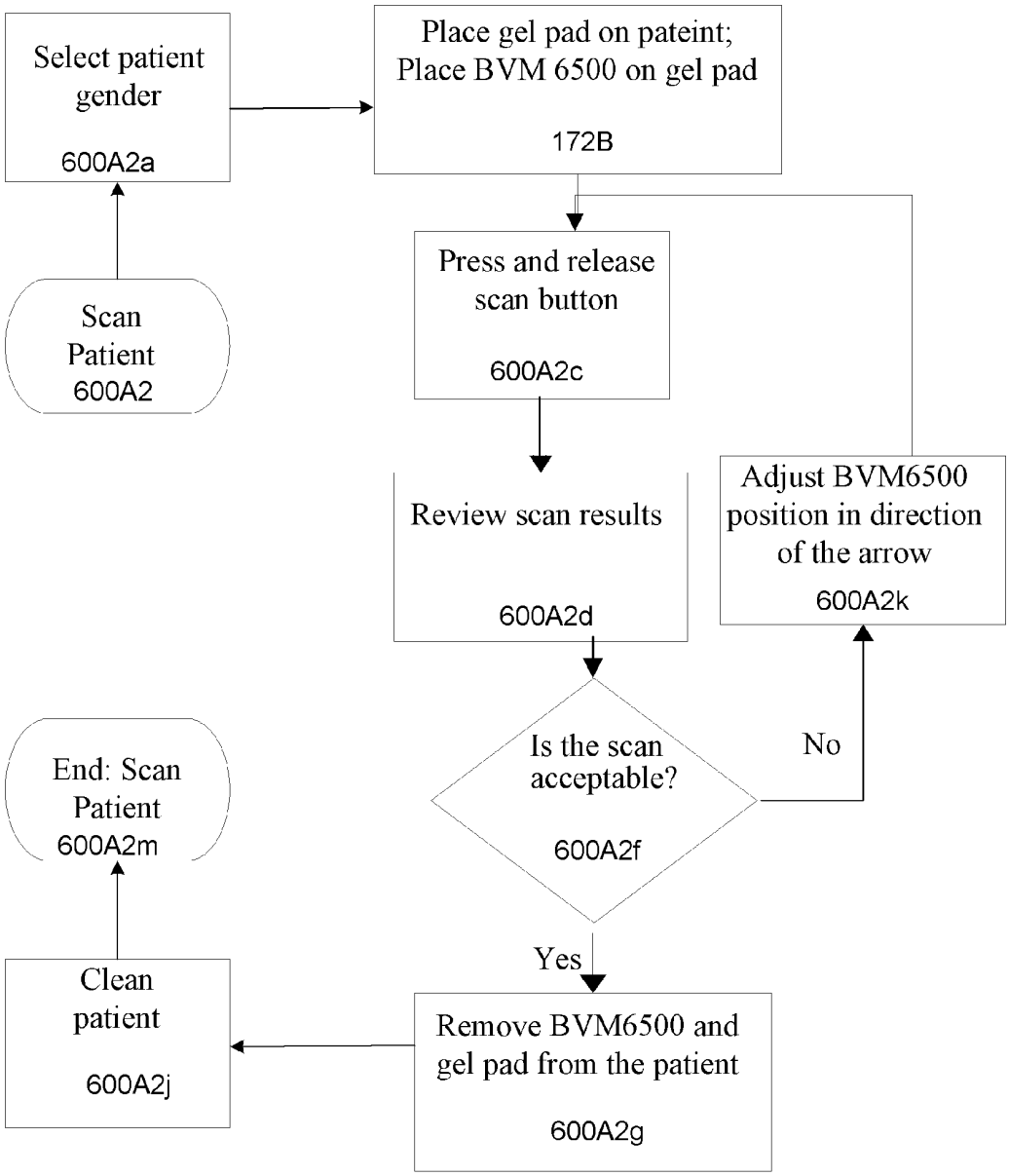
Select patient gender
600A2a
Place gel pad on pateint; Place BVM 6500 on gel pad
172B
Scan Patient
600A2
Press and release scan button
600A2c
Review scan results
600A2d
Adjust BVM6500 position in direction of the arrow
600A2k
Is the scan acceptable?
600A2f
No
Yes
End: Scan Patient
600A2m
Clean patient
600A2j
Remove BVM6500 and gel pad from the patient
600A2g

Fig. 57

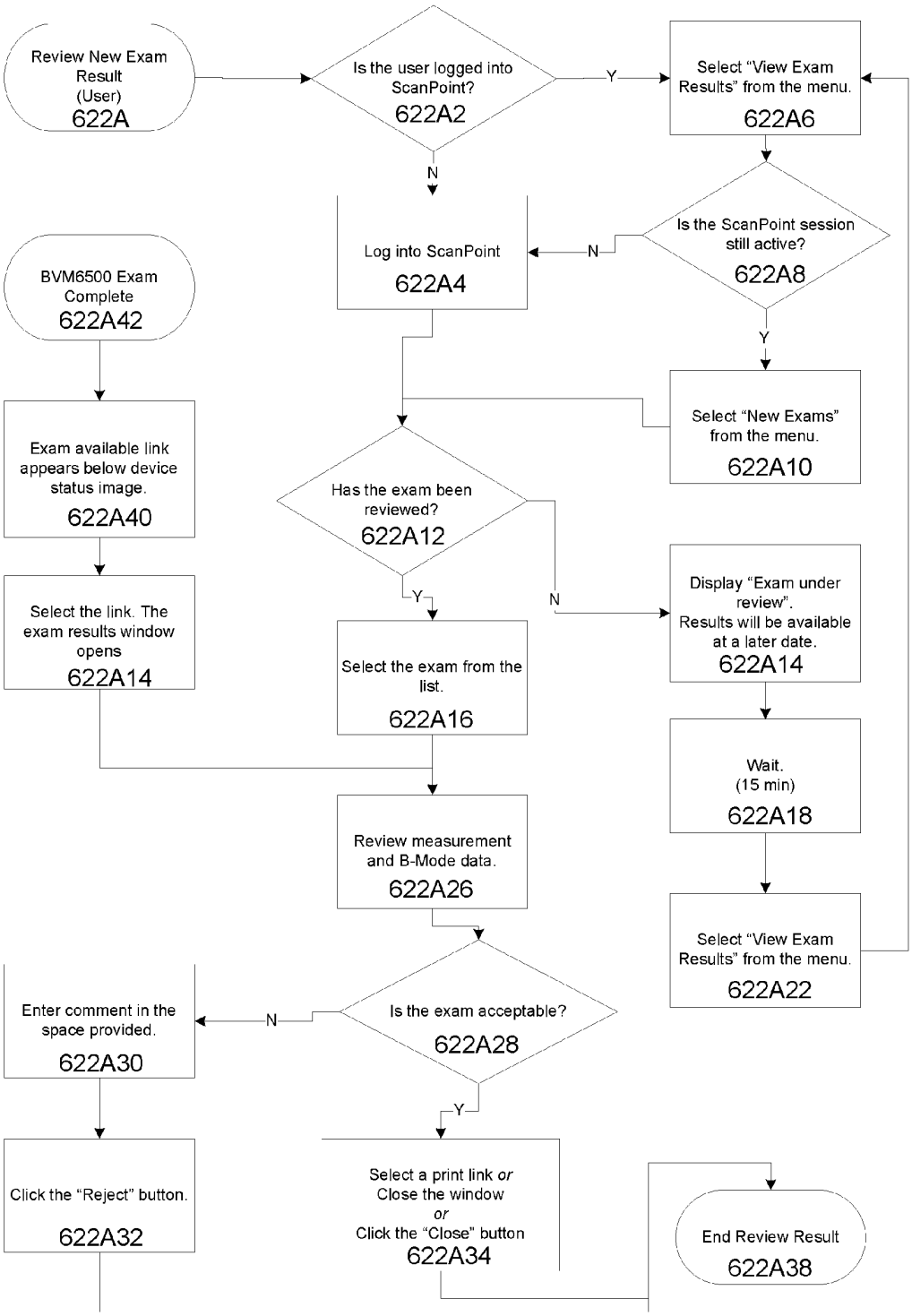
Review New Exam Result (User) 622A
Is the user logged into ScanPoint? 622A2
Y
N
Select "View Exam Results" from the menu. 622A6
Is the ScanPoint session still active? 622A8
N
Y
Log into ScanPoint 622A4
BVM6500 Exam Complete 622A42
Select "New Exams" from the menu. 622A10
Exam available link appears below device status image. 622A40
Has the exam been reviewed? 622A12
Y
N
Select the link. The exam results window opens 622A14
Select the exam from the list. 622A16
Display "Exam under review". Results will be available at a later date. 622A14
Wait. (15 min) 622A18
Review measurement and B-Mode data. 622A26
Select "View Exam Results" from the menu. 622A22
Enter comment in the space provided. 622A30
N
Is the exam acceptable? 622A28
Y
Click the "Reject" button. 622A32
Select a print link or Close the window or Click the "Close" button 622A34
End Review Result 622A38

Fig. 58

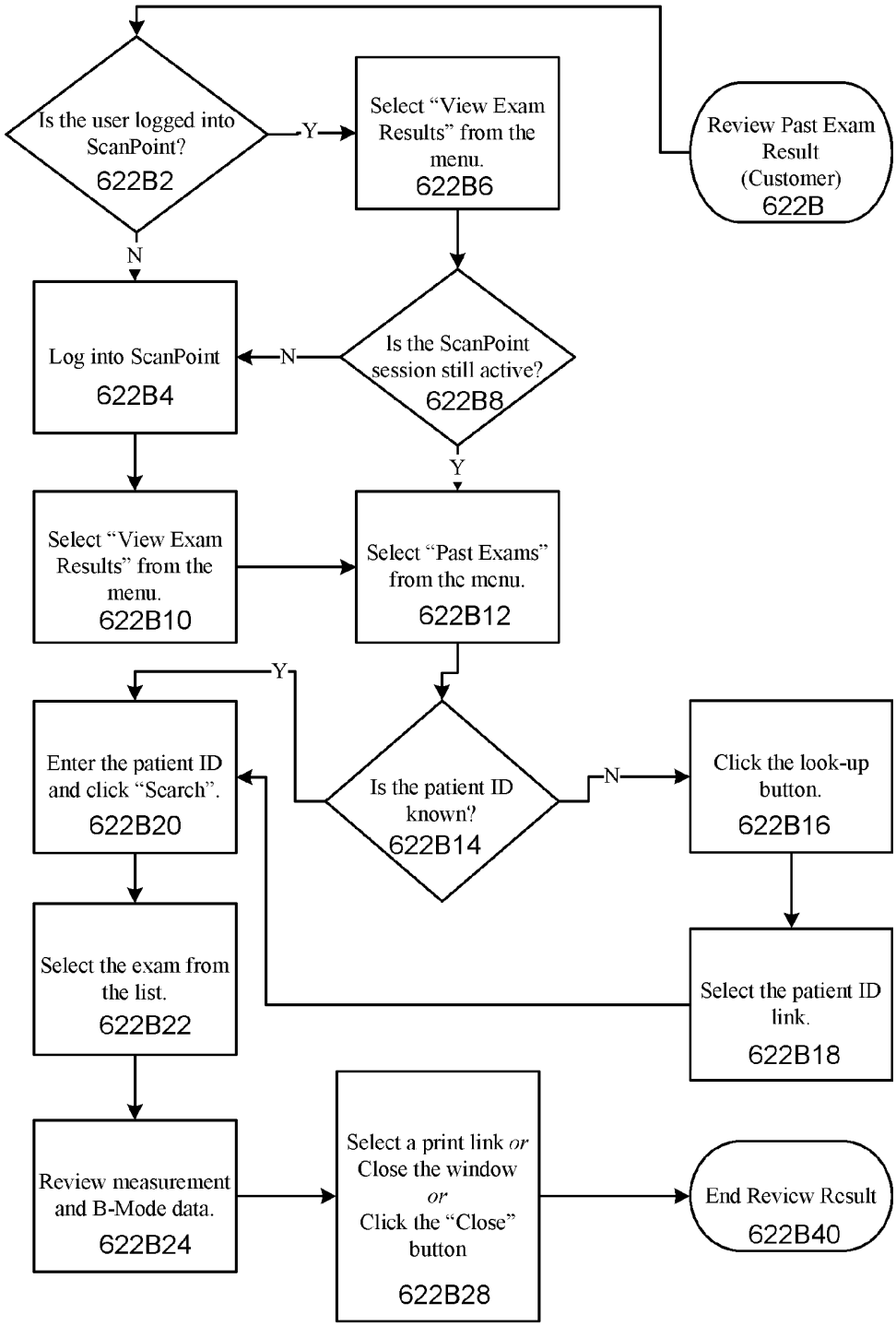
Is the user logged into ScanPoint?
622B2
Y
Select "View Exam Results" from the menu.
622B6
Review Past Exam Result (Customer)
622B
N
Log into ScanPoint
622B4
N
Is the ScanPoint session still active?
622B8
Y
Select "View Exam Results" from the menu.
622B10
Select "Past Exams" from the menu.
622B12
Y
Enter the patient ID and click "Search".
622B20
Is the patient ID known?
622B14
N
Click the look-up button.
622B16
Select the exam from the list.
622B22
Select the patient ID link.
622B18
Review measurement and B-Mode data.
622B24
Select a print link *or* Close the window *or* Click the "Close" button
622B28
End Review Result
622B40

Fig. 59

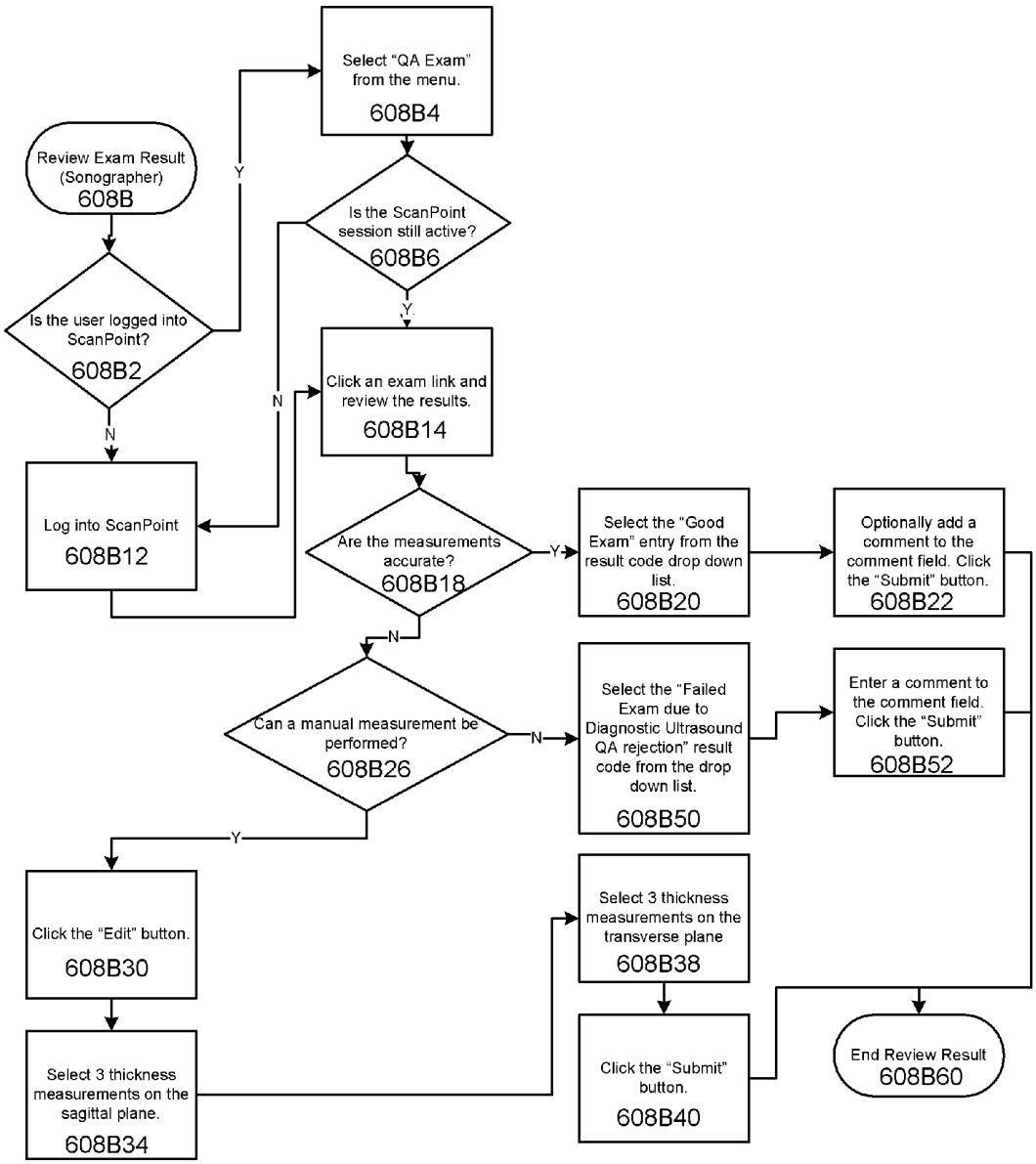
Review Exam Result (Sonographer) 608B
Is the user logged into ScanPoint? 608B2
Y
N
Select "QA Exam" from the menu. 608B4
Is the ScanPoint session still active? 608B6
Y
N
Log into ScanPoint 608B12
Click an exam link and review the results. 608B14
Are the measurements accurate? 608B18
Y
N
Select the "Good Exam" entry from the result code drop down list. 608B20
Optionally add a comment to the comment field. Click the "Submit" button. 608B22
Can a manual measurement be performed? 608B26
N
Y
Select the "Failed Exam due to Diagnostic Ultrasound QA rejection" result code from the drop down list. 608B50
Enter a comment to the comment field. Click the "Submit" button. 608B52
Click the "Edit" button. 608B30
Select 3 thickness measurements on the sagittal plane. 608B34
Select 3 thickness measurements on the transverse plane 608B38
Click the "Submit" button. 608B40
End Review Result 608B60

Fig. 60

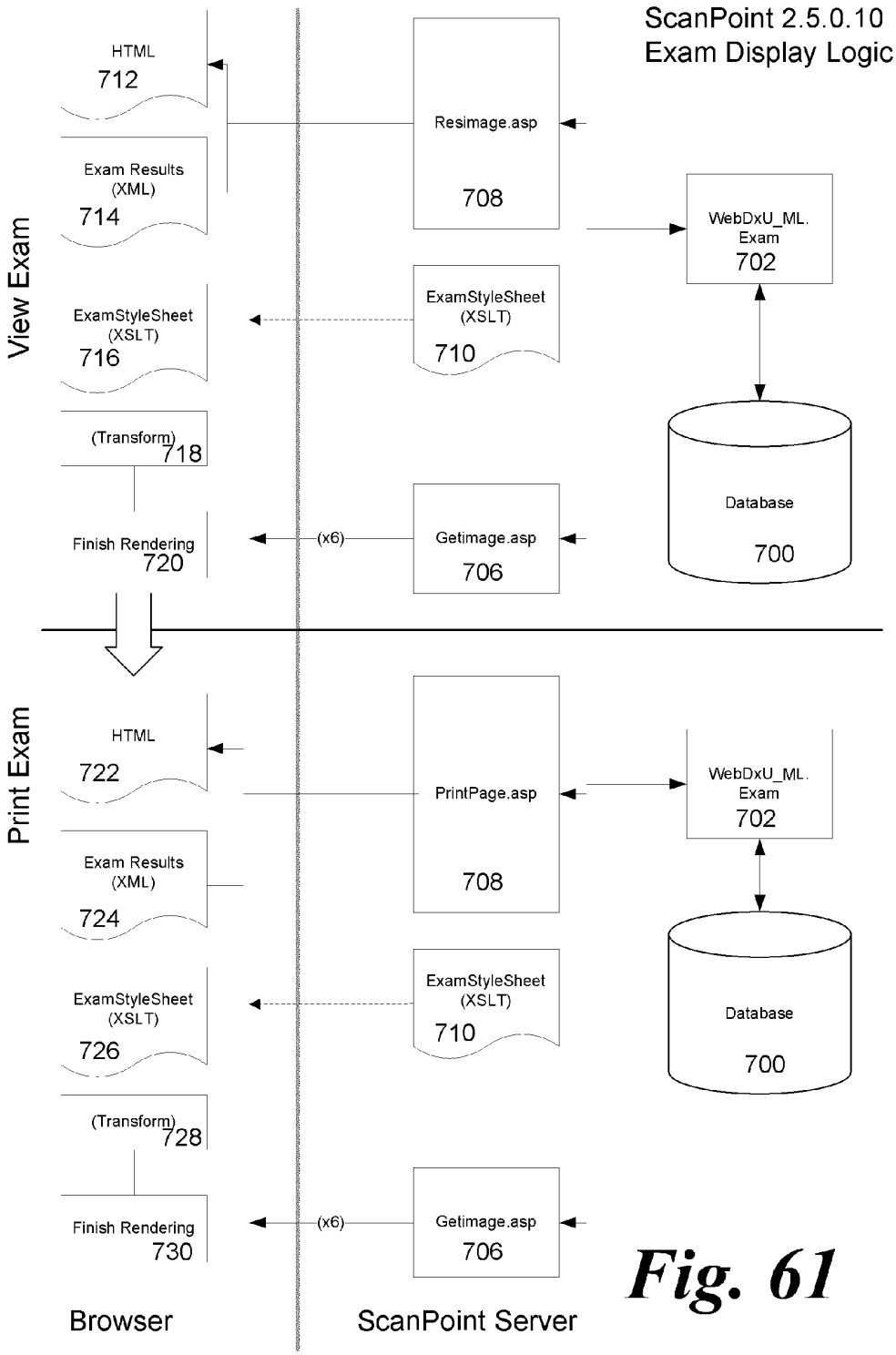
ScanPoint 2.5.0.10
Exam Display Logic
View Exam
HTML
712
Exam Results
(XML)
714
ExamStyleSheet
(XSLT)
716
(Transform)
718
Finish Rendering
720
Resimage.asp
708
ExamStyleSheet
(XSLT)
710
(x6)
Getimage.asp
706
WebDxU_ML.
Exam
702
Database
700
Print Exam
HTML
722
Exam Results
(XML)
724
ExamStyleSheet
(XSLT)
726
(Transform)
728
Finish Rendering
730
PrintPage.asp
708
ExamStyleSheet
(XSLT)
710
(x6)
Getimage.asp
706
WebDxU_ML.
Exam
702
Database
700
Browser
ScanPoint Server

Fig. 61

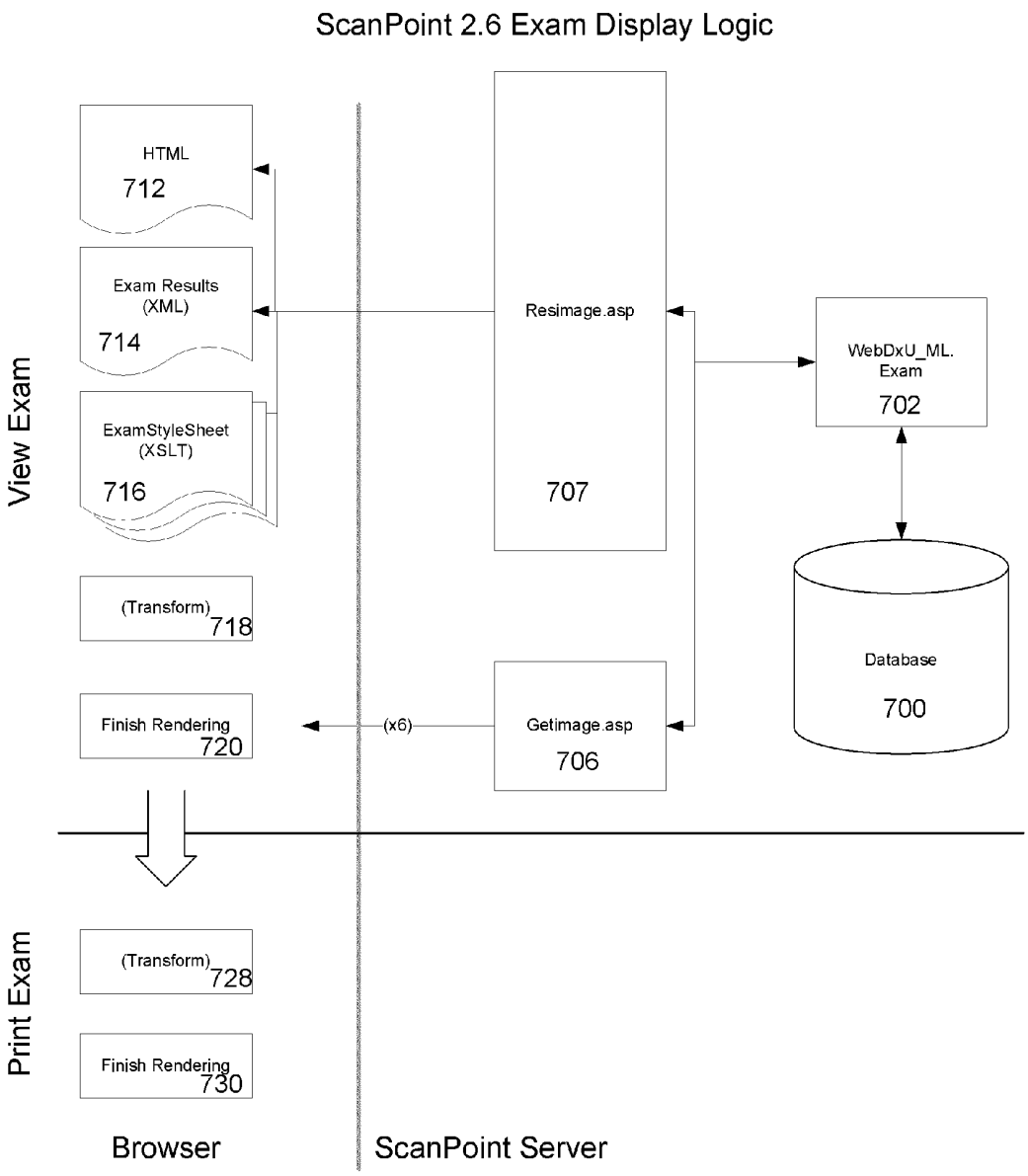
ScanPoint 2.6 Exam Display Logic
HTML
712
Exam Results
(XML)
714
ExamStyleSheet
(XSLT)
716
View Exam
(Transform)
718
Finish Rendering
720
Resimage.asp
707
WebDxU_ML.
Exam
702
Database
700
(x6)
Getimage.asp
706
(Transform)
728
Finish Rendering
730
Print Exam
Browser
ScanPoint Server

Fig. 62

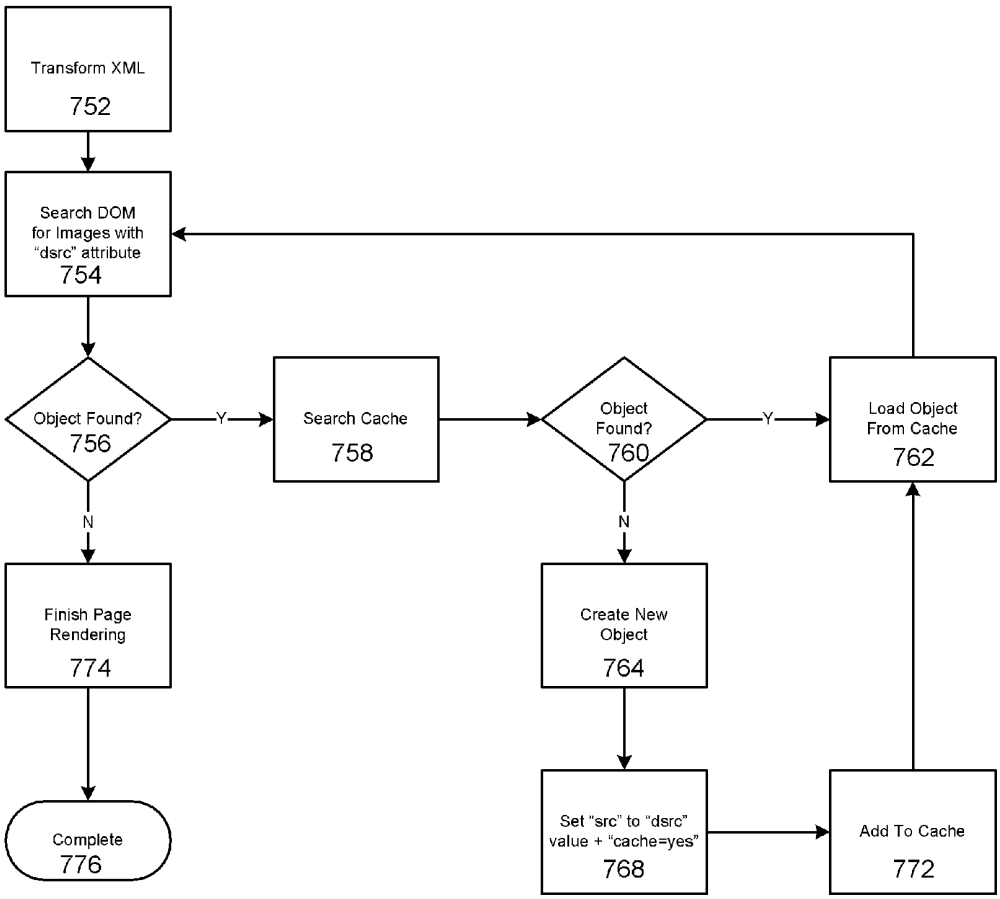
Transform XML
752
Search DOM for Images with "dsrc" attribute
754
Object Found?
756
Y
Search Cache
758
Object Found?
760
Y
Load Object From Cache
762
N
N
Finish Page Rendering
774
Create New Object
764
Complete
776
Set "src" to "dsrc" value + "cache=yes"
768
Add To Cache
772

Fig. 63

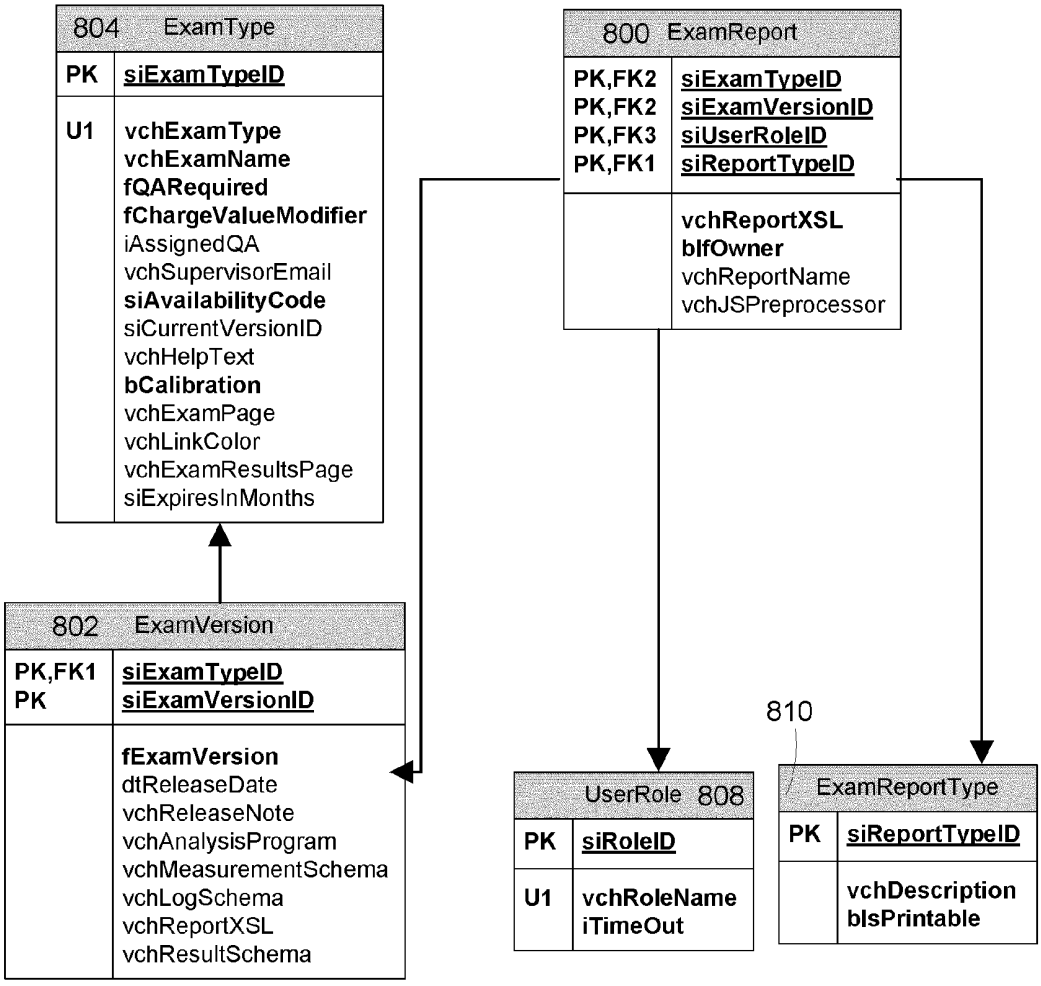
804 ExamType
PK siExamTypeID
U1 vchExamType
vchExamName
fQARequired
fChargeValueModifier
iAssignedQA
vchSupervisorEmail
siAvailabilityCode
siCurrentVersionID
vchHelpText
bCalibration
vchExamPage
vchLinkColor
vchExamResultsPage
siExpiresInMonths
800 ExamReport
PK,FK2 siExamTypeID
PK,FK2 siExamVersionID
PK,FK3 siUserRoleID
PK,FK1 siReportTypeID
vchReportXSL
blfOwner
vchReportName
vchJSPreprocessor
802 ExamVersion
PK,FK1 siExamTypeID
PK siExamVersionID
fExamVersion
dtReleaseDate
vchReleaseNote
vchAnalysisProgram
vchMeasurementSchema
vchLogSchema
vchReportXSL
vchResultSchema
UserRole 808
PK siRoleID
U1 vchRoleName
iTimeOut
810
ExamReportType
PK siReportTypeID
vchDescription
blsPrintable

Fig. 64

ClonedExams 820	
PK	iOriginalExamID
	iNewExamID iUserID siOriginalResultCode dtTimeStamp

Fig. 65

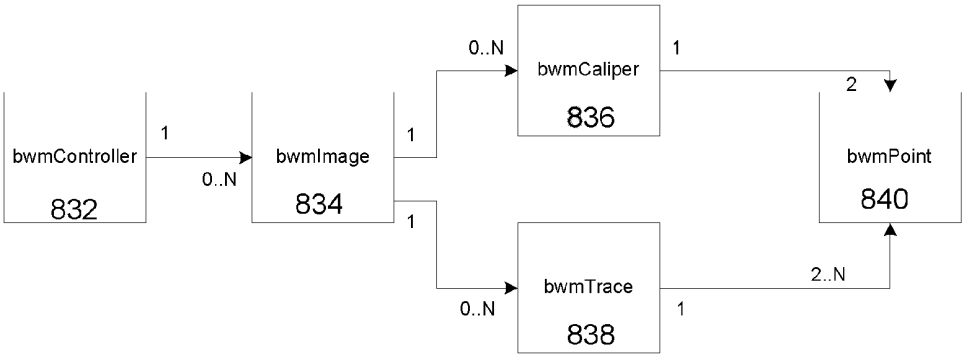

Fig. 66

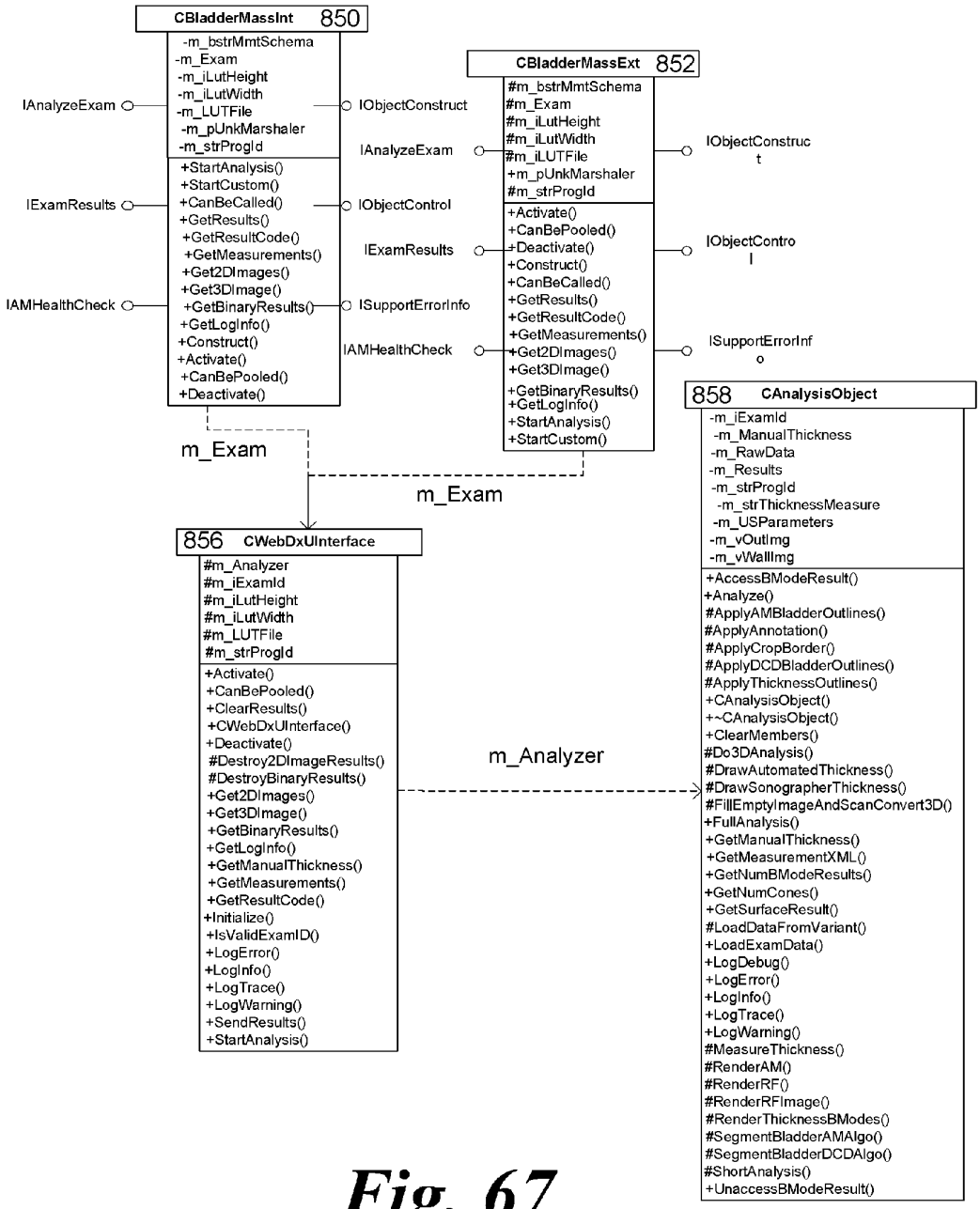
CBladderMassInt 850
-m_bstrMmtSchema
-m_Exam
-m_iLutHeight
-m_iLutWidth
-m_LUTFile
-m_pUnkMarshaler
-m_strProgId
+StartAnalysis()
+StartCustom()
+CanBeCalled()
+GetResults()
+GetResultCode()
+GetMeasurements()
+Get2DImages()
+Get3DImage()
+GetBinaryResults()
+GetLogInfo()
+Construct()
+Activate()
+CanBePooled()
+Deactivate()
IAnalyzeExam
IExamResults
IAMHealthCheck
IObjectConstruct
IObjectControl
ISupportErrorInfo
CBladderMassExt 852
#m_bstrMmtSchema
#m_Exam
#m_iLutHeight
#m_iLutWidth
#m_iLUTFile
+m_pUnkMarshaler
#m_strProgId
+Activate()
+CanBePooled()
+Deactivate()
+Construct()
+CanBeCalled()
+GetResults()
+GetResultCode()
+GetMeasurements()
+Get2DImages()
+Get3DImage()
+GetBinaryResults()
+GetLogInfo()
+StartAnalysis()
+StartCustom()
IAnalyzeExam
IExamResults
IAMHealthCheck
IObjectConstruct
IObjectControl
ISupportErrorInfo
m_Exam
m_Exam
856 CWebDxUInterface
#m_Analyzer
#m_iExamId
#m_iLutHeight
#m_iLutWidth
#m_LUTFile
#m_strProgId
+Activate()
+CanBePooled()
+ClearResults()
+CWebDxUInterface()
+Deactivate()
#Destroy2DImageResults()
#DestroyBinaryResults()
+Get2DImages()
+Get3DImage()
+GetBinaryResults()
+GetLogInfo()
+GetManualThickness()
+GetMeasurements()
+GetResultCode()
+Initialize()
+IsValidExamID()
+LogError()
+LogInfo()
+LogTrace()
+LogWarning()
+SendResults()
+StartAnalysis()
m_Analyzer
858 CAnalysisObject
-m_iExamId
-m_ManualThickness
-m_RawData
-m_Results
-m_strProgId
-m_strThicknessMeasure
-m_USParameters
-m_vOutImg
-m_vWallImg
+AccessBModeResult()
+Analyze()
#ApplyAMBladderOutlines()
#ApplyAnnotation()
#ApplyCropBorder()
#ApplyDCDBladderOutlines()
#ApplyThicknessOutlines()
+CAnalysisObject()
+~CAnalysisObject()
+ClearMembers()
#Do3DAnalysis()
#DrawAutomatedThickness()
#DrawSonographerThickness()
#FillEmptyImageAndScanConvert3D()
+FullAnalysis()
+GetManualThickness()
+GetMeasurementXML()
+GetNumBModeResults()
+GetNumCones()
+GetSurfaceResult()
#LoadDataFromVariant()
+LoadExamData()
+LogDebug()
+LogError()
+LogInfo()
+LogTrace()
+LogWarning()
#MeasureThickness()
#RenderAM()
#RenderRF()
#RenderRFImage()
#RenderThicknessBModes()
#SegmentBladderAMAlgo()
#SegmentBladderDCDAlgo()
#ShortAnalysis()
+UnaccessBModeResult()

Fig. 67

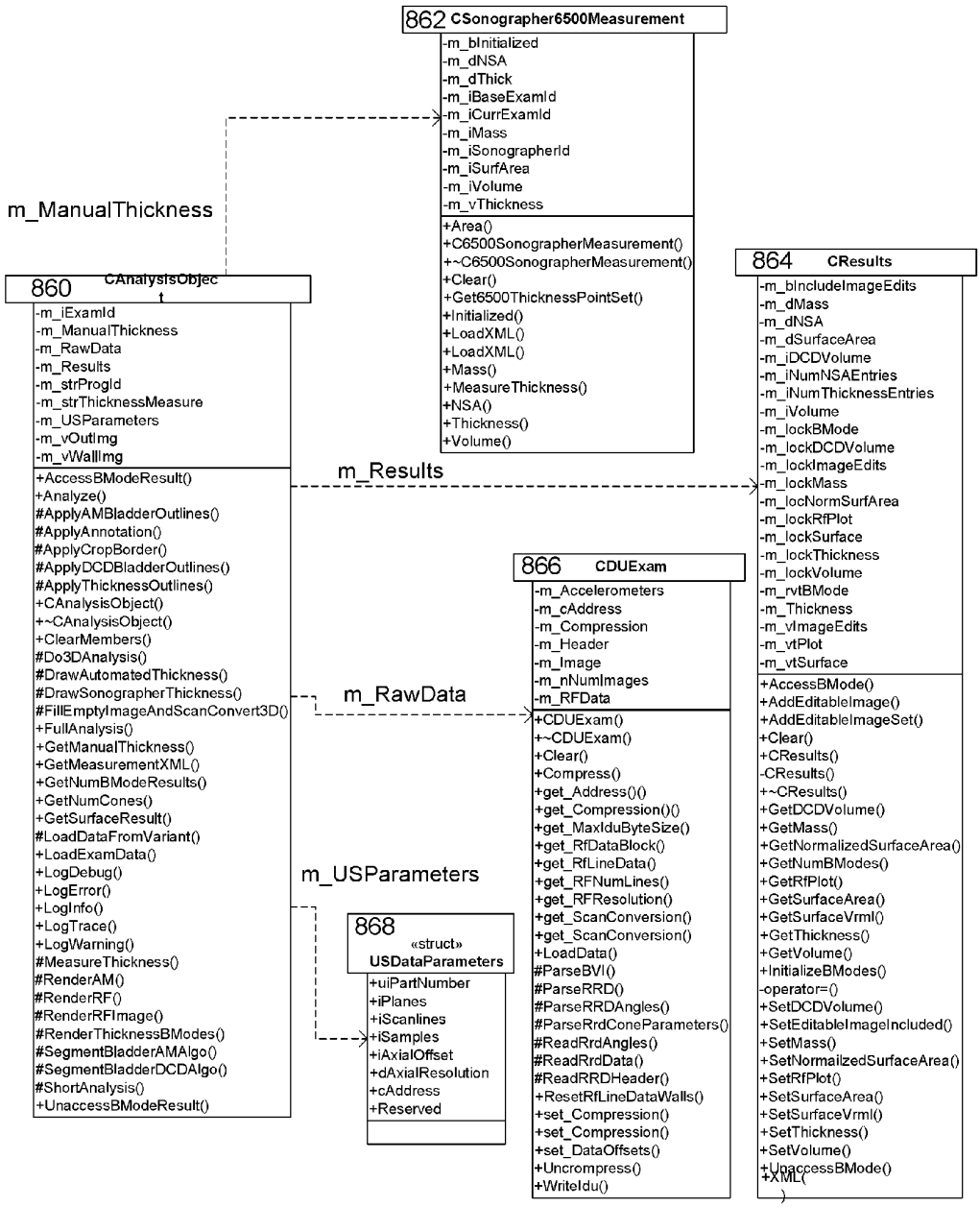
862 CSonographer6500Measurement
-m_bInitialized
-m_dNSA
-m_dThick
-m_iBaseExamId
-m_iCurrExamId
-m_iMass
-m_iSonographerId
-m_iSurfArea
-m_iVolume
-m_vThickness
+Area()
+C6500SonographerMeasurement()
+~C6500SonographerMeasurement()
+Clear()
+Get6500ThicknessPointSet()
+Initialized()
+LoadXML()
+LoadXML()
+Mass()
+MeasureThickness()
+NSA()
+Thickness()
+Volume()
m_ManualThickness
860 CAnalysisObject
-m_iExamId
-m_ManualThickness
-m_RawData
-m_Results
-m_strProgId
-m_strThicknessMeasure
-m_USParameters
-m_vOutImg
-m_vWallImg
+AccessBModeResult()
+Analyze()
#ApplyAMBladderOutlines()
#ApplyAnnotation()
#ApplyCropBorder()
#ApplyDCDBladderOutlines()
#ApplyThicknessOutlines()
+CAnalysisObject()
+~CAnalysisObject()
+ClearMembers()
#Do3DAnalysis()
#DrawAutomatedThickness()
#DrawSonographerThickness()
#FillEmptyImageAndScanConvert3D()
+FullAnalysis()
+GetManualThickness()
+GetMeasurementXML()
+GetNumBModeResults()
+GetNumCones()
+GetSurfaceResult()
#LoadDataFromVariant()
+LoadExamData()
+LogDebug()
+LogError()
+LogInfo()
+LogTrace()
+LogWarning()
#MeasureThickness()
#RenderAM()
#RenderRF()
#RenderRFImage()
#RenderThicknessBModes()
#SegmentBladderAMAlgo()
#SegmentBladderDCDAlgo()
#ShortAnalysis()
+UnaccessBModeResult()
m_Results
m_RawData
m_USParameters
868 «struct» USDataParameters
+uiPartNumber
+iPlanes
+iScanlines
+iSamples
+iAxialOffset
+dAxialResolution
+cAddress
+Reserved
866 CDUExam
-m_Accelerometers
-m_cAddress
-m_Compression
-m_Header
-m_Image
-m_nNumImages
-m_RFData
+CDUExam()
+~CDUExam()
+Clear()
+Compress()
+get_Address()()
+get_Compression()()
+get_MaxIduByteSize()
+get_RfDataBlock()
+get_RfLineData()
+get_RFNumLines()
+get_RFResolution()
+get_ScanConversion()
+get_ScanConversion()
+LoadData()
#ParseBVI()
#ParseRRD()
#ParseRRDAngles()
#ParseRrdConeParameters()
#ReadRrdAngles()
#ReadRrdData()
#ReadRRDHeader()
+ResetRfLineDataWalls()
+set_Compression()
+set_Compression()
+set_DataOffsets()
+Uncrompress()
+WriteIdu()
864 CResults
-m_bIncludeImageEdits
-m_dMass
-m_dNSA
-m_dSurfaceArea
-m_iDCDVolume
-m_iNumNSAEntries
-m_iNumThicknessEntries
-m_iVolume
-m_lockBMode
-m_lockDCDVolume
-m_lockImageEdits
-m_lockMass
-m_locNormSurfArea
-m_lockRfPlot
-m_lockSurface
-m_lockThickness
-m_lockVolume
-m_rvtBMode
-m_Thickness
-m_vImageEdits
-m_vtPlot
-m_vtSurface
+AccessBMode()
+AddEditableImage()
+AddEditableImageSet()
+Clear()
+CResults()
-CResults()
+~CResults()
+GetDCDVolume()
+GetMass()
+GetNormalizedSurfaceArea()
+GetNumBModes()
+GetRfPlot()
+GetSurfaceArea()
+GetSurfaceVrml()
+GetThickness()
+GetVolume()
+InitializeBModes()
-operator=()
+SetDCDVolume()
+SetEditableImageIncluded()
+SetMass()
+SetNormailzedSurfaceArea()
+SetRfPlot()
+SetSurfaceArea()
+SetSurfaceVrml()
+SetThickness()
+SetVolume()
+UnaccessBMode()
+XML()

Fig. 68

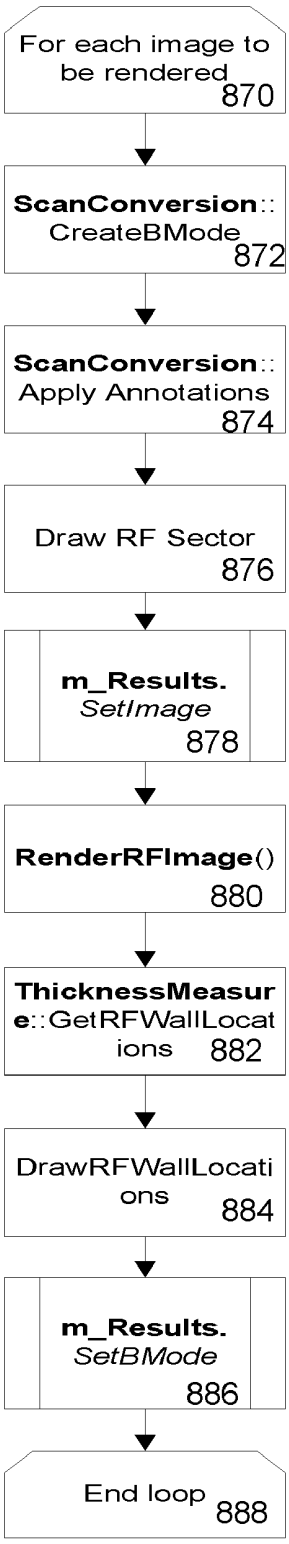
For each image to be rendered
870
ScanConversion:: CreateBMode
872
ScanConversion:: Apply Annotations
874
Draw RF Sector
876
m_Results. SetImage
878
RenderRFImage()
880
ThicknessMeasure::GetRFWallLocations
882
DrawRFWallLocations
884
m_Results. SetBMode
886
End loop
888

Fig. 69

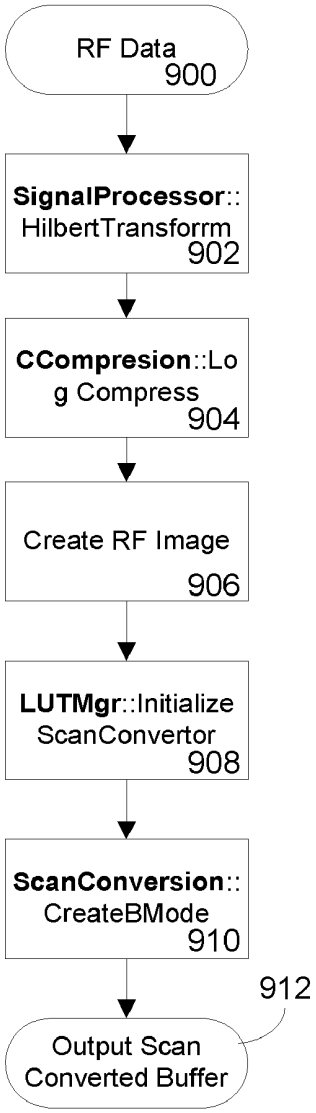
RF Data
900
SignalProcessor:: HilbertTransforrm
902
CCompresion::Log Compress
904
Create RF Image
906
LUTMgr::Initialize ScanConvertor
908
ScanConversion:: CreateBMode
910
912
Output Scan Converted Buffer

Fig. 70

ULTRASOUND SYSTEM AND METHOD FOR MEASURING BLADDER WALL THICKNESS AND MASS

PRIORITY CLAIM

[0001] This application claims priority to U.S. patent application Ser. No. 11/061,867 filed Feb. 17, 2005.

[0002] This application claims priority to U.S. Provisional Patent Application Ser. No. 60/566,823, filed Apr. 30, 2004; to U.S. Provisional Patent Application Ser. No. 60/566,818, filed Apr. 30, 2004; and to U.S. Provisional Patent Application Ser. No. 60/545,576, filed Feb. 17, 2004. This application claims priority to U.S. patent application Ser. No. 11/064,114 filed Feb. 17, 2005.

[0003] This application also claims priority to U.S. application Ser. No. 11/010,539 filed Dec. 13, 2004, which claims priority to PCT/EP03/07807 filed Jul. 17, 2003, which claims priority to UK Application Serial No. 0218547.8 filed Aug. 9, 2002; and U.S. patent application Ser. No. 10/704,996, filed Feb. 3, 2005, which claims priority to PCT/EP03/07807 filed Jul. 17, 2003, which claims priority to UK Application Serial No. 0218547.8 filed Aug. 9, 2002.

[0004] This application is also a continuation-in-part of and claims priority to U.S. patent application Ser. No. 10/704,996, filed Nov. 10, 2003, which claims priority to, and is a continuation-in-part of U.S. patent application Ser. No. 10/701,955 filed Nov. 5, 2003, which claims priority to U.S. patent application Ser. No. 10/633,186, filed Jul. 31, 2003, which claims priority to U.S. patent application Ser. No. 10/443,126 filed May 12, 2003, which claims priority to U.S. Provisional Patent Application Ser. No. 60/423,881, filed Nov. 5, 2002 and to U.S. Provisional Patent Application Ser. No. 60/400,624, filed Aug. 2, 2002.

[0005] This application is also a continuation-in-part of, and claims priority to U.S. patent application Ser. No. 10/165,556, filed Jun. 7, 2002.

[0006] This application is also a continuation-in-part of, and claims priority to Patent Cooperation Treaty (PCT) Application Serial Number PCT/US03/24368, filed Aug. 1, 2003, which claims priority to U.S. Provisional Patent Application Ser. No. 60/423,881, filed Nov. 5, 2002, and U.S. Provisional Patent Application Ser. No. 60/400,624, filed Aug. 2, 2002.

[0007] This application is also a continuation-in-part of, and claims priority to Patent Cooperation Treaty (PCT) Application Serial No. PCT/US03/14785, filed May 9, 2003, which is a continuation of U.S. patent application Ser. No. 10/165,556, filed Jun. 7, 2002.

[0008] This application is also a continuation-in-part of, and claims priority to U.S. patent application Ser. No. 10/633,186, which claims priority to U.S. Provisional Patent Application Ser. No. 60/423,881, filed Nov. 5, 2002, and U.S. Provisional Patent Application Ser. No. 60/400,624, filed Aug. 2, 2002, and to U.S. Patent Application Serial Number 10/443,126, filed May 20, 2003, which claims priority to U.S. Provisional Patent Application Ser. No. 60/423,881, filed Nov. 5, 2002, and to U.S. Provisional Patent Application No. 60/400,624, filed Aug. 2, 2002.

[0009] This application also claims priority to U.S. Provisional Patent Application Ser. No. 60/470,525, filed May 12, 2003, and to U.S. patent application Ser. No. 10/165,556, filed Jun. 7, 2002. All of the foregoing applications are incorporated by reference in their entirety, as if fully set forth herein.

[0010] All of the foregoing applications are incorporated by reference in their entirety, as if fully set forth herein.

FIELD OF THE INVENTION

[0011] This invention relates generally to ultrasound imaging systems and methods, and more particularly, to ultrasound systems and methods used in diagnosing various disease states.

BACKGROUND OF THE INVENTION

[0012] A variety of ultrasound methods may be used to evaluate a bladder dysfunction. In general, such methods estimate a bladder volume containing an amount of urine. For example, U.S. Pat. No. 6,110,111 to Barnard discloses an ultrasound system for estimating bladder pressure by comparing the estimated bladder surface area with the surface area of a comparable sphere. According to Barnard, as the bladder surface area approaches the surface area of the comparable sphere, a greater pressure within the bladder is inferred.

[0013] Other bladder measurements are possible using ultrasound methods, and are similarly useful in the diagnosis of several different bladder conditions. For example, a bladder wall thickness and bladder mass may be estimated using ultrasound, and may be used to indicate a bladder outlet obstruction and/or a bladder distension. In general, a bladder outlet obstruction results in an elevated internal pressure in the bladder that must be overcome by the surrounding muscle as the bladder contracts during urination. Accordingly, an undesired hypertrophy of the bladder muscle often results. Symptoms of bladder muscle hypertrophy generally include increased bladder wall thickness and increased bladder wall mass. See, for example, P. N. Matthews, J. B. Quayle, A. E. A. Joseph, J. E. Williams, K. W. Wilkinson and P. R. Riddle; "The Use of Ultrasound in the Investigation of Prostatism", British Journal of Urology, 54:536-538, 1982; and C. J. Cascione, F. F. Bartone and M. B. Hussain; "Transabdominal Ultrasound Versus Excretory Urography in Preoperative Evaluation of Patients with Prostatism", Journal of Urology, 137:883-885, 1987). Using an estimated bladder wall thickness to infer a bladder wall volume, or, alternately, a bladder wall mass (obtained by multiplying the estimated bladder wall volume by a specific gravity of the bladder tissue) yields a value that is generally independent of the bladder volume. While the bladder wall thins as the volume increases, the total bladder wall volume (or the bladder wall mass) remains generally unchanged.

[0014] Another indicator of the bladder condition is bladder distension. As the bladder volume increases in response to increased internal bladder pressure, the bladder walls elongate and decrease in thickness, resulting in the distention. Bladder distention is generally associated with numerous bladder ailments, including incontinence and hyperdistension. Incontinence occurs when sphincter muscles associated with the bladder are unable to retain urine within the bladder as the bladder pressure and bladder distension increases. In many individuals, incontinence occurs when the bladder volume achieves a consistent maximum volume in the individual. Consequently, if the maximum volume is known, and if the bladder volume can be measured while the volume is approaching the maximum value, incontinence may be prevented. When hyperdistension occurs, the bladder fills with an excessive amount urine and generates an internal bladder

pressure that may cause serious adverse effects, including renal damage, renal failure, or even death of the patient from autonomic dysreflexia if the patient has spinal cord damage.

[0015] It is further observed that normal bladder response is relatively constant at small bladder volumes in typical adult humans. Accordingly, normal healthy adults encounter little physical difficulty voiding, and typically leave less than about 50 milliliters (ml) of urine in the bladder. Thus at the present time, it is relatively easy to distinguish a normal post-void-residual (PVR) volume from an abnormal PVR volume that may be indicative of a potential medical problem. At low bladder volumes, bladder distension information is not typically useful since normal humans have widely varying bladder capacities. Thus, it is more difficult to establish a volume threshold at which over-distension occurs or when incontinence occurs for a selected individual. Consequently, as the bladder fills, measurement of bladder distension becomes more useful as an indicator of hyperdistension and bladder capacity in an individual.

[0016] Current ultrasound methods measure bladder wall thicknesses using one-dimensional (A-mode) and two-dimensional (B-mode) ultrasound modes. Unfortunately, the application of these current methods to determine bladder wall thickness are susceptible to operator error, are time consuming, and generally lead to inaccurate estimations of the bladder wall thickness. For example, in one known ultrasound method, an operator applies an ultrasound probe to an external portion of the patient and projects ultrasound energy into the patient to image a bladder region. Since the operator must repeatedly reposition the ultrasound probe until a bladder wall image is sufficiently visible, inaccuracies may be introduced into the ultrasound data. Consequently, current ultrasound methods to determine bladder wall thickness is an unreliable or ineffective means to measure bladder distension.

[0017] Thus, there is a need for an ultrasound method and system that permits a bladder wall thickness to be accurately measured.

SUMMARY OF THE INVENTION

[0018] Systems and methods for ultrasound imaging an abdominal region in a patient to detect and measure underlying organ structures, and in particular, to image a bladder to determine the thickness, volume and mass of the bladder detrussor are disclosed. In an aspect of the invention, echogenic data is obtained by scanning the abdominal region to obtain a three-dimensional scancone assembly comprised of two-dimensional scanplanes, or an array of three-dimensional distributed scanlines. Selected two-dimensional and one-dimensional algorithms are then applied to the echogenic data to measure the bladder wall thickness and surface area.

[0019] The pixel location of initial wall loci are determined in two-dimensional scanplanes via B-mode echo signal processing algorithms applied to scanlines crossing the organ wall. The pixel location of the initial wall loci serve as an initial approximation of wall location from which more exacting algorithms are applied to either reconfirm the initially selected wall loci, or more likely, to select other loci positions. The reconfirmed or newly selected loci positions are achieved by the application of higher resolving, echo signal processing algorithms to define final wall loci pixel locations. Thereafter, verification of the final wall loci pixel locations are established by cost function analysis using neighboring final pixel locations of scanlines within the same scanplane.

[0020] The final wall pixel loci as determined include the organ outer-wall and the organ inner-wall pixel locations. The distance separating the organ outer-wall and inner-wall final pixel loci determines the thickness of the organ wall. B-mode algorithms applied to the final outer-wall loci pixel locations, as determined by the A-mode algorithms, determine the outer boundary of the organ wall within a given scanplane. Surface area of the inner-wall boundary is determined by analysis of the scanplane arrays within the scancone. Organ wall volume is calculated as a product of organ wall surface area and thickness. Organ wall mass is determined as a product of organ wall volume and density. When the organ is a bladder, the bladder wall thickness and wall mass is calculated to provide information to assess bladder dysfunction.

[0021] The collection of two-dimensional and one-dimensional algorithms includes ultrasound B-mode based segmentation and specialized snake algorithms to determine the surface area of the organ wall and to provide an initial front wall location. The initial front wall location determined by the B-mode algorithms is sufficiently precise to be further processed by the one-dimensional algorithms. The one-dimensional algorithms are unique sequences of A-mode based algorithms applied to the echogenic ultrasound scanlines to further improve the accuracy and precision of wall location loci as initially determined by the B-mode algorithms.

[0022] In accordance with the preferred embodiment of the invention, a microprocessor-based ultrasound apparatus, placed on the exterior of a patient, scans the bladder of the patient in multiple planes with ultrasound pulses, receives reflected echoes along each plane, transforms the echoes to analog signals, converts the analog signals to digital signals, and downloads the digital signals to a computer system.

[0023] Although a variety of scanning and analysis methods may be suitable in accordance with this invention, in a preferred embodiment the computer system performs scan conversion on the downloaded digital signals to obtain a three-dimensional, conically shaped image of a portion of the bladder from mathematical analysis of echoes reflecting from the inner (submucosal) and outer (subserosal) surfaces of the bladder wall. The conical image is obtained via ultrasound pulse echoing using radio frequency (RF) ultrasound (approximately 2-10 MHz) to obtain a three-dimensional array of two-dimensional scanplanes, such that the scanplanes may be a regularly spaced array, an irregular spaced array, or a combination of a regularly spaced array and irregularly spaced array of two-dimensional scanplanes. The two-dimensional scanplanes, in turn are formed by an array of one-dimensional scanlines (ultrasound A-lines), such that the scanlines may be regularly spaced, irregularly spaced, or a combination of regularly spaced and irregularly spaced scanlines. The three-dimensional array of two-dimensional scanplanes results in a solid angle scan cone.

[0024] Alternatively, a solid angle scan cone is obtained by three-dimensional data sets acquired from a three-dimensional ultrasound device configured to scan a bladder in a three-dimensional scan cone of three-dimensional distributed scanlines. The three-dimensional scan cone is not a three-dimensional array of two-dimensional scanplanes, but instead is a solid angle scan cone formed by a plurality of internal and peripheral one-dimensional scanlines. The scanlines are ultrasound A-lines that are not necessarily confined within a scanplane, but would otherwise occupy the inter-scanplane spaces that are in the three-dimensional array of two-dimensional scanplanes.

[0025] The solid angle scan cones, either as a three-dimensional array of two-dimensional scanplanes, or as a three-dimensional scan cone of three-dimensional distributed scanlines, provides the basis to locate bladder wall regions or surface patches of the inner and outer surfaces of the bladder wall. The location of each surface patch is determined and the distance or thickness between the inner and outer surface patches is measured. The bladder wall mass is calculated as a product of the surface area of the bladder, the bladder wall thickness, and the specific gravity of the bladder wall. The entire bladder wall or various regions, including anterior, posterior, and lateral portions of the bladder, may be measured for thickness and mass. Preferred embodiments of the programs to analyze scanline or scanplane data to determine bladder thickness and mass employ algorithms.

[0026] An alternate embodiment of the invention configures the downloaded digital signals to be compatible with a remote microprocessor apparatus controlled by an Internet web-based system. The Internet web-based system has multiple programs that collect, analyze, and store organ thickness and organ mass determinations. The alternate embodiment can measure the rate at which internal organs undergo hypertrophy over time. The programs can include instructions to permit disease tracking, disease progression, and provide educational instructions to patients.

BRIEF DESCRIPTION OF THE DRAWINGS

[0027] The preferred and alternative embodiments of the present invention are described in detail below with reference to the following drawings:

[0028] FIG. **1** is a side elevational view of an ultrasound transceiver according to an embodiment of the invention;

[0029] FIG. **2** is an isometric view of an ultrasound scancone that projects outwardly from the transceiver of FIG. **1**;

[0030] FIG. **3**A is a plan view of an ultrasound scanplane representation of an ultrasound scancone that projects outwardly from the transceiver of FIG. **1**;

[0031] FIG. **3**B is an isometric view of an ultrasound scancone that projects outwardly from the transceiver of FIG. **1**;

[0032] FIG. **3**C is a scancone that is generated by the transceiver of FIG. **1**;

[0033] FIG. **3**D is a plan view of the scancone of FIG. **3**C;

[0034] FIG. **3**E is side-elevational view of the scanplane of FIG. **3**C and FIG. **3**D;

[0035] FIG. **4**A is an isometric view of the transceiver of FIG. **1** applied to an abdominal region of a patient;

[0036] FIG. **4**B is a perspective view of the transceiver of FIG. **1** positioned in a communication cradle according to another embodiment of the invention;

[0037] FIG. **5** is a partially-schematic view of an imaging system according to another embodiment of the invention;

[0038] FIG. **6** is a partially-schematic view of a networked imaging system according to still another embodiment of the invention;

[0039] FIG. **7** is a cross sectional view of a selected anatomical portion that will be used to further describe the various embodiments of the present invention;

[0040] FIG. **8** is a cross sectional view of the anatomical region of FIG. **7** as the region is imaged by the transceiver of FIG. **1**;

[0041] FIGS. **9**A through **9**D are four exemplary and sequential ultrasound images obtained from a male subject during an ultrasound examination;

[0042] FIGS. **10**A through **10**D are four exemplary and sequential ultrasound images obtained from a female subject during an ultrasound examination;

[0043] FIG. **11** is an exemplary, non-rectified echogenic signal received along a selected scanline during ultrasound imaging of a bladder;

[0044] FIG. **12** is an exemplary processed echogenic signal pattern from the selected scanline of the bladder imaging of FIG. **15**;

[0045] FIG. **13** is the processed echogenic signal pattern of FIG. **12** that further shows a waveform that is generated by additional processing of the rectified waveform;

[0046] FIG. **14** is a method algorithm of the particular embodiments;

[0047] FIG. **15** is a flowchart that describes a method for scanning a bodily organ, according to an embodiment of the invention;

[0048] FIG. **16** is a diagram that describes a method for determining incident angles;

[0049] FIG. **17** is an idealized diagram of an echogenic envelope having an intensity pattern that crosses a front bladder organ wall;

[0050] FIG. **18** is an envelope of a scanline having an echogenic intensity distribution that crosses highly reflective adipose;

[0051] FIG. **19** is a B-mode ultrasound image that shows a family of wall layer locations corresponding to the candidate points of FIG. **18**;

[0052] FIG. **20** is a diagrammatic view of a plurality of candidate wall points that result from an echogenic distribution;

[0053] FIG. **21**A is a flowchart of a method for identifying an outer wall location according to an embodiment of the invention;

[0054] FIG. **21**B is a flowchart of a method for identifying an inner wall location according to an embodiment of the invention;

[0055] FIG. **22** is an exemplary graph of a cost function generated along a selected scanline;

[0056] FIG. **23** is an exemplary scanplane of an internal anatomical region having a sector of scanlines superimposed on the scanplane;

[0057] FIG. **24** is an expanded portion of the scanplane **42** of FIG. **24** that shows the initial front wall location in greater detail;

[0058] FIG. **25** is an expansion of the sub-algorithm **172** of FIGS. **14** and **15**;

[0059] FIG. **26** is an expansion of the sub-algorithm **180** of FIG. **14**;

[0060] FIG. **27** is an expansion of the sub-algorithm **180**A of FIG. **26**;

[0061] FIG. **28** is an expansion of the sub-algorithm **180**C of FIG. **26**;

[0062] FIG. **29** is an expansion of the sub-algorithm **180**J of FIG. **26**;

[0063] FIG. **30** is an expansion of the sub-algorithm **184** of FIG. **14**;

[0064] FIG. **31** is an expansion of the sub-algorithm **188** of FIG. **14**;

[0065] FIG. **32** is an expansion of the sub-algorithm **192** of FIG. **31**;

[0066] FIG. **33** is an expansion of the sub-algorithm **192**A of FIG. **32**;

[0067] FIG. **34** is an expansion of the sub-algorithm **192**C of FIG. **32**;
[0068] FIG. **35** is an expansion of the sub-algorithm **192**C**10** of FIG. **34**;
[0069] FIG. **36** is an expansion of the sub-algorithm **192**E of FIG. **32**;
[0070] FIGS. **37**A-D are B-mode scans overlaid with interface tracings;
[0071] FIGS. **38**A-D are B-mode scans overlaid with interface tracings;
[0072] FIGS. **39**A-D are B-mode scans overlaid with interface tracings;
[0073] FIGS. **40**A-B are normal and magnified B-mode scans overlaid with interface tracings;
[0074] FIGS. **41**A-B are normal and magnified B-mode scans overlaid with interface tracings;
[0075] FIG. **42** is an alternative-algorithm of FIG. **15**;
[0076] FIGS. **43**A-B are B-mode scans overlaid with interface tracings;
[0077] FIGS. **44**A-B are B-mode scans overlaid with interface tracings;
[0078] FIGS. **45**A-B are B-mode scans overlaid with interface tracings;
[0079] FIGS. **46**A-B are B-mode scans overlaid with interface tracings;
[0080] FIGS. **47**A-B are B-mode scans overlaid with interface tracings;
[0081] FIGS. **48**A-B are B-mode scans overlaid with interface tracings;
[0082] FIG. **49** is a method algorithm for the Internet System;
[0083] FIG. **50** is a screen shot of four image panels;
[0084] FIG. **51** is a screen shot of two image panels;
[0085] FIG. **52** is a screen shot of six image panels;
[0086] FIG. **53** is a screen shot of Exam Quality Report;
[0087] FIG. **54** is a screen shot of two image panels; and
[0088] FIG. **55** is a scanplane image overlaid with inner and outer wall tracings using algorithms of the Internet System.

DETAILED DESCRIPTION OF TIE PREFERRED EMBODIMENT

[0089] FIG. **1** is a side elevational view of an ultrasound transceiver **10**. Transceiver **10** includes a transceiver housing **18** having an outwardly extending handle **12** suitably configured to allow a user to manipulate transceiver **10**. The handle **12** includes a trigger **14** that allows the user to initiate an ultrasound scan of a selected anatomical portion, and a cavity selector **16**, described below. Transceiver **10** includes a transceiver dome **20** that contacts a surface portion of the patient when the selected anatomical portion is scanned to provide an appropriate acoustical impedance match and to properly focus ultrasound energy as it is projected into the anatomical portion. The transceiver **10** further includes an array of separately excitable ultrasound transducer elements (not shown in FIG. **1**) positioned within the housing **18**. The transducer elements are suitably positioned within the housing **18** to project ultrasound energy outwardly from the dome **20**, and to permit reception of acoustic reflections generated by internal structures within the anatomical portion. The array of ultrasound elements may include a one-dimensional, or a two-dimensional array of piezoelectric elements that are moved within the housing **18** by a motor, of a transceiver dome **20** that contacts a surface portion of the patient when the selected anatomical portion is scanned, or other similar actuation means to scan the selected anatomical region. Alternately, the array may be stationary with respect to the housing **18** so that the selected anatomical region is scanned by selectively energizing the elements in the array. Transceiver **10** includes a display **24** operable to view processed results from the ultrasound scan, and to allow operational interaction between the user and the transceiver **10**. Display **24** may be configured to display alphanumeric data that indicates a proper and/or optimal position of the transceiver **10** relative to the selected anatomical portion. In other embodiments, two- or three-dimensional images of the selected anatomical region may be displayed on the display **24**. The display **24** may be a liquid crystal display (LCD), a light emitting diode (LED) display, a cathode ray tube (CRT) display, or other suitable display devices operable to present alphanumeric data and/or graphical images to a user.

[0090] Still referring to FIG. **1**, the cavity selector **16** is structured to adjustably control the transmission and reception of ultrasound signals to the anatomy of a patient. In particular, the cavity selector **16** adapts the transceiver **10** to accommodate various anatomical details of male and female patients. For example, when the cavity selector **16** is adjusted to accommodate a male patient, the transceiver **10** is suitably configured to locate a single cavity, such as a urinary bladder in the male patient. In contrast, when the cavity selector **16** is adjusted to accommodate a female patient, the transceiver **10** is configured to image an anatomical portion having multiple cavities, such as a bodily region that includes a bladder and a uterus. Alternate embodiments of the transceiver **10** may include a cavity selector **16** configured to select a single cavity scanning mode, or a multiple cavity-scanning mode that may be used with male and/or female patients. The cavity selector **16** may thus permit a single cavity region to be imaged, or a multiple cavity region, such as a region that includes a lung and a heart to be imaged.

[0091] To scan a selected anatomical portion of a patient, the transceiver dome **20** of the transceiver **10** is positioned against a surface portion of a patient that is proximate to the anatomical portion to be scanned. The user then actuates the transceiver **10** by depressing trigger **14**. In response, transceiver **10** transmits ultrasound signals into the body, and receives corresponding return echo signals that are at least partially processed by the transceiver **10** to generate an ultrasound image of the selected anatomical portion. In a particular embodiment, the transceiver **10** transmits ultrasound signals in a range that extends from approximately about two megahertz (MHz) to approximately about ten MHz.

[0092] In one embodiment, the transceiver **10** is operably coupled to an ultrasound system that is configured to generate ultrasound energy at a predetermined frequency and/or pulse repetition rate and to transfer the ultrasound energy to the transceiver **10**. The system also includes a processor that is configured to process reflected ultrasound energy that is received by the transceiver **10** to produce an image of the scanned anatomical region. Accordingly, the system generally includes a viewing device, such as a cathode ray tube (CRT), a liquid crystal display (LCD), a plasma display device, or other similar display devices, that may be used to view the generated image. The system may also include one or more peripheral devices that cooperatively assist the processor to control the operation of the transceiver **10**, such a keyboard, a pointing device, or other similar devices. The ultrasound system will be described in greater detail below. In still another particular embodiment, the transceiver **10** may

be a self-contained device that includes a microprocessor positioned within the housing **18** and software associated with the microprocessor to operably control the transceiver **10**, and to process the reflected ultrasound energy to generate the ultrasound image. Accordingly, the display **24** is used to display the generated image and/or to view other information associated with the operation of the transceiver **10**. For example, the information may include alphanumeric data that indicates a preferred position of the transceiver **10** prior to performing a series of scans. In yet another particular embodiment, the transceiver **10** may be operably coupled to a general-purpose computer, such as a laptop or a desktop computer that includes software that at least partially controls the operation of the transceiver **10**, and also includes software to process information transferred from the transceiver **10**, so that an image of the scanned anatomical region may be generated.

[0093] Although transceiver **10** of FIG. **1** may be used in any of the foregoing embodiments, other transceivers may also be used. For example, the transceiver may lack one or more features of the transceiver **10**. For example, a suitable transceiver may not be a manually portable device, and/or may not have a top-mounted display, or may selectively lack other features or exhibit further differences.

[0094] FIG. **2** is an isometric view of an ultrasound scancone **30** that projects outwardly from the transceiver **10** of FIG. **1** that will be used to further describe the operation of the transceiver **10**. The ultrasound scancone **30** extends outwardly from the dome **20** of the transceiver **10** and has a generally conical shape comprised of a plurality of discrete scanplanes having peripheral scanlines **31**A-**31**F that define an outer surface of the scancone **30**. The scanplanes also include internal scanlines **34**A-**34**C that are distributed between the respective peripheral scanlines **31**A-**31**F of each scanplane. The scanlines within each scanplane are one-dimensional ultrasound A-lines that taken as an aggregate define the conical shape of the scancone **30**.

[0095] With reference still to FIG. **2** and now also to FIG. **3**A, an ultrasound scancone **40** formed by a rotational array of two-dimensional scanplanes **42** projects outwardly from the dome **20** of the transceiver **10**. The plurality of scanplanes **40** are oriented about an axis **11** extending through the transceiver **10**. Each of the scanplanes **42** are positioned about the axis **11** at a predetermined angular position θ. The scanplanes **42** are mutually spaced apart by angles θ_1 and θ_2. Correspondingly, the scanlines within each of the scanplanes **42** are spaced apart by angles Φ_1 and Φ_2. Although the angles θ_1 and θ_2, are depicted as approximately equal, it is understood that the angles θ_1 and θ_2 may have different values. Similarly, although the angles Φ_1 and Φ_2 are shown as approximately equal, the angles Φ_1 and Φ_2 may also have different angles.

[0096] Referring now also to FIG. **3**B, the peripheral scanlines **44** and **46**, and an internal scanline **48** is further defined by a length r that extends outwardly from the transceiver **10** (FIG. **3**A). Thus, a selected point P along the peripheral scanlines **44** and **46** and the internal scanline **48** may be defined with reference to the distance r and angular coordinate values Φ and θ.

[0097] With continued reference to FIGS. **2**, **3**A and **3**B, the plurality of peripheral scanlines **31**A-E and the plurality of internal scanlines **34**A-D are three-dimensional-distributed A-lines (scanlines) that are not necessarily confined within a scanplane, but instead may sweep throughout the internal regions and along the periphery of the scancone **30** (FIG. **2**). Thus a given point P within the scancone **30** may be identified by the coordinates r, Φ, and θ whose values can vary. The number and location of the internal scanlines emanating from the transceiver **10** may thus be distributed within the scancone **30** at different positional coordinates as required to sufficiently visualize structures or images within the scancone **30**. As described above, the angular movement of the transducer may be mechanically effected, or it may be electronically generated. In either case, the number of lines and the length of the lines may vary, so that the tilt angle Φ sweeps through angles approximately between −60° and +60° for a total arc of approximately 120°. In one embodiment, the transceiver **10** is configured to generate a plurality of scanlines between the first limiting scanline **44** and the second limiting scanline **46** of approximately about seventy-seven, each having a length of approximately about 18 to 20 centimeters (cm).

[0098] As previously described, the angular separation between adjacent scanlines **34** (FIG. **2**) may be uniform or non-uniform. For example, and in another particular embodiment, the angular separation Φ_1 and Φ_2 (as shown in FIG. **2**) may be about 1.5°. Alternately, and in another particular embodiment, the angular separation Φ_1 and Φ_2 may be a sequence wherein adjacent angles are ordered to include angles of 1.5°, 6.8°, 15.5°, 7.2°, and so on, where a 1.5° separation is between a first scanline and a second scanline, a 6.8° separation is between the second scanline and a third scanline, a 15.5° separation is between the third scanline and a fourth scanline, a 7.2° separation is between the fourth scanline and a fifth scanline, and so on. The angular separation between adjacent scanlines may also be a combination of uniform and non-uniform angular spacings, for example, a sequence of angles may be ordered to include 1.5°, 1.5°, 1.5°, 7.2°, 14.3°, 20.2°, 8.0°, 8.0°, 8.0°, 4.3°, 7.8°, so on.

[0099] After a scanplane **42** is generated, the transceiver **10** rotates the transducer through a rotational angle θ (FIG. **3**A) to position the transducer assembly within the transceiver **10** to a different angular increment, to generate another scanplane. As the transducer assembly is rotated in the direction θ, a series of scanplanes is generated, with each scanplane slightly rotated in relation to the prior scanplane by a selected increment of the rotational angle θ. As previously described, the increment between adjacent scanplanes may be uniform or no uniform. For example, and with reference still to FIG. **3**B, in another particular embodiment, each scanplane **42** may be projected at an approximately 7.5° rotational angle increment. In other embodiments, the angular increment may be non-uniform and arranged in a sequence wherein the spacing between adjacent scanplanes includes 3.0°, 18.5°, 10.2°, and so on. Accordingly, an increment of approximately 3.0° is present between a first scanplane and a second scanplane, an increment of approximately 18.5° is present between the second scanplane and a third scanplane, and an increment of approximately 10.2° is present between the third scanplane and a fourth scanplane, and so on. The scanplane interval may also be a combination of uniform and non-uniform rotational angle increments, such as, for example, a sequence of incremental angles ordered in a sequence including 3.0°, 3.0°, 3.0°, 18.5°, 10.2°, 20.6°, 7.5°, 7.5°, 7.5°, 16.0°, 5.8° and so on.

[0100] FIG. **3**C is a scancone **40** that is generated by the transceiver **10**. The scancone **40** includes a dome cutout **41** near an apex of the scancone **40** that is formed, at least in part, to the presence of the transceiver dome **20** (as shown in FIG. **1**). Referring now to FIG. **3**D, a plan view of the scancone **40**

of FIG. **3**D is shown. The dome cutout **41** is positioned at an approximate center of the scancone **40**, with each of the scanplanes **42** mutually spaced apart by the angular increment θ. Although the scancone **40** includes forty-eight scanplanes **42** that are mutually uniformly spaced apart, the number of scanplanes **42** in the scancone **40** may include at least two, but can be varied to include any desired number of scanplanes **42**.

[0101] FIG. **3**E is side-elevational view of the scanplane **42** of FIG. **3**C and FIG. **3**D that includes approximately about seventy-seven scanlines **48** that extend outwardly from the dome cutout **41**. Other scancone configurations are possible. For example, a wedge-shaped scancone, or other similar shapes may be generated by the transceiver **10** (FIG. **1**).

[0102] FIG. **4**A is an isometric view of the transceiver **10** of FIG. **1** applied to an abdominal region of a patient, which is representative of a data acquisition method for a bladder wall mass determination in the patient. In contact with the patient is a pad **67** containing a sonic coupling gel to minimize ultrasound attenuation between the patient and the transceiver **10**. Alternatively, sonic coupling gel may be applied to the patient's skin. The dome **20** (not shown) of the transceiver **10** contacts the pad **67**. The transceiver **10** may the used to image the bladder trans-abdominally, and initially during a targeting phase, the transceiver **10** is operated in a two-dimensional continuous acquisition mode. In the two-dimensional continuous mode, data is continuously acquired and presented as a scanplane image as previously shown and described. The data thus acquired may be viewed on a display device, such as the display **24**, coupled to the transceiver **10** while an operator physically translates the transceiver **10** across the abdominal region of the patient. When it is desired to acquire data, the operator may acquire data by depressing the trigger **14** of the transceiver **10** to acquire real-time imaging that is presented to the operator on the display device.

[0103] FIG. **4**B is a perspective view of the transceiver **10** of FIG. **1** positioned in a communication cradle **50** according to another embodiment of the invention. The communication cradle **50** is operable to receive the transceiver **10**, and to transfer data and/or electrical energy to the transceiver **10**. In another particular embodiment of the invention, the cradle **50** may include a data storage unit configured to receive imaging information generated by the transceiver **10** (not shown), and may also include a data interface **13** that may be employed to transfer the acquired imaging information to other processors or systems for further image processing. In a particular embodiment, the data interface may include a universal serial bus (USB) interface having a connecting cable **53**. In other embodiments, the data interface **13** may include a FIREWIRE interface, an RS-232 interface, or other similar and known interface devices. In still another particular embodiment, the data interface **13** may be used to transfer programmed instructions to a processing device positioned within the transceiver **10**.

[0104] FIG. **5** is a partially schematic view of an imaging system **51** according to another embodiment of the invention. The system **51** includes at least one transceiver **10** in communication with a computer device **52** that is further in communication with a server **56**. The at least one transceiver **10** is operable to project ultrasound energy into a patient and to receive the resulting ultrasound echoes, as previously described. The ultrasound echoes may be converted to digital signals within the transceiver **10**, or alternately within the computer device **52** that is coupled to the transceiver **10**. Similarly, the digital signals may be stored and processed in the transceiver **10**, or within the computer device **52** to generate ultrasound images that may be viewed on a display **54** that is coupled to the computer device **52**. In either case, the transceiver **10** may be coupled to the computer device **52** by the connecting cable **53**, or by means of a wireless link, such as an ETHERNET link, or an infrared wireless link. The transceiver **10** and/or the computer device **52** are configured to process the digital signals using algorithms that will be explained in greater detail below.

[0105] Still referring to FIG. **5**, the computer device **52** may communicate information to the server **56**, which is configured to receive processed images and/or image data from the computer device **52** and/or the transceiver **10**. The server **56** may include any computer software and/or hardware device that is responsive to requests and/or issues commands to or from at least one client computer (not shown in FIGURE **5**). The server **56** is coupled to the computer device **52** by a local communications system **55**, such as a telephone network or a local area network (LAN) or other similar networks.

[0106] The operation of the imaging system **51**. Each transceiver **10** may be separately and independently used to project ultrasound information into a selected region of the patient and to transmit the signals proportional to the received ultrasound echoes to the computer device **52** for storage and/or further processing. If the image processing occurs in the computer device **52**, each computer device **52** includes imaging software having instructions to prepare and analyze a plurality of one dimensional images from the stored signals and to transform the plurality of images into a plurality of two-dimensional scanplanes, as previously described. Additionally, the imaging software programs may also present three-dimensional renderings from the plurality of two-dimensional scanplanes. Each computer device **52** may also include instructions to perform other additional ultrasound image enhancement procedures, which may include instructions to implement the image processing algorithms.

[0107] In another embodiment of the system **51**, the imaging software programs and other instructions that perform additional ultrasound enhancement procedures are located on the server **56**. Each computer device **52** coupled to the system **51** receives the acquired signals from the transceiver T**0** using the cradle **50** and stores the signals in the memory of the computer device **52**. The computer device **52** subsequently retrieves the imaging software programs and the instructions to perform the additional ultrasound enhancement procedures from the server **56**. Thereafter, each computer device **52** prepares the one-dimensional images, the two-dimensional images, and the three-dimensional renderings, as well as enhanced images from the retrieved imaging and ultrasound enhancement procedures. Results from the data analysis procedures may then be sent to the server **56** for storage.

[0108] In still another embodiment of the system **51**, the imaging software programs and the instructions to perform the additional ultrasound enhancement procedures are located in the server **56** and executed on the server **56**. Each computer device **52** in the system **51** receives the acquired signals from the transceiver **10** and sends the acquired signals to the memory of the computer **52** through the cradle **50**. The computer device **52** subsequently sends the stored signals to the server **56**. In the server **56**, the imaging software programs and the instructions to perform the additional ultrasound enhancement procedures are executed to prepare the one-dimensional images, two-dimensional images, three-dimen-

sional renderings, and enhanced images from the signals. Results from the data analysis procedures may be stored by the server **56**, or alternatively, sent to a client computer coupled to the server for archival storage, or for other purposes.

[0109] FIG. **6** is a partially schematic view of a networked imaging system **61** according to still another embodiment of the invention. Many of the elements of the present embodiment have been discussed in detail in connection with other embodiments, and in the interest of brevity, will not be discussed further. The networked imaging system **61** includes a public data network **64** interposed between the computer device **52** and the server **66**. The public data network **64** may include a LAN, a WAN, or the Internet. Accordingly, other computational devices associated with the public data network **64** may communicate imaging data and/or ultrasound images with the portable computing devices **52** and the server **56**. Although two transceivers **10** are shown in the networked imaging system **61** shown in FIG. **6**, fewer that two, or more than two transceivers **10** may be present. The public data network **64** advantageously permits the system **61** to communicate images and data to other computer devices and/or processors.

[0110] FIG. **7** is a cross sectional view of a selected anatomical portion that will be used to further describe the various embodiments of the present invention. As shown in FIG. **7**, the transceiver **10** is placed over the anatomical portion, which may include a urinary bladder and surrounding tissues of a male patient. Also shown, the dome **20** of the transceiver is placed in contact with a sonic coupling gel contained within a pad **67** to minimize ultrasound attenuation between the patient and the transceiver **10**. Alternatively, the dome **20** may be placed in contact with a sonic coupling gel applied on the patient's skin. A wall of the urinary bladder may be divided into three distinct and observable layers, including an outer wall layer (visceral peritoneum), an opposing inner wall layer, and an inter-wall layer positioned between the outer layer and the inner layer. In general, muscular contraction in the bladder results from muscular tissue in the inter-wall layer, so that urine within the bladder may be excreted. The bladder wall thickness typically varies between about 1.0 millimeter (mm) and about 4.0 millimeters (mm). Since the volume of the bladder wall is a product of an area of the bladder and the thickness of the bladder wall, an estimation of the bladder wall volume is reasonably accurate if the surface area determination of the bladder wall and the thickness of the bladder wall is sufficiently precise. Assuming the thickness of the bladder wall is substantially uniform around the bladder, a bladder wall mass can be calculated as a product of the bladder wall volume and an estimation of the density of the wall tissue. The bladder wall mass calculations are thus similarly limited by the accuracy of the bladder wall surface area determination and the bladder wall thickness measurement.

[0111] FIG. **8** is a cross sectional view of the anatomical region of FIG. **7** as the region is imaged by the transceiver **10**. As previously described, the transceiver **10** is operable to image the anatomical region by generating a scanplane **42** that is further comprised of a plurality of scanlines **48**. In FIG. **8**, the partial scanplane **42** is superimposed on a B-mode ultrasound image of the anatomical region in order to illustrate the plurality of scanlines **48** crossing the front bladder wall (e.g., the wall closer to the dome **20**) and extending through the bladder to the back wall of the bladder.

[0112] FIGS. **9**A through **9**D are four exemplary and sequential ultrasound images obtained from a male subject during an ultrasound examination. The ultrasound images were obtained using lower resolving B-mode algorithms, and show a bladder volume surrounded by a bladder wall. In FIGS. **9**A through **9**D, the front and back walls of the bladder are shown surrounding a generally darker bladder volume. As shown in FIGS. **9**A through **9**D, the front wall and the back wall of the bladder are relatively poorly defined.

[0113] FIGS. **10**A through **10**D are four exemplary and sequential ultrasound images obtained from a female subject during an ultrasound examination. The ultrasound images in FIGS. **10**A through **10**D were also obtained using lower resolving B-mode algorithms. In FIGS. **10**A through **10**D, the bladder is similarly poorly defined, and a uterine structure is detected beyond the bladder. The bladder front wall (BFW) and an opposing bladder back wall (BBW) along with the uterine front wall (UFW) and a uterine back wall (UBW) are imaged, but are still rather poorly defined. Thus, the ability to easily discern the front and back walls of a uterus and a bladder from the same female subject using selected wall locations obtained from B-mode imaging is difficult to establish. In particular, the determination of the narrower distances between the outer and inner wall layer locations of the uterus or bladder is often very difficult to establish.

[0114] FIG. **11** is an exemplary, non-rectified echogenic signal received along a selected scanline during ultrasound imaging of a bladder. The echogenic signal pattern includes an outer wall reflection, which is shown as a solid line, which results from a reflection that occurs at the outer wall of a bladder (as best seen in FIG. **7**), and an inner wall reflection (as also shown in FIG. **7**), resulting from a reflection occurring at an inner wall of the bladder, which is shown as a dashed line. Since the non-rectified inner wall reflection and the outer wall reflection signals at least partially overlap, it may be difficult to accurately discern a location of the inner wall of the bladder from the outer wall location.

[0115] FIG. **12** is an exemplary processed echo signal pattern from the selected scanline of the bladder imaging of FIG. **8**. The outer wall and inner wall reflection signals are algebraically summed and rectified to generate a signal envelope waveform. Rectification is achieved by performing a Hilbert transform to the algebraically summed waveform. The positive signal envelope waveform obtained by the Hilbert transform advantageously allows a central location of the outer and the inner layers of the front organ walls to be accurately located since the envelope exhibits a more pronounced signal peak corresponding to the outer and the inner walls.

[0116] FIG. **13** is the processed echogenic signal pattern of FIG. **12** that further shows a waveform that is generated by additional processing of the rectified waveform. The waveform (represented by a dotted line in FIG. **13**) may be generated by processing the rectified waveform of FIG. **12** using an A-mode algorithm so that selected bladder wall locations may be more easily identified. The processed rectified waveform is generally sharper and/or exhibits peaks that permit various maximum points on the processed rectified waveform may be easily identified. Once identified, the maximum waveform points may then be used to select candidate points for further bladder wall imaging, described below.

[0117] FIG. **14** is a method algorithm of the particular embodiments. The method algorithm **170** is comprised of 8 sub-algorithms that culminate in the calculation of the mass of the organ wall. In block **172**, the ultrasound probe is posi-

tioned over the abdomen of a patient and a scan is commenced to acquire at least a portion of an organ wall image. The echoes are received and processed in the next block, block **176**. A block **176** signals are generated from the echoes in proportion to their signal strength and the signals are processed and presented as a 2-D ultrasound image in the format of two-dimensional scanplanes. This is commonly referred to as B-mode ultrasound. The next block is block **180** in which the desired organ in the 2-D scanplanes is selected and wall loci of the organ wall in at least one scanplane is delineated. Algorithm **170** continues with block **184** in which the initial wall delineation from the 2-D scanplane is now further refined or adjusted. The adjustment of the 2-D wall loci position is achieved by applying a 1-D analysis of the scanline echo signals to obtain inner and outer wall layer loci. The next block is block **188** in which the thickness of the organ wall is calculated as a difference between the inner and outer wall layer loci as determined from block **184**. The algorithm **170** continues with block **192** in which 2-D scanplanes obtained from B-mode ultrasound are assembled into a 3D array and the wall surface area of the organ wall is calculated. In block **300**, the volume of the organ wall is calculated as a product of the thickness as determined from block **188** and the surface area as determined from block **192**. Finally, in block **400**, the mass of the organ wall is calculated as a product of the volume obtained from block **300** and the tissue density of the organ wall.

[0118] FIG. **15** is a flowchart that will be used to describe a method **170** for scanning a bodily organ, according to an embodiment. At block **172**, ultrasound energy is projected into the bodily organ, and reflections from various internal structures are acquired, that constitutes raw ultrasound data The raw data may be collected, for example, using the device shown in FIG. **1**, or in any of the other disclosed embodiments described herein. Block **184** describes the procedures to obtain points for the inner and outer wall layers. At block **184**A, the raw data is processed to generate an RF envelope, as earlier described and shown in FIG. **16** and FIG. **17**. In addition, at block **176**, B-mode scans of the bodily organ are also compiled. Based upon the B-mode data acquired at block **176**, a family of bladder wall locations may be generated, as will be described below.

[0119] At block **184**C, incident angles for each of the scanlines projected into the bodily organ are calculated as will also be described below. In general terms, the calculation of the incident angle permits better discrimination between an inner wall and an outer wall of the organ. At block **184**E, candidate points that characterize the position of the inner wall, the outer wall and the position of intermediate layers between the inner wall and the outer wall are determined. The determination of candidate points will also be described in greater detail below. Based upon the candidate points generated at block **184**E, candidate walls may be generated at block **184**G. The candidate walls comprise a family of possible wall locations, which will be further processed, as described below.

[0120] Still referring to FIG. **15**, at block **184**J, an inner wall layer location is identified from amongst the candidate walls determined at block **184**G. An outer wall location is also identified at block **184**L, which represents a refined estimate of an actual outer wall layer location. The determination of the inner wall location and the outer wall location will be described in greater detail below. Based upon the inner wall layer and the outer wall layer determinations at blocks **184**J and **184**L, respectively, and the incident angle determinations at block **184**C, a wall thickness may be determined at block **188**. A surface area of the bodily organ may be determined based upon the B-mode data collected at block **192**. Based upon the surface area determination at block **192** and the wall thickness determination at block **188**, an organ volume value **300** and an organ mass value **400** for the organ wall may then be determined by routine calculation.

[0121] In FIG. **16**, a method for determining incident angles will now be described. The scancone **20** of the transceiver **10** (FIG. **1**) projects ultrasound energy towards an anatomical portion that includes a front wall of a bodily organ, such as a urinary bladder. In general, the scancone **20** is positioned at an angle Ω with respect to a normal direction relative to the bladder wall of a patient. A wall thickness is defined by a distance between an inner wall and an outer wall of the bladder along the surface normal T. Also, the inner and outer walls are most clearly discerned on scanlines that are normal to the bladder surface. Accordingly, the incident angle of each of the scanlines **48** of the scanplane **42** is supplied. A first vector R_1 extends along a first scanline having a tilt angle ϕ_1 and a second vector R_2 extends along a second scanline having a tilt angle ϕ_2. Accordingly, a vector R_{12} that is a difference between the first vector R_1 and the second vector R_2 extends between R_1 and R_2.

[0122] In general, the vector $\vec{R}$ extends from the cone vertex at an incident angle ϕ. In the interest of clarity of illustration, a two-dimensional representation of $\vec{R}$ is shown in FIG. **18**. It is understood, however, that the vector $\vec{R}$ is oriented in three-dimensional space. Accordingly, in the description that follows, the vector $\vec{R}$ may be expressed in equation E1 as:

$$\vec{R}=(R\cos\Phi, R\sin\Phi, 0) \quad \text{E1}$$

where, R is the distance between the cone vertex and a segmentation point positioned on the front wall. The two adjacent neighbor points, $\vec{R}_1$ and $\vec{R}_2$, are expressed similarly in equation E2 and E3:

$$\vec{R}_1=(R_1\cos\Phi_1, R_1\sin\Phi_1, 0) \quad \text{E2}$$

$$\vec{R}_2=(R_2\cos\Phi_2, R_2\sin\Phi_2, 0) \quad \text{E3}$$

The surface vector, $\vec{R}_{12}$, may be expressed in terms of the two adjacent points, $\vec{R}_1$ and $\vec{R}_2$ by a vector addition, as follows in equation E4:

$$\vec{R}_{12}=\vec{R}_2-\vec{R}_1 \quad \text{E4}$$

The surface normal vector T is orthogonal to the surface vector, $\vec{R}_{12}$. When the vector T is rotated through an angle θ about the y-axis, a rotation matrix and an orthogonal matrix may be defined, respectively, as follows:

$$\begin{bmatrix} \cos\theta' & 0 & -\sin\theta' \\ 0 & 1 & 0 \\ \sin\theta' & 0 & \cos\theta' \end{bmatrix} \text{ and } \begin{bmatrix} 0 & -1 & 0 \\ 1 & 0 & 0 \\ 0 & 0 & 1 \end{bmatrix}$$

where in the present case, θ' is an angle between the orthogonal plane, and if the image is in a first plane, the angle θ' will be zero, and if the image is the 13th plane (in a 24-plane image), the angle θ' will be the incident angle of the broadside scanline relative to the first plane.

Therefore, a surface normal vector, $\vec{R}_{12}^{\perp ccw}$ may be calculated using the above rotation and orthogonal matrices as described in equation E5.

$$\vec{R}_{12}^{\perp ccw} = \begin{bmatrix} \cos\theta' & 0 & -\sin\theta' \\ 0 & 1 & 0 \\ \sin\theta' & 0 & \cos\theta' \end{bmatrix} \begin{bmatrix} 0 & -1 & 0 \\ 1 & 0 & 0 \\ 0 & 0 & 1 \end{bmatrix} \vec{R}_{12} \quad \text{E5}$$

[0123] The angle between the two vectors, $\vec{R}$ and $\vec{R}_{12}^{\perp ccw}$ is the incident angle θ, which may be determined as follows in equation E6:

$$\theta = \vec{R} \angle \vec{R}_{12}^{\perp ccw} = \cos^{-1}\left(\frac{\vec{R} \cdot \vec{R}_{12}^{\perp ccw}}{\|\vec{R}\| \cdot \|\vec{R}_{12}^{\perp ccw}\|} \right) \quad \text{E6}$$

[0124] where "||•||" indicates a vector length and "•" is the dot product of the two vectors.

[0125] The above method can be extended to calculate the incidence angle in a three-dimensional space. In case of such a three dimensional extension, a two-dimensional plane is fit to all points in the neighborhood of point R. The normal direction to this plane is determined $\vec{R}_{12}^{\perp ccw}$ and then the incidence angle is calculated as in Equation E6. To fit the plane to a neighborhood of points and determine the normal direction to the plane, an eigenvector-based approach is used. First calculate a 3 by 3 covariance matrix C for all the points in the neighborhood of point $\vec{R}$. The eigenvalues and the eigenvectors of this 3 by 3 matrix are then calculated. Thereafter, the normal direction is determined the eigenvector corresponding the smallest eigenvalue.

[0126] FIG. **17** is a diagram that shows an idealized envelope having echogenic intensity distributed along a scanline similar to the scanline **48** of FIG. **8** that crosses the front bladder wall. In FIG. **17**, only the echogenic pattern of the front bladder wall is shown, so that the strongly echogenic patterns caused by adipose and peritoneum tissues are not shown. The front wall profile shown in FIG. **17** is bimodal, and where the proximal wall outer layer generates an outer layer peak having a signal midpoint maxima near a distance value of 30, a middle layer (bladder muscle) having a signal minima near a distance value of 50, and a distal inner layer peak that presents another signal midpoint maxima near a distance value of 70. A search region for candidate points may therefore include at least the distance between the exterior slopes the outer and inner layers peaks, indicated by the vertical lines that intersect near a distance value of 25 for the outer layer peak and near a distance value of 75 for the inner layer peak.

[0127] FIG. **18** is an actual echogenic envelope distribution along a scanline that crosses highly reflective adipose and peritoneum tissues. The echogenic distribution is therefore more complex than the distribution shown in FIG. **17**, since signal variation and/or noise are included. FIG. **18** also shows a plurality of possible candidate points that may be used to identify the inner and the outer wall layers of the bladder. The inner and outer wall layer candidate points are present as local peak maxima, and are shown by ovals in FIG. **18**. The candidate points are determined by one-dimensional A-mode algorithms applied to the distribution, as will be discussed in more detail below. Accordingly, FIG. **18** shows, for example, a total of fifteen local maxima, which correspond to fifteen inner and outer layer candidate points, although either more than fifteen, or fewer than fifteen candidate points may be present in other similar distributions.

[0128] Still referring to FIG. **18**, the inner and outer wall layer candidate points are developed by higher resolution one-dimensional algorithms applied to scanlines **48**, (FIG. **8**) which use an initial inner layer anchor point determined by a two-dimensional segmentation algorithm having generally less resolution. The initial inner layer anchor point on the scanline **48**, which in the present example are determined by the two-dimensional B-mode segmentation algorithms, are shown in FIG. **18** as a diamond with dashed lines. The segmentation anchor point serves as a reference point that permits the adequacy of the one-dimensional inner and outer wall layer candidate points to be determined.

[0129] With continued reference to FIG. **18**, localized peaks P**1**, P**2**, P**3**, and P**4** are shown that resemble the outer-inner layer bimodal pattern of FIG. **17**. For example, in the region between a distance **65** and a distance **71**, the peaks P**2** and P**3** appear to closely approximate the bimodal pattern of FIG. **17** since the signal magnitude of the point P**2** is approximately the same as for the point P**3**. A local minimum is present between the points P**2** and P**3**, which correspond to two minor maxima. If the region between and including P**2** and P**3** represents a front bladder wall, then the higher magnitude P**1** could be indicative of the more reflective peritoneal or adipose tissues that are anterior or proximate to the dome **20** (FIGS. **7** or **8**).

[0130] Although the combination of the candidate points P**2** and P**3** appear to present a favorable candidate for the location of the outer and inner bladder walls, respectively, other combinations are possible. For example, the points P**1** and P**2**, and the points P**3** and P**4** may also represent the location of the outer and inner bladder walls. Moreover, any combination of the fifteen local maxima or candidate points shown in FIG. **20** may be used to determine a location of the front wall. Algorithms will be described below that may be implemented to select envelope peak candidates within a particular scanline **48** with enhanced confidence. Accordingly, a peak combination representing the location of the bladder wall may be identified with increased accuracy.

[0131] FIG. **19** is a B-mode ultrasound image that shows a family of wall layer locations corresponding to the candidate points of FIG. **18** assembled from adjacent scanlines **48**. The continuous white line shown in FIG. **19** represents an initial inner wall location of the bladder superimposed onto the image as determined by the two-dimensional B-mode segmentation algorithms. The dashed lines shown in FIG. **19** represent candidates for the location of outer wall layers that, in the present case, progress outwardly towards the dome cutout **41** (FIGS. **3**C through **3**E). The family of seven dashed lines indicate the seven possible outer layer wall locations, some of which are overlapping with the initial inner wall as determined by the two-dimensional B-mode segmentation algorithms.

[0132] As shown in FIG. **19**, the application of all the candidate points (FIG. **18**) suggests that estimates of the thickness of the bladder wall can vary from nearly zero, to multiple centimeters. Algorithms to identify an optimum set of candidate points from the group of all of the candidate points generated is therefore preferable to select the final wall

locations so that a bladder wall thickness within an expected range is determined. In general, an expected range of bladder wall thicknesses is between approximately about one millimeter and about four millimeters. Accordingly, a search range from about −2 millimeters and about 10 millimeters may be used to search for candidate points on scanlines having large incident angles from the initial front inner wall location. The search range can also be determined based on the volume of urine in the bladder. For a given volume assuming a spherical bladder, we can calculate the minimum and the maximum expected wall thickness based on smallest and largest expected bladder masses. A smallest expected bladder mass value may be around 10 grams while a largest expected bladder mass value may be around 100 grams. Candidate points so identified may be defined as inner layer and outer layer candidate points.

[0133] FIG. **20** is a diagrammatic view of a plurality of candidate wall points that result from an echogenic distribution, such as the distribution shown in FIG. **19**. In FIG. **20**, for example, twenty-five wall envelope maxima are identified as candidate points in a relevant portion of the scanplane **42** (FIGS. **8**, **15**) selected from a series of truncated scanlines **48**A through **48**K from FIG. **19** that are selected from the scanplane **42**. The total number of candidate points may be determined by a candidate points algorithm according to an embodiment of the invention, which will be described in further detail below. The wall layer locations are determined from the segmented front wall (FIG. **20**) and the incident angle Ω of a selected scanline **48** (FIG. **15**). As shown in FIG. **15**, the wall thickness is defined along a surface normal extending outwardly from the front wall of the bladder wall. Alternate embodiments of the methods described for FIG. **16** permits the determination of organ wall thicknesses from non-normal incidence angles.

[0134] Of the wall candidate points shown in FIG. **20**, nine of the candidate points are determined by the algorithms below to properly characterize a location of the nearest outer layer. The foregoing candidate points are shown in FIG. **20** as lightly shaded circles, while the remaining points, shown as dark circles, are retained as candidate points for an inner layer location determination. As shown in FIG. **20**, the nine selected candidate points closely correlate with a candidate outer wall layer. An outer wall selection method algorithm identifies and selects the outer layer points from the plurality of scanlines **48**A through **48**K. The algorithm reduces the total number of candidate points while preserving appropriate candidate points.

[0135] FIG. **21**A is a flowchart that will now be used to describe a method **220** for identifying an outer wall location based upon the candidate points, according to an embodiment of the invention. As an initial matter, all candidate points are selected for the analysis described below. In block **222**, the outer wall location is first assumed to be at least 0.78 millimeters (mm) away from the inner wall, so that an initial wall thickness is at least about 0.78 mm. Accordingly, the equivalent sample distance is about 0.8 mm (about 20 RF sample points). At block **224**, for each of the scanlines **48**A through **48**K (see FIG. **20**), at least one upper most candidate point is selected for each of the respective scanlines **48**A through **48**K. In one particular embodiment, at least four uppermost candidate points are selected, and characterize the outer wall location, an inside wall location, and a muscular membrane positioned between the outer wall location and the inner wall location. At block **226**, the selected candidate points are tested for consecutiveness. Any of the selected candidate points that are more than a predetermined distance away from an assumed inner wall location are rejected. In another particular embodiment, any point candidate point that is more than about 1.2 mm (about 30 RF sample points) away from the assumed inner wall location is discarded. At block **228**, of the remaining candidate points, any candidate point having an intensity that is less than about one-half of the intensity among the selected candidates are also rejected. The foregoing blocks in the method are performed for incident angles greater than about 0.2 radian (about 10 degrees). Once the candidate points for the outer wall location have been selected, at block **230**, a cost function is employed in order correlate an outer wall location with the candidate points. The cost function is based on the least-square error between the candidate wall locations and the candidate points. The candidate walls are calculated from the known incident angles by varying the wall thickness from 0 to about 78.4 mm. The cost function, Ci, is calculated by the following expression of equation E8:

$$C_i = \left(\frac{1}{n} \sum_{k=1}^{n} \sqrt{\min(|W_k - C|)} \right)^2 \quad \text{E8}$$

[0136] Where n is the number of scanlines, W_k is the candidate wall location, and C are the candidate points. An exemplary cost function distribution that characterizes an outer wall location is shown in FIG. **19**. Accordingly, an outer wall location is selected by identifying a minimum point in the distribution.

[0137] With reference now to FIG. **21**B, a flowchart of a method **240** for identifying an inner wall location is shown, in accordance with another embodiment of the invention. At block **242**, an inner wall range is restricted to fall within a predetermined range with respect to the outer wall location. In a particular embodiment of the invention, the predetermined range is between approximately about −0.4 mm and approximately about 1.0 mm relative to the outer wall location. At block **244**, the intensity of a candidate point is assessed, and if the intensity of the candidate points are greater than approximately about one half of the intensity of a candidate point having a maximum intensity in the inner wall zone, the candidate points are retained. At block **246**, if the intensity of a candidate point is less than that of any of the candidate points selected in block **244**. During the foregoing inner wall selection, the process is performed only if the incident angle is greater than about 0.2 radian (about 10 degrees). The inner wall location is then selected by reverting to block **248**, so that a minimum in cost function distribution may be determined.

[0138] Due to acoustic reverberation of the transceiver dome **20** and to additional noise introduced through segmentation, the front wall segmentation of a bodily organ, such as a bladder, may be unacceptable as a thickness measurement estimation. Accordingly, it has been determined that a well-defined wall segmentation may be fitted using a second order polynomial, although other higher order polynomials may be used. The second order polynomial least squares curve fitting will now be described. The segmented points, y_i, are known and the second degree polynomial, f(x) is expressed in equation E9 as:

$$f(x)=ax^2+bx+c \quad \text{E9}$$

The least-square error, π, may be expressed by equation E10:

$$\Pi = \sum_{i=1}^{n} [y_i - f(x_i)]^2 = \sum_{i=1}^{n} [y_i - (ax_i^2 + bx_i + c)]^2 \quad \text{E10}$$

π is therefore minimized by varying the coefficient a, b, and c. Consequently, each of the partial derivatives of π with respect to each coefficient is set to zero, as shown below in equation E11-13:

$$\frac{\partial \Pi}{\partial a} = 2\sum_{i=1}^{n} x_i^2 [y_i - (ax_i^2 + bx_i + c)] = 0 \quad \text{E11}$$

$$\frac{\partial \Pi}{\partial b} = 2\sum_{i=1}^{n} x_i [y_i - (ax_i^2 + bx_i + c)] = 0 \quad \text{E12}$$

$$\frac{\partial \Pi}{\partial c} = 2\sum_{i=1}^{n} [y_i - (ax_i^2 + bx_i + c)] = 0 \quad \text{E13}$$

[0139] Expanding the above equations, the following expressions are obtained as shown in equation E14-E16:

$$\sum_{i=1}^{n} x_i^2 y_i = a\sum_{i=1}^{n} x_i^4 + b\sum_{i=1}^{n} x_i^3 + c\sum_{i=1}^{n} x_i^2 \quad \text{E14}$$

$$\sum_{i=1}^{n} x_i y_i = a\sum_{i=1}^{n} x_i^3 + b\sum_{i=1}^{n} x_i^2 + c\sum_{i=1}^{n} x_i \quad \text{E15}$$

$$\sum_{i=1}^{n} y_i = a\sum_{i=1}^{n} x_i^2 + b\sum_{i=1}^{n} x_i + c\sum_{i=1}^{n} 1 \quad \text{E16}$$

[0140] Expressing the foregoing in matrix form, the following matrix equation is obtained in equation E17:

$$\begin{bmatrix} \sum_{i=1}^{n} x_i^2 y_i \\ \sum_{i=1}^{n} x_i y_i \\ \sum_{i=1}^{n} y_i \end{bmatrix} = \begin{bmatrix} \sum_{i=1}^{n} x_i^4 & \sum_{i=1}^{n} x_i^3 & \sum_{i=1}^{n} x_i^2 \\ \sum_{i=1}^{n} x_i^3 & \sum_{i=1}^{n} x_i^2 & \sum_{i=1}^{n} x_i \\ \sum_{i=1}^{n} x_i^2 & \sum_{i=1}^{n} x_i & \sum_{i=1}^{n} 1 \end{bmatrix} \begin{bmatrix} a \\ b \\ c \end{bmatrix} \quad \text{E17}$$

[0141] Therefore, the coefficients a, b, and c for the least squares analysis may be determined as shown in equation E18:

$$\begin{bmatrix} a \\ b \\ c \end{bmatrix} = \begin{bmatrix} \sum_{i=1}^{n} x_i^4 & \sum_{i=1}^{n} x_i^3 & \sum_{i=1}^{n} x_i^2 \\ \sum_{i=1}^{n} x_i^3 & \sum_{i=1}^{n} x_i^2 & \sum_{i=1}^{n} x_i \\ \sum_{i=1}^{n} x_i^2 & \sum_{i=1}^{n} x_i & \sum_{i=1}^{n} 1 \end{bmatrix}^{-1} \begin{bmatrix} \sum_{i=1}^{n} x_i^2 y_i \\ \sum_{i=1}^{n} x_i y_i \\ \sum_{i=1}^{n} y_i \end{bmatrix} \quad \text{E18}$$

[0142] If the least-square error between the wall segmentation and the second order polynomial is greater than about five pixels it is rejected from the further processing.

[0143] A method for determining a wall thickness, T will now be described. The inner wall location and the outer wall locations previously determined (see FIGURE **21**A and FIG. **21**B) may be used to find the wall thickness by forming a difference between the outer and inner wall locations:

T=(Outerwall−Innerwall)·RF_resolution

RF_resolution is the length of a single RF sample, typically but not exclusively 0.08 millimeters. Since a plurality of scancones are developed during an ultrasound examination, and each scancone has a pair of orthogonal planes having corresponding thickness estimations, a median value may be calculated and accordingly constitutes a best estimate of the wall thickness.

[0144] FIG. **22** is an exemplary graph of a cost function generated along a selected scanline, which was employed in the methods described in FIG. **21**A and FIG. **21**B. The cost function is thus minimal at a final outer wall layer location exhibiting minimum thickness values. The cost function may therefore be used to identify the minimum thickness value since it is proximate to the minimum cost value.

[0145] FIG. **23** is an exemplary scanplane **42** of an internal anatomical region having a sector of scanlines **48** superimposed on the scanplane **42**. The scanlines **48** cross an inner layer border initially determined by the two-dimensional B-mode segmentation algorithms discussed above, in connection with FIGS. **14** and **15**. The initially determined inner layer border provides a first wall location from which, at the scanline level, a one-dimensional A-mode algorithm may be applied to rectified RF envelopes to determine the nearest outer layer candidates and the nearest inner layer candidates. Either at the scanplane or scanline level, the nearest outer layer candidate points amount to a second wall location. Similarly, the nearest inner layer candidate points amount to a third wall location.

[0146] FIG. **24** is an expanded portion of the scanplane **42** of FIG. **23** that shows the initial front wall location in greater detail. The expanded portion of the scanplane **42** shows the outer and inner layer borders of the initial front wall location as determined by the one-dimensional A-mode algorithms with the two-dimensional B-mode inner layer border. Compared with FIG. **19**, six of the outer layer candidates were eliminated leaving the nearest outer layer boundary line as shown. The nearest outer layer boundary amounts to the second position loci. Also shown is a nearest inner layer boundary displaced anteriorly to the initial front wall boundary layer as determined from two-dimensional segmentation algorithms.

[0147] FIG. **25** expands sub-algorithm **172** of FIGS. **14** and **15**. The sub-algorithm **172** is comprised of three blocks. In block **172**A, the patient is palpated to determine the location of the synthesis pubis or as commonly known the pubic bone. Above the synthesis pubis location, a sonic gel pad or a sonic gel is applied and the scanner is either placed in the gel that is applied to the patient or on the sonic gel pad. The sonic gel and the sonic gel pad serve to minimize attenuation of the ultrasound that transverses between the transceiver dome **20** of the transceiver **10** and the patient. The next block is **172**C and the scan button is pressed on the transceiver **10** so that a rotational array of 2-D scanplanes is acquired. The method then proceeds to block **176** from FIG. **14**.

[0148] FIG. **26** expands sub-algorithm **180** of FIG. **14**. The sub-algorithm **180** is comprised of eight process or decision routines. The first process is block **180**A and is called Find Initial Wall. From block **180**A is the next block **180**B that is Find Centroid. Thereafter, block **180**C is Fixed Initial Walls. After Fix Initial Walls is a decision block in which the question is asked, "Is it uterus?" The decision block **180**D. If it is a uterus, "yes", the next process is Clear Walls block **180**E. Thereafter, the volume is displayed at in process **180**H and the process continues on to process **180**J. Referring back to decision diamond **180**D, if the organ is not a uterus, "no" then we proceed to decision **180**F in which the question is asked, "Is volume less than 40 ml.?" If the answer is "no" to the decision diamond **180**F, then the volume is displayed at terminator **180**H and the algorithm then proceeds to sub-algorithm **180**J. If at decision diamond **180**F the answer is "yes" to the query, "Is volume less than 40 ml.?" Another decision diamond is presented **180**G. At decision diamond **180**G, the query is asked, "Is it a bladder region?" If the answer is "no" then the sub-algorithm **180** proceeds to the Clear Walls of block **180**E and thence to terminator **180**H Volume Displayed. If at the decision diamond **180**G, the answer is "yes" to the query, "Is it a bladder region?" then the volume is displayed at terminator **180**H and the process then continues on to algorithm **180**J. In sub-algorithm **180**, an interface line is overweighed on the B-mode scanplane image to approximate an initial location for an organ wall, for example, a uterus or a bladder. This initial interface line is used as a seed or initial reference point in which to further use as a basis to adjust the determination for the inner and outer wall layers of the organ wall. Furthermore, in this algorithm, the detected region in the scanplane is determined to be or not to be a bladder or a uterus. This occurs specifically when the gender button of the transceiver **10** indicates that the scan is for a female. If the regions indeed found to be a uterus, it is cleared and a zero volume is displayed. For a non-uterus region, such as a bladder, if the volume is very small, then checks are made on the size of a signal characteristic inside the detected region to ensure that it is a bladder and not another tissue. If a region is indeed a bladder region it is computed and displayed on the output.

[0149] FIG. **27** expands sub-algorithm **180**A of FIG. **26**. The sub-algorithm **180**A is comprised of 11 processes loops, decisions, and terminators. Sub-algorithm **180**A begins with process **180**A**2** in which the Local Average is calculated for the 15 to 16 samples that functions as a low pass filter (LPF) to reduce noise in the signal. Other embodiments allow for calculating averages from less than 15 and more than 16 samples. Next is block **180**A**4** in which the gradient is calculated using a central difference formulation and has taken over seven sample sets. The process at block **180**A**4** then proceeds to a beginning loop limit **180**A**6**. In block **180**A**6**, each sample is examined in a detection region. Thereafter, at decision diamond **180**A**8**, the query is, "Is gradient minimum?" If the answer is "no" then another query is presented at decision diamond **180**A**18**, the query being, "Looking for BW and gradient maximum?" BW refers to for back wall. If the answer to the query in block **180**A**18** is "no" then the end of the loop limit is proceeded to at block **180**A**30**. Thereafter, from the end of the loop limit at **180**A**30**, the terminator end find initial walls is reached at block **180**A**40**. Returning now to the decision diamond **180**A**8**, if the answer to the query, "Is gradient minimum?" "yes" then another query is presented in decision diamond **180**A**10**. The query in **180**A**10** is "Is candidate FW/BW best?" FW is refers to front wall and BW refers to back wall. If the answer to the query in block **180**A**10** is "no", then the process **180**A**62** is used in which the front wall is saved and another back wall is looked for. If the query to in **180**A**10** is "yes" then the process is Save Candidate occurs at block **180**A**14**. Thereafter, the process returns to beginning loop **180**A**6** to resume. Returning to the decision diamond **180**A**10**, should the answer be "yes" to the query, "Is candidate FW/BW best, then the process proceeds to block **180**A**12** in which the candidate is assigned as a pair for back wall/front wall." Thereafter from block **180**A**12** is returned to the beginning loop **180**A**6** and then the process will then terminate at end of each sample at end loop **180**A**30** and thence to terminator **180**A**40** for end find initial walls sub-algorithm. Sub-algorithm **180**A attempts to find the best front wall and back wall pair for the inner and outer wall layer plotting points. The best front wall and back wall pair in each scanline is defined as the front wall and back wall pair for which the difference in the back wall gradient and front wall gradient sometimes referred to as the tissue delta, is the maximum and the smallest local average between the front wall and back wall pair is the minimum for the pixel values.

[0150] FIG. **28** is an expansion of the sub-algorithm **180**C of FIG. **27**. Sub-algorithm **180**C is comprised of several processes decision diamonds and loops. Sub-algorithm **180**C operates on a scanplane by scanplane basis where the first scanplane to be processed is one that is closest to the central aid of the initial walls and then the remaining scanplanes are processed moving in either direction of that initial scanplane. Sub-algorithm **180**C begins at block **180**C**2** referred to as Start Fix Initial Walls. The first process is at block **180**C**4** in which the center line is corrected if necessary. The center line is defined as the line on that scanplane with the maximum gradient difference between the front wall and the back wall. The correction of the front wall and the back wall location at any line is carried out by a match filtering like step where the best location within a search limit is defined as the one for which the difference between points immediately outside the bladder and points immediately inside the bladder is maximum. Of course, this applies to any organ other than the bladder, as the bladder is used here as an example of a particular embodiment. Thereafter, at block **180**C**6**, the front wall and back wall means are calculated for five central lines. The pixel main intensity is computed and if this intensity is less than expected from the noise at that depth, the lines are cleared and the algorithm proceeds to the next plane as shown in decision diamond **180**C**8** to the query, "Is BW level less than noise?" where BW means the back wall (or posterior wall) of the bladder. If the answer is "yes" to this query, at block **180**C**10**, the process Clear Wall Data is initiated and from that proceeds to terminator **180**C**50** End Fix Initial Walls. Returning to the decision diamond **180**C**8**, if the answer is "no" to the query, "Is BW level less than noise?" then the sub-algorithm **180**C proceeds to the process at block **180**C**12** described as Fix 3 Central Lines. From this point through the end of sub-algorithm **180**C, the purpose is first correct the lines to the left of the central lines, called the left half plane (LHP) until either the edge of the bladder or the edge of the ultrasound cone is found. After the algorithm corrects the LHP, it proceeds to correct the lines to the right of the central lines, called the right half plane. Because the same steps are used for all lines, regardless of their position to the left of center or to the right of center, the process blocks **180**C**16** through **180**C**42** are used for both the LHP and once for the right half plane. The "line index" of process **180**C**14**

indicates an identifier for the current line that is processed. The line index is set to 2 indices less than the center line to start processing the LHP. The looping procedure started in block **180C16** continues looping while the line index is a valid index (i.e. it corresponds to a scanline). Sub-loop **180C18** is started with the intent of adjusting the initial wall locations, sub-process **180C20**, to their correct location if any correction is necessary. This loop, terminated at process **180C24**, completes two iterations. The first iteration uses sub-process **180C20** to correct the front wall of the bladder on the current line and the second iteration to correct the back wall of the bladder, although the ordering of which wall is corrected first can be interchanged. Once the wall locations have been corrected of the current line have been corrected, sub-algorithm **180C** proceeds to sub-process **180C28**, "Check Wall Growth". This sub-process ensures that the length of the scanline that intersects the bladder in the current line does not grow significantly with respect to the previous line that has already been corrected. In the preferred embodiment, the length of the scanline intersecting the bladder is constrained to be less than 1.125 times longer than in the previous line. If the loop bounded by sub-processes **180C16** and **180C42** is being applied to the LHP, then the previous line is one index number greater than the current line index. Otherwise the previous line index is one index number less than the current index. After completing sub-process **180C28**, sub-process **180C30** "Check Wall Consistency" verifies that the portion of the current scanline that intersects the bladder overlaps the portion of the previous scanline that intersects the bladder. After completing sub-process **180C30**, decision **180C32** queries "If working LHP?" (i.e. the loop bounded by terminators **180C16** and **180C42** is being applied to the lines left of center). If the answer to the query is yes, then the sub-process **180C34** "Decrement line index" decreases the line index by one index number. Decision **180C36** queries "If line index is invalid". The loop bounded by terminators **180C16** and **180C42** is applied to the next, and now current, scanline. If the decremented line index corresponds to an invalid value, the edge of the LHP has been reached. Sub-process **180C38** is called to reset the line index to the first line to the right of center that has not been adjusted. The loop bounded by terminators **180C16** and **180C42** will now be applied to the right half plane (RHP). Returning to decision **180C32**, if the answer to the query is "No", sub-process **180C40** "Increment line index" results with the line index being increased by one index number. Loop terminator **180C42** cause the loop to return to **180C16** as long as the line index corresponds to an actual scanline. As soon as that condition is violated, the loop terminator will cause sub-algorithm **180C** to proceed to the terminator **180C50**, "End Fix Initial Walls".

[0151] FIG. **29** is an expansion of the sub-algorithm **180J** of FIG. **26**. The procedures within sub-algorithm **180J** provide a decision tree used for ascertaining whether a uterus has been detected. The definitions of the abbreviations in the flow chart blocks are Max E, Max V1, Max V2, ValMean, and MaxVM. Max means maximum, E means enhancement, V1 means volume 1, V2 means volume 2, ValMean refers to a measurement of the minimum local average pixel intensity of the region inside the region identified as urine inside the bladder, Max VM is a pre-defined threshold against which VALMEAN is tested. If VALMEAN is greater than MAXVM, the region identified as urine inside the bladder isn't really urine and the boundaries are actually an outline of the uterus. Depending on the hardware platform used for the various embodiments of the transceiver **10**, the decision tree for the sub-algorithm **180J** of FIG. **26**. The sub-algorithm **180J** begins from sub-algorithm **180H** in which a decision diamond Enhancement<MaxE (maximum enhancement) at decision diamond **180J2** is reached. If the answer is "yes" for enhancement, then another decision diamond **180J4** is reached and the query is a Volume<Max V1 (maximum Volume 1) is made. If the answer is "yes" to this query, then the determination at terminator **180J6** is reached and the organ that is being examined is a uterus. Thereafter, the algorithm continues to block **184** of FIG. **14**. Returning to the decision diamond **180J4**, if the answer is "no" to the query Volume<Max V1, then another decision diamond **180J8** is reached having the query "Is the Volume<Max V2?" (Maximum Volume 2). If the answer is "yes", then the next decision diamond is **180J10** is reached with the query, "Is the ValMean>MaxVM?" If the answer is "yes", then terminus **180J6** is reached and the organ being viewed is the uterus. If the answer is "no", then terminus **180J20** is reached and the organ being viewed is a bladder, the algorithm then completes block **184** of FIG. **14**. Returning back to decision diamond **180J8**, if the answer is "no" to the query, "Is the volume<than MaxV2", then the answer is that a bladder is being viewed as indicated by the terminal **180J20**." From terminus **180J20** the algorithm continues to block **184** of FIG. **14**.

[0152] FIG. **30** is an expansion of an alternate embodiment of the sub-algorithm **184** of FIG. **14**. The processes within sub-algorithm **184** are procedures taken between blocks **180** and **188** of FIG. **31**. The sub-algorithm **184** is comprised of block **184A2** in which 1-D scanline signals are examined for scanlines crossing the organ wall. Thereafter at block **184A4**, the echo signals are rectified using a Hilbert Transform to obtain an A-mode radio frequency (RF) envelope along scanlines crossing the organ wall. Sub-algorithm **184** continues with block **184A6** where the scanline RF envelope is examined for candidate points of inner and outer wall layers of the organ wall. Thereafter at block **184A10** the candidate points are plotted for the inner and outer wall layers of the organ wall on scanlines within the 2-D scanplanes. Finally, the sub-algorithm **184** is completed with the process described at block **184A12** in which the best candidate points are determined for the inner and outer wall layers of the organ wall being examined on scanlines using a least cost analysis algorithm previously described above.

[0153] FIG. **31** is an expansion of the sub-algorithm **188** of FIG. **14**. Sub-algorithm block **188** is between sub-algorithms **184** and **192** of FIG. **14**. There are two sub processes in **188** depending upon how the organ wall thickness is calculated depending upon either a single value or a group of values. For a single value at block **188A2**, the organ wall thickness is calculated as a difference between one pair of best inner and outer layer wall candidates from one scanline. Alternatively, at block **188A4**, the organ wall thickness is calculated as a mean of the differences between a plurality of best inner and outer wall layer candidates pairs of more than one scanline crossing the organ. Both blocks **188A2** and **188A4** are then continued to sub-algorithm **192**.

[0154] FIG. **32** is an expansion of the sub-algorithm **192** of FIG. **31**. Sub-algorithm **192** is between sub-algorithm **180A** and thickness measurement **188**. Sub-algorithm **192** starts with block **192A** morphological cleanup. The processes of sub-algorithm **192** identifies potential front wall and back wall pairs on A-mode scanlines that potentially look like an

organ of interest, for example, a bladder in which a dark region which is surrounded by bright echos on the front and of the back of the organ being viewed. The sub-algorithm **192** uses some shape and anatomical knowledge to clean up the potential front walls and back walls in the morphological cleanup block **192**A. The morphological cleanup is needed because there may be missing wall pairs that appear spurious and further more are further obscured by speckle and other noise associated with ultrasound-based images. Such a speckle and other ultrasound-based noise may give a front and back walls that are unnecessarily jagged. The morphological cleanup at block **192**A serves for correcting errors due to this jaggedness and for regularizing or smoothing these wall locations. The morphological cleanup block **192**A uses mathematical morphology and a sequence of morphological operations that are applied to the initial wall data. The mathematical operations will be described in figures below. After execution of the morphological cleanup process at block **192**A, there may be more than one potential region that represents an organ of interest say the bladder. If there is more than one region, then the largest three-dimensional region is assumed to be the bladder and is selected for further processing. This selection of the largest region occurs at the next block **192**B. After the largest region selection is determined, another smoothing and cleanup process is applied at block **192**C mainly a process referred to as snake smoothing. A variant of the snake-smoothing algorithm was developed and is described in the figures below. The boundary output from this snake smoothing algorithm step **192**C is used to calculate the surface area of the bladder using an algorithm described below. The initial points that are used in sub-algorithm **192** are those that were already obtained to have high confidence. Those that were not high confidence wall points are filtered and removed. The high confidence front wall locations are then used to initialize the RF base thickness measurement as described above and as further elucidated below. Parallel with the snake smoothing algorithm **192**C, a block **192**D is implemented in which high confidence front walls are selected or chosen. After snake smoothing has been implemented at block **192**E surface area measurement is then conducted.

[0155] FIG. **33** is an expansion of the sub-algorithm **192**A of FIG. **32**. Several steps are applied to initial wall data. A series of morphological openings and closings are used with increasingly large kernel sizes and are applied to the pre-scan converted data. This kind of filter is known as "alternating sequential filter" and further described in P. Soille and J. F. Rivest, *Principles and Applications of Morphological Image Analysis*. In the expansion of sub-algorithm **192**A, gaps are filled between planes and the image sequence. As an example, the sub-algorithm **192**A is represented by a series of close and open processes that are shown in eleven process boxes and conclude with an erode box. The first close process box is **192A1** which then proceeds to a first open process box **192A2** and further proceeds to the following series described below. The series of morphological openings and closings are used with increasingly large kernel sizes and are applied to the pre-scan converted data. The first operation is a closing with a structuring element 3 planes deep designated in block **192A1** as 1×1×3. This step fills in the gaps between planes that extend to less than 3 planes. Next, in open block **192A2**, a structuring element 3 planes deep is opened which removes outlier regions between the planes that extend for less than 3 planes. Thereafter, at block **192A3**, the data is closed in a 1×1×5 sequence and then reopened at block **192A4** in a 1×1×5 sequence. That is the structuring elements of 5 planes deep in blocks **192A3** and **192A4**. The open and close algorithm continues with open block **192A5** and close block **192A6** in which this series of morphological operations aim to fill gaps and remove outliers within a plane. In open block **192A5**, a small opening using a structure element 3 scanlines wide is implemented and this serves to remove outliers that are less than 3 scanlines wide. This step is then followed by block **192A6** in which a closing process is implemented that closes all gaps in the wall locations less than 3 scanlines wide. Thereafter, another open and close pair of processes are applied at open block **192A7** and close block **192A8**. The open block **192A7** is of a 1×5×1 configuration and the close processing block **192A8** is of a 1×5×1 operation. Thereafter, an open and close processing is done in a 1×7×1 configuration at block **192A9** and block **192*a*10**, respectively. In these two blocks, outliers are removed and gaps are filled for 5 and 7 scanlines, respectively. Thereafter, at open processing block **192A11**, a 15×11×1 configuration is implemented in which 15 samples long and 11 scanlines wide are processed to help select for the proper points. In open block **192A11**, the main purpose is to remove erroneous front wall locations that are affected by the dome reverberation artifact dissociated with ultrasound echo reverberations of the dome **20** if the transducer **10**. The final step of sub-algorithm **192**A is an erode processing block **192A12** in which the morphological processing erodes the front and back walls by 5 samples. That is, this is a 5×1×1 configuration in which the step shrinks the front walls and the back walls inside to allow the snake to expand and search for the best location.

[0156] FIG. **34** expands sub-algorithm **192**C of FIG. **32**. Sub-algorithm **192**C is for snake smoothing and is comprised of several processing and terminator steps. Snake processing uses an active contour known as a snake and is basically a way to link edges or other image features by minimizing a cost function for a contour passing through the image features. The cost function typically includes a cost that favors contours that are close to the desired image features on the image and a cost that favors smooth and short contours.

[0157] The minimum cost contour is found by using an iterative method starting with an initial contour that is fairly close to the desired contour. This initial contour is minimized iteratively and the motion of the contour between iterations resembles the motion of a snake; therefore the name of the algorithm. The snake moves under two forces—(1) an image-based force that tries to move the contour closer to image edges, and (2) a regularizing force that tries to make the contour smooth and short. At the end of the iterations, a contour is developed which balances the two forces using the following sub-algorithms of snake smoothing algorithm **192**C of FIGS. **32** and **34**.

[0158] A combination of two images is used to define image-based forces. The first image is a gray scale image that is inputted at starting terminus **192C4**. Thereafter, a heat and shock filter at block **192C6** is applied which respectfully serve to optimize a detection of the gray scale image. The two images are incorporated into the snake metric using the following logic. Looking along a direction normal to the snake curve, the optimal snake location has the maximum difference between the gray scale intensities outside the curve and the gray scale intensities inside the curve and it lies on a location that is identified as an edge point. This occurs at the edge detection process block **192C8**. After heat and shock filtration at block **192C6** and after edge detection at **192C8**, a

2-D snake algorithm is applied as described further in block **192**C**10** of FIG. **34**. At **192**C**10**, an initial bladder outline or other organ of interest outlined is provided to processing block **192**C**10**. The initial bladder outline is inputted from input terminal **192**C**2**. After application of the 2-D snake process **190**C**10** to the input 2-D scanplane image of **192**C**4**, an overlay with initial bladder outline of **192**C**2**, a final bladder outline is generated at terminus **192**C**20**. Discussing below an amplification of the 2-D snake algorithm **192**C**10** is further described.

[0159] FIG. **35** expands sub-algorithm **192**C**10** of FIG. **34**. The expansion of this algorithm serves to make the snake an iterative sequence of the following two steps—(a) moving the contour in a direction normal to the contour where each normal direction that is searched becomes the best image metric, and (b) smoothing the deformed contour using regularization constraints. In the application of the sub-algorithm, each point along the curve is examined and image pixels are sampled normal to each point and the image metric is calculated at each normal location within a pre-specified search range. Thus, beginning at the loop at **202**, each point of the curve is readied for processing. Thereafter at processing block **204** a normal to the point on the curve is found. Thereafter at block **206**, a normal to the image metric is computed provided that filtered images from block **216** and edge image **218** are available. The image metric at each point uses the gray scale pixel intensities inside and outputs the curve and also uses the edge image obtained respectfully from the filtered image block **216** and edge image block **218**. The contour point is moved to a location where the image metric is optimal, i.e., the gray scale intensity difference is maximal and the location corresponds to an edge location. This is denoted in block **208** selected best location. Thereafter, the processing loop is ended at block **210** and the processing points on the curve is completed. Next is a smoothing of a contour that is carried out at block **212**, smooth curve. Of the contour, it is carried out by multiplying the vectors representing the X and Y coordinance of the contour with a smoothing matrix. Following the smooth curve **212** block is a decision diamond for the termination of the Max iterations has been reached and if it has, then the 2-D snake algorithm **192**C**10** is completed at terminus **220**. If it has not, the procedure returns to the opening loop **202** of the sub-algorithm. Referring now to the filtered image block **216** of the edge image block **218**, the snake algorithm are applied to obtain the best computed image metric along the normal block **206** based upon examining every detected front wall layer location within a small search region on the same scanline around the detected front wall layer location. If no edges are found within the search area, the wall location is considered of low confidence and is removed from the output wall locations. However, if an edge point exists within that search region, and the intensity difference between the pixels outside and inside the organ wall, for example, a bladder wall on an enhanced image is maximal, the location is considered a high confidence location. The output wall location for such a point is moved to this high confidence location.

[0160] FIG. **36** expands sub-algorithm **192**E of FIG. **32**. Sub-algorithm **192**E concerns the procedures for obtaining a surface area measurement and comprises a series of processing steps. Starting with block **192**E**2**, the segmented front and back walls are supplied to a fill bladder region procedure in block **192**E**4**. The fill bladder region procedure creates a pre-scan converted, for example, in polar coordinate form, volume where all the pixels inside the bladder are filled in with a non-zero pixel value such as **255**. Then all the pixels outside are set to zero. The next procedure is in block **192**E**6**, a 3-D scan convert process. The 3-D scan convert process is a conversion procedure applied to convert the polar coordinate pre-scan image to a Cartesian coordinate system. The size of the Cartesian volume created is 150×150×150. This Cartesian volume data is then smoothed as indicated in block **192**E**8** 3-D image smoothing. The smoothing step uses a Gaussian smoothing window of approximately 11×11×11 pixels. The kind of filtering used in the Gaussian smoothing is preferable to generate a smooth output organ surface as would be for a bladder surface. In the next block **192**E**10**, a general iso-surface procedure is implemented. The general iso-surface procedure uses the Marching Cubes algorithm described in Lorensen and Cline (W. E. Lorensen and H. E. Cline, "Marching Cubes: A High Resolution 3D Surface Construction Algorithm," *Computer Graphics*, vol. 21, pp. 163-169, July 1987.) Marching Cubes algorithm is applied to create iso-surface of the organ region such as a bladder. An iso-value of 127.5 is used to decide where to place the iso-surface on the smooth image. Everything greater than this iso-value of 127.5 is considered inside the bladder or the organ of interest and less than this value is considered outside the bladder or organ of interest. In the next step process **192**E**12**, the organ surface is then decimated and smoothed to reduce the number of vertices. The surface is then triangulated at process step **192**E**14** in order to represent the entire surface using a mesh of triangles. This triangulated surface is then outputted as a VRML for potential display and is also used for the calculation and surface area and other properties. The triangulated surface is used for surface area calculation. As shown in the FIG. **36**, the triangulated surface is also output as a VRML file in terminus **192**E**16**. The surface properties, surface area, etc. are calculated as indicated in block **192**E**18**. Thereafter, at terminus **192**E**20**, the surface area is outputted for report.

[0161] FIGS. **37**A-D are B-mode scans overlaid with interface tracings obtained by the algorithms previously described. FIGS. **37**A and B are sagittal plane (plane 1) images and FIGS. **37**C and D are transverse images. A line along the back wall in FIG. **37**A is seen and a more jagged line in FIG. **37**B is shown as a consequence of noisy signals. FIGS. **37**C and **37**D show the cleanup of the interface tracings along the organ wall boundaries, in this case a bladder after being subjected to the morphological cleanup, sub-algorithm **192**A of FIG. **32**. Note the loss of the jagged interface tracings of **37**B substantially smooth over and as an interface tracing **37**D.

[0162] FIGS. **38**A-D are B-mode scans overlaid with interface tracings before and after application of the morphological cleanup algorithms. As with FIGS. **37**A-D, FIGS. **38**A and B are sagittal images and FIGS. **38**C and D are transverse images. Again, note the difference between FIGS. **38**B whether a substantial jagging along the back wall that clearly goes into the tissue and whereas morphological cleanup there is a substantially closer interface tracing along the boundary

[0163] FIGS. **39**A-D are B-mode scans overlaid with interface tracings. This is yet another iteration of the morphological cleanup process in which a truer fidelity is achieved demarcating in this **2**-D scan images a more precise interface tracing demarcating the bladder from surrounding tissue after application of the snake algorithms.

[0164] FIGS. **40**A-B are normal and magnified B-mode scans overlaid with interface tracings. FIG. **40**A is a normal view and has a white square looking at the bladder wall area. FIG. **40**B is an expansion of the white square perimeter of FIG. **40**A in which the inner and outer wall layers are shown delineated as separate tracings. There is a high degree of resolution by using the algorithms of the preceding as discussed previously.

[0165] FIGS. **41**A-B are normal and magnified B-mode scans overlaid with interface tracings. Similar to the tracings of FIGS. **40**A and B, a normal view of FIG. **41**A is shown with an enclosed square which is magnified in the FIG. **41**B to show comparable high resolution interface tracings of the inner and outer wall layers of the front wall organ wall, in this case, a bladder. The front wall muscles as detected for the bladder wall in FIG. **40**B and FIG. **41**B are used for the thickness calculation measurements of FIG. **32**.

[0166] FIG. **42** is an alternative-algorithm of FIG. **15**. Raw data is first brought under processing block **172** and thereafter the raw data is split between segmentation of the organ and calculate wall area block **192** and finding the extent (search region) of proximate organ wall to the transceiver block **250**. After block **250**, the inner wall layer of proximate organ wall to transceiver is achieved at block **252**. Thereafter, at block **254**, find outer wall layer of the proximate organ wall to transceiver is implemented. Thereafter, at block **256**, the thickness of the proximate wall as a difference between the inner and outer wall layers is then calculated. Thereafter, the two parallel fracture combined merge at block **300** in which the organ wall volume is calculated and thereafter ends with block **400** in which the organ wall mass is calculated. All the processing here—**250**,**252**,**254**,**256** is carried out on 2D or 1D data.

[0167] FIGS. **43**A-B are B-mode scans overlaid with interface tracings. A scanplane **500** is shown having a bladder **500**C which is delineated along its tissue cavity boundary by a front bladder wall **500**A and a back bladder wall **500**B. FIG. **43**B is another scanplane from the same patient and shows the initial wall locations of a scanplane **502** about the bladder **502**C in which the front wall **502**A and back wall **502**B is delineated by interface tracings.

[0168] FIGS. **44**A-B are B-mode scans overlaid with interface tracings. FIG. **53**A is a scanplane **506** and **53**B shows a scanplane **508** from the same patient. In contrast to the scanplane in FIGS. **43**A and B, the boundaries are more difficult to set with the tracings and show that parts of the bladder as delineated as **506**C and **508**A, respectively are comparably delineated with **506**A as the front wall and **506**B as the back wall in scanplane **506**. Similarly, the delineation of partial where only part of a front wall **508**A is shown as a interface tracing and part of the rear wall **508**B is shown as interface tracing. In this case here in FIG. **43**A and **43**B, would receive the benefit of filling in the likely candidate points in the gaps set are between the front and rear wall interface tracings.

[0169] FIGS. **45**A-B are B-mode scans overlaid with interface tracings. The interface tracings for scanplanes **510** and **512**, respectively of FIGS. **45**A and B show a partially delineated bladder that goes off scale. The bladder is respectfully represented as **510**C and **512**C and the figures and the respective front walls are **510**A and **512**A and the rear walls are **512**B and **510**B. Of interest to note is that using the method the algorithms of the system is that the outer wall layer and inner wall layer is more clearly delineated. The outer wall layer in scanplane **510** is shown as **510**D and the inner wall layer is shown more clearly as **510**A for the front wall. The rear wall does not shown this delineation with tracings at this point.

[0170] FIGS. **46**A-B are B-mode scans overlaid with interface tracings. The interface tracings as shown in the previous FIGS. **46**A and B show the front wall tracings for the inner and outer wall layers. In scanplane **514** of FIG. **46**A, the outer wall layer of **514**D is shown and inner wall layer **514**A is shown of a partially revealed bladder. Also shown in scanplane **514**, is the partial back wall delineation along tracing **514**B. In FIG. **46**B, scanplane **516** shows a slight proportion of the inner wall layer of **516**A and the outer layer of **516**B and only a very small portion of the back wall **516**B.

[0171] FIGS. **47**A-B are B-mode scans overlaid with interface tracings. FIG. **47**A concerns scanplane **518** and FIG. **47**B concerns scanplane **520**. In scanplane **518**, the outer layer wall of **518**D may be seen traced with the inner layer wall **518**A. The back wall **518** B is shown partially traced. In FIG. **47**B scanplane **520** is sequential with scanplane **518** of FIG. **47**A and another view of the delineated bladder may be seen. Due to the differences in the scanplanes, the relatively full bladder may be seen where the proximate or forward bladder wall is seen delineated with the inner wall **520** and the outer layer wall **520**D. Also, visible is the delineation for the back wall **520**B that goes off image.

[0172] FIGS. **48**A-B are B-mode scans overlaid with interface tracings using the preceding algorithms. FIG. **48**A and **48**B present to a sequential scanplane from a different patient with different views of the bladder available. In scanplane **522**, the inner layer **522**A of the proximate or forward bladder wall is shown delineated and the outer layer **522**B is shown delineated with the interface tracings. The back wall **522**B is shown slightly delineated and off image. Similarly, FIG. **48**B shows scanplane **524**A with only a portion of the bladder visible, but nevertheless the inner layer **524**A is shown with the interface tracing along with the outer layer **524**D with an interface tracing for the proximate forward bladder wall. Only a portion of the back wall of **524**B is visible.

[0173] FIG. **49** is a method algorithm for the Internet System used to measure organ wall mass. In FIG. **49**, the exam valuation is for a BVM 6500 transceiver end block **600**. Block **600** is composed of a user block **600**A, a sonographer block **600**B, and ScanPoint database block **600**C, and a ScanPoint application block **600**D. The Internet system **600** uses a coordinated interplay between the user block **600**A dismounted for **600**B via database ScanPoint software **600**C and the ScanPoint application software of **600**D. The user begins the exam evaluation **600** by scanning the patient at procedural block **600A2**. Thereafter, at procedural block **600A4**, the exam is off-loaded to the ScanPoint server. The ScanPoint server block **604** receives the analysis and stores the results from the exam uploaded from block **600A4**. Thereafter, the results are saved in the ScanPoint database **600**C at procedural block **606**. A sonographer experienced to review the images and results from the ScanPoint database **600**C at procedural block **606** reviews the exam at block **608**. Thereafter, a decision diamond **610** occurs in the sonographer column **600**B where the query is as presented, "Are the automated results good?". If the answer is "no", the another decision diamond is presented at **614** with the query, "Can the exam be corrected?". If the answer is "yes" to the query in decision diamond **614**, at block **615**, the results are edited and submitted for re-analysis. Returning back to decision diamond **610**, if the answer is "yes" to the query, "Are the automated results good?" the

procedure returns to the ScanPoint database **600**C column where at block **612** the exam is marked available to user. Upon successful assessment by a sonographer at decision diamond **610**, and after being marked available for user at procedural block **612**, the exam results are made available to the user at block **624** wherein it then becomes accepted by the user for evaluation at block **628** within the user column **600**A. In block **628**, the user accepts or rejects the results after the sonographer has approved it. The accepted to rejected results from procedural block **628** is then sent to the ScanPoint database and stored at procedural block **640**. In the ScanPoint **600**C. Returning to the sonographer, column **600**B at procedural **615**, there are two options that occur at ScanPoint database **600**C and ScanPoint application **600**D. In the ScanPoint database column **600**C, a procedural block **616** for clone exam is available. In the cloned exam procedure, the exam may be repeated as desired by the sonographer. Alternatively, in the ScanPoint application software **600**D at procedural block **618**, the results of the scan may be analyzed and stored. Thereafter, returning to the ScanPoint column **600**C, the results that are saved are marked clone and the exam results are made available to the user. Thereafter, at block **624**, the exam results are made available to the user and from block **624** and the user column **600**A the user then reviews the exam results at block **628** and decides to accept or reject the results. Thereafter, the user returns to the ScanPoint database column **600**C and the results are saved and a charge for the exam is made if necessary procedural block **630**. From preceding detailed description of the major operation processes of the exam evaluation **600**, it can be seen that the bladder mass exam is deployed via the Internet system as a reviewed exam. An experienced sonographer reviews the exam and the resulting data is re-analyzed as needed. As shown in the user column **600**A, the user is free to scan a patient prior to after preparing an exam in ScanPoint. In starting block **600A2**, the user performs the following steps substantially similar to that described in sub-algorithm **172** of FIG. **15**. First, the patient is palpated to determine the location of the symphysis pubis or the pubic bone approximately two centimeters or one inch above the patient's symphysis pubis along the patient's midline the transceiver **10** is placed. Prior to that, either a sonic gel pad is placed at this location or a ultrasound conveying gel is applied to the patient's skin. Thereafter, the transceiver **10** currently a BVM 6500 scanner is placed in the center of the gel pad or near the center of the applied gel. Then, the scan button is released to acquire the rotational array of 2-D scanplanes referred to as V-Mode™ scan. Once the V-Mode™ scan trademark is completed, the results are conveyed as indicated in the flowchart of FIG. **49**. The particular embodiment to the transceiver **10** specifically the BVM 6500 scanner can notify the user, through display presented arrows, whether or not the aim of transceiver **10** needs to be adjusted to acquire the organ of interest, in this case a bladder, so as to acquire the bladder in a more reasonably centered location. Attempts to prove the aim at this point are recommended, but optional. That the organ of interest in this case, a bladder is properly centered is verified by getting consistent readings through multiple repositions. It is suggested that at least three volume readings be acquired that are consistent. As previously indicated in the Internet system method of FIG. **49**, the exams uploaded to the ScanPoint software and is available soon thereafter for review by a sonographer. The sonographer reviews the raw data uploaded to the ScanPoint database and analyzes the organ volume surface area and wall mass. The sonographer can assess the results as is, reject the exam outright, or edit the exam. If the sonographer accepts or rejects the exam, the result is immediately available to the user. If the sonographer chooses to edit the exam, a new window opens on the computer display. In this window, sonographer will trace inner and outer bladder wall layers on both the sagittal plane and on the transverse plane by selecting a series of points. These measurements will be uploaded to the ScanPoint software database and ScanPoint application. The ScanPoint Internet system will clone the exam results to form a new record and raw data will be re-analyzed with the sonographer's measurement locations. The sonographer's measurement will be added to the zoom thickness measurements after this repeated analysis. After the re-analysis is complete, the results corrected by the sonographer will be presented to the user along with the original thickness measurement result. At this point, the user is free to view the results. The user may accept or reject the exam in the same manner as other exams available and the ScanPoint suite.

[0174] FIG. **50** is a screen shot of four image panels A-D. The screen shots are what is available to be seen by the user or sonographer after his points along the execution of the Internet algorithm as described in FIG. **49**.

[0175] FIG. **51** is a screen shot of two image panels A and B. The screenshot as shown shows two other image panels with two inner face tracings drawn in image B. The two images here are editable as needed.

[0176] FIG. **52** is a screen shot of six image panels A-F. The six screen shots are acquired and show different degrees of image processing and overlaying of interface tracings for the outer at inner wall layers of the proximate or forward organ wall.

[0177] FIG. **53** is a screen shot of Exam Quality Report. The Exam Quality Report has different test options including bladder mass, bladder volume, amniotic fluid volume, etc., as well as different levels of descriptors that categorize whether the particular exam selected is % incomplete or % inconclusive, the number of exams, the percent good they were, the amount of % that are quality assurance rejected or % that are quality assurance edited, or the number in which the user has rejected.

[0178] FIG. **54** is a screen shot of two image panels A and B indicating initial segmentation of a bladder. The bladder that has been segmented is an early stage of organ wall tissue interface resolution as indicated by the relative jagged interface tracings.

[0179] FIG. **55** is a scanplane image overlaid with inner and outer wall tracings using algorithms of the Internet System. An outer wall layer **920** is shown in relation to an inner wall layer tracing **922**. While preferred and alternate embodiments of the invention have been illustrated and described, as noted above, many changes can be made without departing from the spirit and scope of the invention.

[0180] Certain embodiments of the present invention relate to and can be practiced in conjunction with the invention and embodiments described in our co-pending application filed via Express Mail Label No. EV510340886US on Feb. 17, 2005, which is hereby incorporated by reference.

[0181] Accordingly, the scope of the invention is not limited by the disclosure of these preferred and alternate embodiments. Instead, the invention should be determined entirely by reference to the claims that follow.

What is claimed is:

1. A method to measure wall thickness of an organ using an ultrasound transceiver, the method comprising:

positioning an ultrasound transceiver exterior to a patient such that at least a portion of an organ wall is within the range of the transceiver;

transmitting radio frequency ultrasound pulses as scanlines to, and receiving those pulses echoed back from, the external and internal surface of the portion of the organ wall, and based on those pulses, forming at least one two-dimensional image;

selecting wall loci at a first position of the organ wall from the two dimensional image;

adjusting the position of the wall loci by applying a one-dimensional analysis of the pulse echoes associated with the two-dimensional image to a second position and a third position; and

determining the thickness of the organ wall by calculating the difference of the wall loci between the second and third positions.

2. The method of claim **1**, wherein the radio frequency ultrasound pulses are sent to the organ in one or more of the forms selected from the group consisting of a scanplane, a spiral, and a random scanline.

3. The method of claim **2**, wherein the form selected is a scanplane, and the scanplane is associated with an array, the array selected from the group consisting of a translational array, a wedge array, and a rotational array.

4. The method of claim **3**, wherein the scanplane in the array is selected from the group consisting of uniformly spaced, non-uniformly spaced, and a combination of uniformly spaced and non-uniformly spaced scanplanes.

5. The method of claim **4**, wherein the scanplane comprises a plurality of scanlines, the scanlines selected from the group consisting of uniformly space, non-uniformly spaced, and a combination of uniformly space and non-uniformly spaced scanlines.

6. The method of claim **5**, wherein the uniform spacing between each scanplane is approximately 7.5 degrees.

7. The method of claim **5**, wherein the uniform spacing between each scanline is approximately 1.5 degrees.

8. The method of claim **1**, wherein the one-dimensional analysis includes converting the signals of ultrasound echoes associated with the scanlines of the two-dimensional image from a non-rectified signal pattern to a rectified signal pattern.

9. The method of claim **8**, wherein the conversion to the rectified signal pattern is achieved by a Hilbert Transform.

10. The method of claim **8**, wherein peak maxima of the rectified signal pattern of each scanline of the two-dimensional image determines wall loci candidates for the second and third positions.

11. The method of claim **10**, wherein a portion of the rectified signal pattern is analyzed to determine the nearest second position candidate.

12. The method of claim **11**, wherein the nearest second position candidate is determined by vector analysis of each scanline's peak maxima

13. The method of claim **12**, wherein the locus of nearest second position within each scanline is confirmed by candidate point cost analysis of the nearest second position locus of each scanline rectified signal pattern and the nearest second position loci of neighboring scanline rectified signal patterns.

14. The method of claim **10**, wherein the portion of the rectified signal pattern is analyzed to determine the nearest third position candidate.

15. The method of claim **14**, wherein the nearest third position candidate is determined by vector analysis of each scanline's peak maxima.

16. The method of claim **14**, wherein the locus of nearest third position within each scanline is confirmed by candidate point cost analysis of the nearest second position locus of each scanline rectified signal pattern and the nearest third position loci of neighboring scanline rectified signal patterns.

17. The method of claim **12**, wherein thickness is calculated as a difference between the nearest third position candidate and the nearest second position candidate.

18. A method to measure wall volume of an organ using an ultrasound transceiver, the method comprising:

positioning an ultrasound transceiver exterior to a patient such that at least a portion of an organ wall is within the range of the transceiver;

transmitting radio frequency ultrasound pulses as scanlines to, and receiving those pulses echoed back from, the external and internal surface of the portion of the organ wall, and based on those pulses, forming at least one two-dimensional image;

selecting wall loci at a first position of the organ wall from the two dimensional image;

adjusting the position of the wall loci by applying a one-dimensional analysis of the pulse echoes associated with the two-dimensional image to a second position and a third position;

determining the thickness of the organ wall by calculating the difference of the wall loci between the second and third positions;

forming an array of two-dimensional scanplanes, each scanplane having the second and third positions;

determining the area of the organ wall by calculating the area of the second and third position in the array; and

calculating the volume of the organ wall as a product of the area and thickness.

19. The method of claim **18**, wherein the radio frequency ultrasound pulses are sent to the organ in one or more of the forms selected from the group consisting of a scanplane, a spiral, and a random scanline.

20. A method to measure wall mass of an organ using an ultrasound transceiver, the method comprising:

positioning an ultrasound transceiver exterior to a patient such that at least a portion of an organ wall is within the range of the transceiver;

transmitting radio frequency ultrasound pulses as scanlines to, and receiving those pulses echoed back from, the external and internal surface of the portion of the organ wall, and based on those pulses, forming at least one two-dimensional image;

selecting wall loci at a first position of the organ wall from the two dimensional image;

adjusting the position of the wall loci by applying a one-dimensional analysis of the pulse echoes associated with the two-dimensional image to a second position and a third position;

determining the thickness of the organ wall by calculating the difference of the wall loci between the second and third positions;

forming an array of two-dimensional scanplanes, each scanplane having the second and third positions;

determining the area of the organ wall by calculating the area of the second and third position in the array;

determining the volume of the organ wall as a product of the area and thickness; and

calculating the mass of the organ as a product of volume and density.

21. The method of claim **20**, wherein the radio frequency ultrasound pulses are sent to the organ in one or more of the forms selected from the group consisting of a scanplane, a spiral, and a random scanline.

22. A system to measure wall thickness of an organ comprising:

an ultrasound transceiver configured to transmit radio frequency ultrasound pulses as scanlines to and receive the pulses echoed back from the external and internal surfaces of at least a portion of the organ wall and convert to echogenic signal pulses;

a microprocessor configured to receive the echogenic signal pulses, and based on the signals, present at least one two-dimensional image of the organ;

a first software algorithm executable by the microprocessor to identify wall loci of the organ wall displayed in the two-dimensional image;

a second software algorithm executable by the microprocessor to apply a one-dimensional analysis of the signal pulses associated with the two-dimensional image to a second position and a third position; and

a third software algorithm executable by the microprocessor to calculate the thickness of the organ wall as a difference between the second and third positions.

23. The system of claim **22**, wherein the radio frequency ultrasound pulses are sent to the organ in one or more of the forms selected from the group consisting of a scanplane, a spiral, and a random scanline.

24. The system of claim **22**, further comprising a fourth algorithm wherein the second and third positions of the wall loci are overlayed on the scanplane image.

25. The system of claim **24** wherein the thickness of the organ wall is determined from a difference of the second and third positions overlayed on the scanplane image.

26. The system of claim **25** wherein the thickness is limited to a range of thicknesses.

27. The system of claim **26** wherein the range of thicknesses is determined by the volume of the organ.

* * * * *

专利名称(译)	超声系统和测量膀胱壁厚度和质量的方法		
公开(公告)号	US20100036252A1	公开(公告)日	2010-02-11
申请号	US12/497509	申请日	2009-07-02
[标]申请(专利权)人(译)	CHALANA VIKRAM DUDYCHA STEPHEN MCMORROW GERALD YUK JONGTAE TIM谢尔顿 巴纳德BILL		
申请(专利权)人(译)	CHALANA VIKRAM DUDYCHA STEPHEN MCMORROW GERALD YUK JONGTAE TIM谢尔顿 巴纳德BILL		
当前申请(专利权)人(译)	CHALANA VIKRAM DUDYCHA STEPHEN MCMORROW GERALD YUK JONGTAE TIM谢尔顿 巴纳德BILL		
[标]发明人	CHALANA VIKRAM DUDYCHA STEPHEN MCMORROW GERALD YUK JONGTAE SHELTON TIM BARNARD BILL		
发明人	CHALANA, VIKRAM DUDYCHA, STEPHEN MCMORROW, GERALD YUK, JONGTAE SHELTON, TIM BARNARD, BILL		
IPC分类号	A61B8/00		
CPC分类号	A61B8/0858 A61B8/483 G01S7/52036 G01S7/52053 G01S7/52074 G06T2207/30004 G01S15/8909 G06T7/602 G06T2207/10136 G06T2207/20148 G01S7/52085 G06T7/136 G06T7/62		
优先权	60/400624 2002-08-02 US 60/423881 2002-11-05 US		
外部链接	Espacenet USPTO		

摘要(译)

超声波收发器扫描器官并处理回声信号以产生器官的三维，二维和一维信息。利用3-D，2-D和1-D信息来确定器官壁的厚度，表面积，体积和质量。

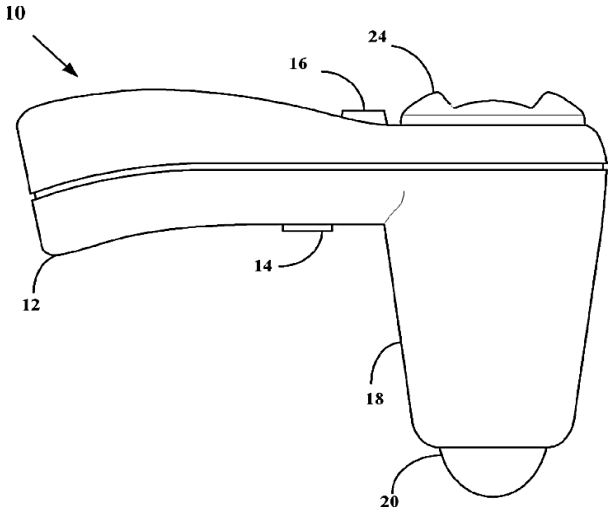
10
24
16
14
12
18
20